Wax ester production in *Rhodococcus*

by

James Round

B.Sc., The University of Victoria, 2011

A THESIS SUBMITTED IN PARTIAL FULFILLMENT OF

THE REQUIREMENTS FOR THE DEGREE OF

DOCTOR OF PHILOSOPHY

in

THE FACULTY OF GRADUATE AND POSTDOCTORAL STUDIES

(Microbiology and Immunology)

THE UNIVERSITY OF BRITISH COLUMBIA

(Vancouver)

December 2018

The following individuals certify that they have read, and recommend to the Faculty of Graduate and Postdoctoral Studies for acceptance, the dissertation entitled:

Wax ester production in *Rhodococcus*

submitted by James Round in partial fulfillment of the requirements for the degree of Doctor of Philosophy in Microbiology and Immunology

Examining Committee:

Lindsay Eltis
Supervisor

Michael Murphy
Supervisory Committee Member

William Mohn
Supervisory Committee Member

Charles Thompson
University Examiner

Vikramaditya Yadav
University Examiner

Additional Supervisory Committee Members:

Steven Hallam
Supervisory Committee Member

Abstract

Rhodococcus is a genus of soil bacteria that are among the best-studied oleaginous bacteria, and have considerable potential for the sustainable production of lipid-based chemicals. Herein, I characterized the biosynthesis of wax esters (WEs) in *Rhodococcus jostii* RHA1 and created tools to develop the biocatalytic potential of rhodococci. In Section 3.1, I established that RHA1 produces WEs and identified key enzymes involved in this production. Specifically, RHA1 produced WEs to 0.0002% of cellular dry weight (CDW) during exponential growth on glucose. These WEs contained 31 to 34 carbon atoms and were saturated. Bioinformatics revealed that RHA1 contains a putative fatty acyl-CoA reductase (FcrA). Purified FcrA catalyzed the NADPH-dependent transformation of stearoyl-CoA to stearyl alcohol with a specific activity of 45±3 nmol/mg·min and dodecanal to dodecanol with a specific activity of 5300±300 nmol/mg·min. A strain of RHA1 overproducing FcrA accumulated WEs to ~13% CDW. In Section 3.2, I expanded the genetic tools available in rhodococci, creating pSYN, a modular integrative-vector. I employed this vector to identify and characterize P_{10}, a strong, potentially constitutive rhodococcal promoter. Various strength promoters were created from P_{10}, resulting in the P_{T2}, P_{T1}, and P_{M6} promoters, which were 1.3-, 2.2-, and 6-fold stronger, respectively, than P_{nit}, a constitutive promoter previously characterized in *Rhodococcus*. RHA1 transformed with a single copy of *fcrA* under the control of these various promoters accumulated WEs. In Section 3.3, I further developed RHA1 as a WE biocatalyst. Screening a variety of enzymes identified WS2 of *Marinobacter hydrocarbonoclasticus* DSM 8798 as an effective wax synthase in RHA1. Cassettes for the co-expression of chromosomally integrated *fcrA* and *ws2* were created and

transformed into RHA1; resulting in a biocatalyst that accumulated WEs to greater than 15% CDW, at yields of 0.05 g/g glucose, while maintaining 80% of the specific growth rate of WT. Accumulated WEs were 29 to 38 carbon atoms in length, of which 75% were unsaturated, with a ~2:1 mix of mono- and diunsaturated species. Overall, this thesis provides insight into the biosynthesis of WEs in rhodococci and facilitates the development of this genus for biocatalytic applications, including the production of high-value neutral lipids.

Lay Summary

Among the best-studied oleaginous bacteria, rhodococci have considerable potential for the sustainable production of lipid-based commodity chemicals such as wax esters. However, many aspects of lipid synthesis in these bacteria are poorly understood. I identified key enzymes for wax ester biosynthesis in rhodococci and exploited them to improve the yield of wax esters in a rhodococcal strain by 75,000-fold. In so doing, this work contributes to the development of novel bioprocesses for an important class of oleochemicals that may ultimately allow us to phase out their unsustainable production from sources such as petroleum and palm oil.

Preface

I identified and designed the research program presented in this thesis in collaboration with Lindsay D. Eltis, with input from Raphael Roccor. Except where noted, the research was conducted primarily by myself. Data was analyzed by myself, and presented following suggestions from Lindsay D. Eltis.

A version of Chapter 3.1 has been published. Round J, Roccor R, Li S-N, Eltis LD. 2017. A fatty acyl-CoA reductase promotes wax ester accumulation in *Rhodococcus jostii* RHA1. Appl Environ Microbiol **83:**e00902-17. I co-wrote the manuscript and conducted all the experiments, except gravimetric measurements of wax ester contents in Section 3.1.5, which were performed by Raphael Roccor.

Table of Contents

Abstract ..... **iii**

Lay Summary ..... **v**

Preface ..... **vi**

Table of Contents ..... **vii**

List of Tables ..... **xiv**

List of Figures ..... **xv**

List of Abbreviations ..... **xvii**

Acknowledgements ..... **xx**

Chapter 1: Introduction **1**

1.1 Microbial Biocatalysts 1

1.1.1 The development of modern microbial biotechnology 2

1.1.2 The era of recombinant biology 6

1.1.3 Gene expression and metabolic engineering 7

1.1.4 Modern and emerging microbial platforms for biocatalyst development 10

1.1.5 Genome editing techniques for engineering biocatalysts 11

1.1.6 Promoters for engineered biocatalysts 15

1.1.7 Non-model bacteria as chassis for engineered biocatalysts 17

1.2 *Rhodococcus* 17

1.2.1 Physiology 18

1.2.2 Phylogeny 19

1.2.3 Biocatalytic potential and state of genetic tools 20

1.3 Bacterial carbon storage 21

1.3.1 PHAs 22

1.3.2 TAGs 24

1.3.3 WEs 24

1.4 TAG biosynthesis in *Rhodococcus* 28

1.4.1 Fatty acid biosynthesis 28

1.4.2 TAG biosynthesis 31

1.4.3 The lipid droplet 33

1.5 Creating a rhodococcal biocatalyst for the production of oleochemicals 35

Chapter 2: Material and Methods 38

2.1 Reagents 38

2.2 Strains and culture conditions 38

2.2.1 Culture conditions 39

2.2.2 Culture media supplements 39

2.3 DNA manipulation, plasmid construction, and gene deletion 40

2.3.1 Cloning of FcrA 44

2.3.2 Deletion of *fcrA* 45

2.3.3 Construction of pSYN 45

2.3.4 Cloning promoters into pSYN 45

2.3.5 Subcloning *fcrA* into pSYN 46

2.3.6 Subcloning synthesized WSs into pTip 46

2.3.7 Subcloning *ws2* into pSYN 46

2.3.8 Construction of pLB 47

2.3.9 Assembly of *fcrA* and *ws2* tandem co-expression cassettes 47

2.3.10 Generation of RHA1 strains harboring tandem co-expression cassettes 47

2.4 Protein production and purification 48

2.4.1 FcrA 48

2.4.2 WSs 49

2.4.3 Mass spectrometry of purified FrcA 50

2.5 FcrA activity assays 50

2.5.1 Spectrophotometric assays 50

2.5.2 *In vitro* fatty alcohol production 51

2.6 Production of neutral lipids and WEs 51

2.7 Lipid extraction and thin layer chromatography (TLC) 52

2.8 Isolation, fractionation, and gravimetric quantification of neutral lipids 52

2.9 GC/MS analyses 53

2.10 Determination of promoter strengths 54

2.11 Transcription start site (TSS) determination 54

2.12 Characterization of RHA1 strains containing *frcA* and *ws2* co-expression cassettes ... 55

2.12.1 Screening of growth characteristics and WE accumulation 55

2.12.2 Determination of dry biomass and WE yields 56

Chapter 3: Results.....57

3.1 FcrA promotes WE accumulation in RHA1 57

3.1.1 Identification and characterization of WEs in RHA1 57

3.1.2 Bioinformatic identification of FcrA 61

3.1.3 Production, purification, and characterization of recombinant FcrA 62

3.1.4 WE production in a Δ*fcrA* mutant..... 66

3.1.5 Overexpression of *fcrA* 67

3.1.6 The role of FARs and WEs in bacterial physiology 69

3.2 Development of synthetic biology tools for rhodococci 70

3.2.1 Creation of pSYN, a modular integrative vector 71

3.2.2 Identification of P_{10} as a strong-constitutive promoter 72

3.2.3 Characterization of P_{10} 76

3.2.4 Demonstration of pSYN for FcrA overproduction 82

3.3 Identification and production of wax synthases in RHA1 85

3.3.1 Identification of WSs in RHA1 85

3.3.2 Co-expression of *fcrA* with characterized WSs. 89

3.3.3 Genomic co-integration of *fcrA* and *ws2* 94

3.3.4 Screening WE accumulating strains 97

3.3.5 Characterization of WE accumulating strains 99

3.3.6 A rhodococcal biocatalyst for the production of WEs 102

Chapter 4: Conclusion 103

4.1 The role of WEs in the physiology of mycolic acid-containing bacteria 103

4.2 Overproduction of FcrA provides *de novo* fatty alcohols for WE synthesis 104

4.3 Synthetic biology tools for rhodococcal biocatalysts 105

4.4 The complexities of lipid biosynthesis in *Rhodococcus* 108

4.5 The potential of rhodococci for the sustainable production of WEs 109

4.6 Remaining questions 112

4.7 Concluding remarks 113

References 114

Appendices 132

Appendix A - Synthesized DNA[a] 132

List of Tables

Table 2.1 Bacterial strains used in this study. 38

Table 2.2 Plasmids used in this study 40

Table 2.3 Primers used in this study 41

Table 3.1 WE levels in RHA1 strains under different growth conditions. 58

Table 3.2 Specific activities of FcrA with various acyl-CoA and fatty aldehyde substrates..... 65

Table 3.3 Candidate genes for identification of strong constitutive promoters. 74

Table 3.4 Characterization of integrative co-expression strains that accumulate WEs. 100

List of Figures

Figure 1.1 Gene expression in prokaryotes..... 9

Figure 1.2 Two-step allelic exchange using *Kan*^{R}-*sacB* cassettes..... 12

Figure 1.3 Advanced genome-editing techniques..... 14

Figure 1.4 PHA synthesis in RHA1..... 23

Figure 1.5 Bacterial WE biosynthesis pathways..... 27

Figure 1.6 Fatty acid synthesis at the FAS1 complex..... 30

Figure 1.7 The Kennedy pathway in RHA1. 32

Figure 3.1 Analyses of WEs in RHA1..... 59

Figure 3.2 WE content of RHA1 under different conditions..... 60

Figure 3.3 Bacterial fatty acyl-CoA reductases. 61

Figure 3.4 Purification and activity of recombinant FcrA..... 64

Figure 3.5 Comparison of WEs in wild-type RHA1 and Δ*fcrA* mutant. 67

Figure 3.6 WE content of RHA1 overproducing FcrA..... 68

Figure 3.7 pSYN, a modular integrative-plasmid for engineering rhodococcal biocatalysts..... 72

Figure 3.8 Characterization of constitutive promoters found in RHA1..... 75

Figure 3.9 Characterization of minimal P_{10} promoters..... 80

Figure 3.10 Transcriptional start sites of the P_{10} promoter..... 81

Figure 3.11 Constitutive overexpression of *fcrA* using pSYN. 83

Figure 3.12 Profile of WEs produced in RHA1 containing an integrated, constitutively expressed copy of *fcrA*..... 84

Figure 3.13 TLC analysis of WE accumulation in *atf* mutants during growth on fatty alcohols. 87

Figure 3.14 TLC analysis of WE accumulation in *atf* mutants during fcrA overproduction. 88

Figure 3.15 Bioinformatic analysis of RHA1 WS/DGATs and characterized WSs..... 89

Figure 3.16 Expression of codon-optimized wax synthases..... 92

Figure 3.17 WE production in RHA1 expressing a chromosomally integrated *fcrA* and plasmid-borne WSs..... 93

Figure 3.18 Assembly of *frcA* and *ws2* expression cassettes..... 96

Figure 3.19 WE production and growth parameters of RHA1 strains containing chromosomally integrated *fcrA* and *ws2* expression cassettes..... 98

Figure 3.20 WE profile of T1/T1 and T2/T1 RHA1 strains containing chromosomal *fcrA* and *ws2*. 101

List of Abbreviations

ABE - Acetone-butanol-ethanol

ACP - Acyl carrier protein

AGPAT - 1-acylglycerol–3-phosphate *O*-acyltransferase

APL - Alkaline pretreated liquor

ARF - Adapter and radiation free

AT - Acetyl transferase

ATP - Adenosine triphosphate

C18:1-CoA - Oleoyl-CoA

C18-CoA - Stearoyl-CoA

CDW - Cellular dry weight

CoA - Coenzyme A

COOL - Codon optimization on-line

CRISPR - Clustered regularly interspaced short palindromic repeats

CV - Column volumes

DAG - Diacylglycerol

DH - Dehydratase

DNA - Deoxyribonucleic acid

DTNB - 5,5'-dithiobis-(2-nitrobenzoic acid)

ED - Entner–Doudoroff

EDTA - Ethylenediaminetetraacetic acid

ER - Enoyl reductase

FAR - Fatty acyl-CoA reductase

FAS - Fatty acid synthase

GC/MS - Gas chromatography mass spectrometry

GPAT - Glycerol-3-phosphate *O*-acyltransferase

HAD - Haloacid dehalogenase

KR - Keto reductase

KS - Keto synthase

LB - Lysogeny broth

LD - lipid droplet

MAGE - Multiplexed automated genome engineering

MBP - Maltose binding protein

MOPS - 3-(N-morpholino)propanesulfonic acid

MPT - Malonyl palmityl transferase

NADH - Nicotinamide adenine dinucleotide

NADPH - Nicotinamide adenine dinucleotide phosphate

NO - Nitric oxide

NRRL - Northern Regional Research Laboratory

NTB^{2-} - 2-nitro-5-thiobenzoate

OD_{600} - Optical density at 600 nm

PA - Phosphatidic acid

PAP2 - Type 2 phosphatidic acid phosphatase

PCR - Polymerase chain reaction

PD630 - *Rhodococcus opacus* PD630

PHA - polyhydroxyalkanoate

RBS - Ribosome binding site

RHA1 - *Rhodococcus jostii* RHA1

RNA - Ribonucleic acid

RPKM - Reads per kilobase per million mapped reads

SDS-PAGE - Sodium dodecyl sulfate polyacrylamide gel electrophoresis

SNARE - Soluble *N*-ethylmaleimide-sensitive factor attachment protein receptor

SNP - Sodium nitroprusside

TAG - Triacylglyceride

TLC - Thin layer chromatography

TSS - Transcriptional start site

UL - Universal linker

UV - Ultra violet

WE - Wax ester

WS - Wax synthase

WS/DGAT - Wax ester synthase/acyl-CoA:diacylglycerol acyltransferase

WT - Wild type

Acknowledgements

I offer my enduring gratitude to the faculty, staff and my fellow students at UBC, who have made this beautiful campus a wonderful place to work and be inspired.

I owe particular thanks to Dr. Lindsay D. Eltis for continually providing guidance, leadership, and the freedom to discovery, explore and make mistakes. You taught me to think and question rigorously, and held me to the highest standards. I will always be better for it.

My friends and lab mates will forever have my gratitude for their unfailing support and encouragement. Kirstin, Raphael, Adam, this has been a wonderful journey.

Special thanks are owed to my family. Phillip, you dragged me up and down mountains, keeping me sane through all the difficulties of this thesis. To my parents, Anne and Adrian Round, who have supported me throughout my years of education. I could not have done this without you. Thank you.

Chapter 1: Introduction

1.1 Microbial Biocatalysts

Since the introduction of agriculture at the end of the Mesolithic period, microorganisms have played a role in the development of human civilization. First used in the fermentation of foods and drink, microorganisms provided a means to preserve foods and to ensure that drinking water was safe (1-3). More specifically, humans used microorganisms to ferment grains, fruits, and dairy products into alcoholic beverages, leavened breads, and products such as yogurt and cheese; occurring as early as the Neolithic period, 4000 to 9000 years ago, in regions of China, the Middle East, and the Mediterranean (3-5). As human civilizations continued to develop, fermentation techniques increased in sophistication. A combination of observation, trial and error, and serendipity resulted in traditions passed down generation-to-generation in written and spoken word. Nevertheless, while civilizations reaped the benefits of early microbial technologies, humankind did not understand the role of microorganisms in fermentation.

It was not until the Age of Enlightenment that we began to understand how microorganisms contribute to fermentation. The first indications that microorganisms were involved in fermentation came when Antoni van Leeuwenhoek developed the microscope in the late 17th century and observed the presence of yeast in the fermentation of alcohol and leavening of bread (6). From this initial discovery, the works of Samuel Johnson, Antoine-Laurent de Lavoisier, and Joseph Louis Gay-Lussac established the importance of yeast in these processes (7). However, it wasn't until 1830s that a series of independent observations and studies suggested that yeast

were alive and growing, rather than just organic catalysts required for fermentation (8). These efforts cumulated in the works of Louis Pasteur who in 1876 conclusively established the role of yeast in fermentation (9, 10). Together, these discoveries founded the scientific fields of microbiology and biochemistry, which subsequently allowed humankind to harness microorganisms as biocatalysts.

1.1.1 The development of modern microbial biotechnology

In the early 1900s, the development of acetone-butanol-ethanol fermentations (ABE) by *Clostridium acetobutylicum* gave rise to modern industrial biotechnology. Building on the works of Pasteur and Shardinger (11), ABE fermentation was developed beyond a scientific curiosity in 1910 by Auguste Fernbach, who aimed to create synthetic rubbers from butadiene and isoprene, which could be chemically derived from butanol and acetone (12). Fernbach's process utilized an isolated bacterium able to ferment potato starch, but suffered from inefficacies and difficulties in scaling, leading to its eventual abandonment. In 1914, Charles Weizmann, who had been associated with the early development of Fernbach's process, isolated *C. acetobutylicum* and independently developed an efficient process for ABE fermentation from corn maize (13). The outbreak of World War One lead to acute shortages of acetone, a vital component for the production of cordite, a smokeless propellant critical to Britain's war effort. Therefore, in 1915, a national effort was undertaken to scale Weizmann's ABE process for the industrial production of acetone. Scaling of Weizmann's process was not trivial, and many fundamental lessons were learned, such as the importance of: aseptic fermentation conditions, regulation of fermentation temperatures, and inoculum purity (12). Furthermore, the development of Weizmann's process

contributed to the development of efficient deep-tank fermentations and the importance of fermentation seed-trains. With the successful scale-up and development of ABE fermentation in 1916, Weizmann's ABE process was developed throughout Allied territories, with Canadian facilities contributing more than 3000 tons of acetone to the war effort (14). While ABE fermentation as an industrial source of acetone and butanol would eventually be replaced by petroleum sources, the lessons learned from the development of ABE processes would be applied to industrial biotechnology's next great achievement, the production of penicillin.

Industrial biotechnology came into its own in the 1940s with the development of large-scale penicillin production. With the rising field of microbiology and the advent of the germ theory of disease by Pasteur and Robert Koch in the 19th century, there was considerable interest in finding therapies for newly discovered microbial diseases in the late 19th and early 20th centuries (11). These works led to two major discoveries: sulphonamide antibiotics by Gerhard Domagk (15), and penicillin by Alexander Fleming (16). While sulphonamide antibiotics could be produced by the technologies of the time, their toxicity and increasing incidences of antibiotic resistance required other solutions (17, 18). Ten years after Fleming's initial discovery, Howard Florey, Ernst Chain, and Norman Heatley at the University of Oxford began to study the application of penicillin as an antibiotic drug. Their team discovered methods to stably extract penicillin from the culture broth of Fleming's *Penicillium* strain, allowing them to conduct clinical trials in animals and humans (11). However, while penicillin was shown to be effective in these early trials, the production was costly, time-consuming, and labor-intensive. It was the advent of World War Two, and the need for new antibacterial treatments that spurred efforts to produce penicillin industrially. In 1941, on behalf of the British government, Florey and Heatley brought

their techniques to the United States for further development. Within three years, a collaborative undertaking between government, academia, and industry, improved penicillin production over 200-fold, allowing it to be used to treat soldiers wounded on the battlefields of Europe, saving thousands of lives.

The development of penicillin production required both fermentation and strain optimization. When Florey and Heatley brought penicillin to America, they were put in touch with Robert Coghill's team of fermentation specialists at the US Department of Agriculture's Northern Regional Research Laboratory (NRRL) (19). Using their experience in fungal fermentation, Coghill's group determined three goals critical to increasing penicillin production: the isolation and selection of better penicillin producing fungi, the optimization of growth media, and the development of submerged fermentations. One of the first breakthroughs was found by Andrew J. Moyer, involving the replacing the brewer's yeast extract fermentation medium with newer corn steep liquor mediums he had developed, resulting in an immediate 30-fold increase in penicillin production (19). This early breakthrough proved critical to convincing government and industry that fermentation and not synthesis was the preferred route for penicillin production. Another of the NRRL contributions to the development of penicillin was the exploration and development of submerged cultures, which proved economically and industrially feasible compared to surface culture methods, and eventually led to the deep-tank fermentation techniques perfected by industry (20). Finally, improvements in fermentation techniques were complemented by the isolation of highly-productive *Penicillium* strains better suited to submerged fermentation (21). Together, the lessons learned from the development of penicillin

production would invigorate the field of industrial biotechnology, leading to many great discoveries through the remaining half of the 20th century.

Post World War Two, the lessons learned in the development of penicillin were applied to other antibiotics and to the production of many small molecules. This brought the world into the antibiotic era, in which new classes of antibiotics were rapidly discovered and isolated from a range of fungal and bacteria sources, such as cephalosporin, streptomycin and neomycin (11). In parallel, scientists developed industrial processes to exploit the primary metabolism of microorganisms to produce a variety of small molecules, such as amino acids, vitamins, nucleotides, alcohols, and organic acids. Many of these processes are still used today (22). Notable examples include the production of amino acids by *Corynebacterium glutamicum*, an actinobacterium that secretes large amounts of glutamate when subjected to membrane stress (23). *C. glutamicum* has been further mutagenized to create industrial strains able to produce other amino acids, in particular lysine (24), and is used to produce more than four million tons of amino acids a year. Vitamins, such as B_{12}, are still produced industrially by *Pseudomonas denitrificans* strains modified through mutagenesis and screening (25). Finally, a range of alcohols and organic acids were produced by a variety of fungi and bacteria (22). While many great bioprocesses were created through the traditional techniques of industrial microbiology, the advent of recombinant DNA technology in the 1970s would be forever change industrial biotechnology.

1.1.2 The era of recombinant biology

Recombinant DNA technologies allowed scientists to rationally modify microorganism. The age of recombinant DNA technologies began in 1973 when Stanley Cohen, Herbert Boyer, and colleagues cloned and propagated recombinant DNA in an *Escherichia coli* plasmid (26, 27). For the first time, the genetic capabilities stored within the DNA of an organism could be isolated and harnessed. This discovery was critical to the advancement of biological science, and catalysed the advancement of supporting DNA technologies, including: DNA hybridization, for detecting cells containing cloned DNA; the production of cDNA from mRNA (28); and DNA sequencing (29, 30). The immense possibilities of these emerging technologies was recognized by Boyer and venture capitalist Robert Swanson, who founded Genentech to take advantage of them. Genentech forged key partnerships between academic and industry experts in recombinant technologies and, in 1977, chemically synthesized, cloned, and expressed the first gene encoding a functional human protein, somatostatin (31). This experience would be critical in Genentech's next endeavour, the production of human insulin. The human insulin gene was synthesized, cloned, and expressed in recombinant *E. coli* by Genentech scientists in 1979 (32). This success spurred a collaboration between Genentech and Eli Lilly that led to the scale-up of industrial production, allowing recombinant insulin to be approved by the United States Food and Drug Administration for the treatment of diabetes in 1982. The production of insulin launched the biopharmaceutical revolution and further highlighted the importance of industrial microbiology.

Recombinant DNA technologies were applied to produce industrial enzymes. With increasingly sophisticated technologies and techniques, private companies used recombinant DNA

technologies to bring industrial enzymes to market faster and cheaper than ever before (33). These included: penicillin amidase, produced in *E. coli* in 1979, for the synthesis of β-lactam antibiotics; α-amylase, cloned in 1982, for liquefying starch in the food industry (11); and in 1987, a lipase from *Humicola lanuginose,* for use in detergents (34). As recombinant DNA technologies improved, these industrially important enzymes were further modified, ensuring their continued relevance in modern industrial processes.

1.1.3 Gene expression and metabolic engineering

A cell's phenotype, including its biocatalytic activity, is largely determined by the protein activities present at a given time (Figure 1.1). Transcription is a major determinant of what proteins are present in the cell under a given set of conditions. Gene transcription is initiated at promoters, specific sequences of DNA that bind RNA polymerase (35). In bacteria, most promoters are composed of two regions, the -10 and -35 boxes, which are hexameric nucleotide sequences that sit approximately ten and thirty-five nucleotides upstream of the transcriptional start site and bind the sigma factor of the RNA polymerase holoenzyme (36, 37). Once bound, the interaction between RNA polymerase and the sigma factor changes, allowing promoter escape and the processive transcription of DNA into mRNA (38). The affinity of the sigma factor for the promoter sequence determines the frequency at which transcription is initiated, and thereby defines the strength of the promoter (39). Transcription can also be influenced positivity or negatively by transcription factors that modulate the binding of the RNA polymerase to promoters. Transcription ends at specific nucleotide sequences called terminators, which usually occur after a gene or operon and prevent the spurious expression of genes (35).

Protein production in the cell is also regulated at the level of translation. Translation is initiated at the ribosome binding site (RBS), located approximately eight nucleotides upstream of the start codon of a gene, which recruits the ribosome. Both the affinity of the RBS sequence for the ribosome and secondary structure within the RBS region affect the frequency of ribosome binding and therefore the amount of protein produced during the lifetime of an mRNA molecule (40). Ultimately, both the strength of the promoter and RBS control the level of enzyme expressed from a gene.

Recombinant DNA technologies and understanding gene expression enabled the metabolic engineering of microorganisms to create powerful industrial biocatalysts. Metabolic engineering was described as a scientific discipline in the 1990s when genetic tools created opportunities to modify the flux of carbon, nitrogen, and other elements through metabolic pathways (41). Researchers aimed to rationally improve product formation or the cellular properties of microorganisms to benefit industrial processes (42). This included understanding metabolic networks and metabolic flux distributions (43), such as the elucidation of lysine production in *C. glutamicum* (44), as well as using recombinant DNA technologies to create novel metabolic pathways and change the expression of existing ones. The latter is exemplified by the production of ascorbic acid in *Erwinia herbicol* (45) and polyhydroxybutyrate in *E. coli* (46). These discoveries and applications highlighted the potential of this field, and prompted research that continues to this day.

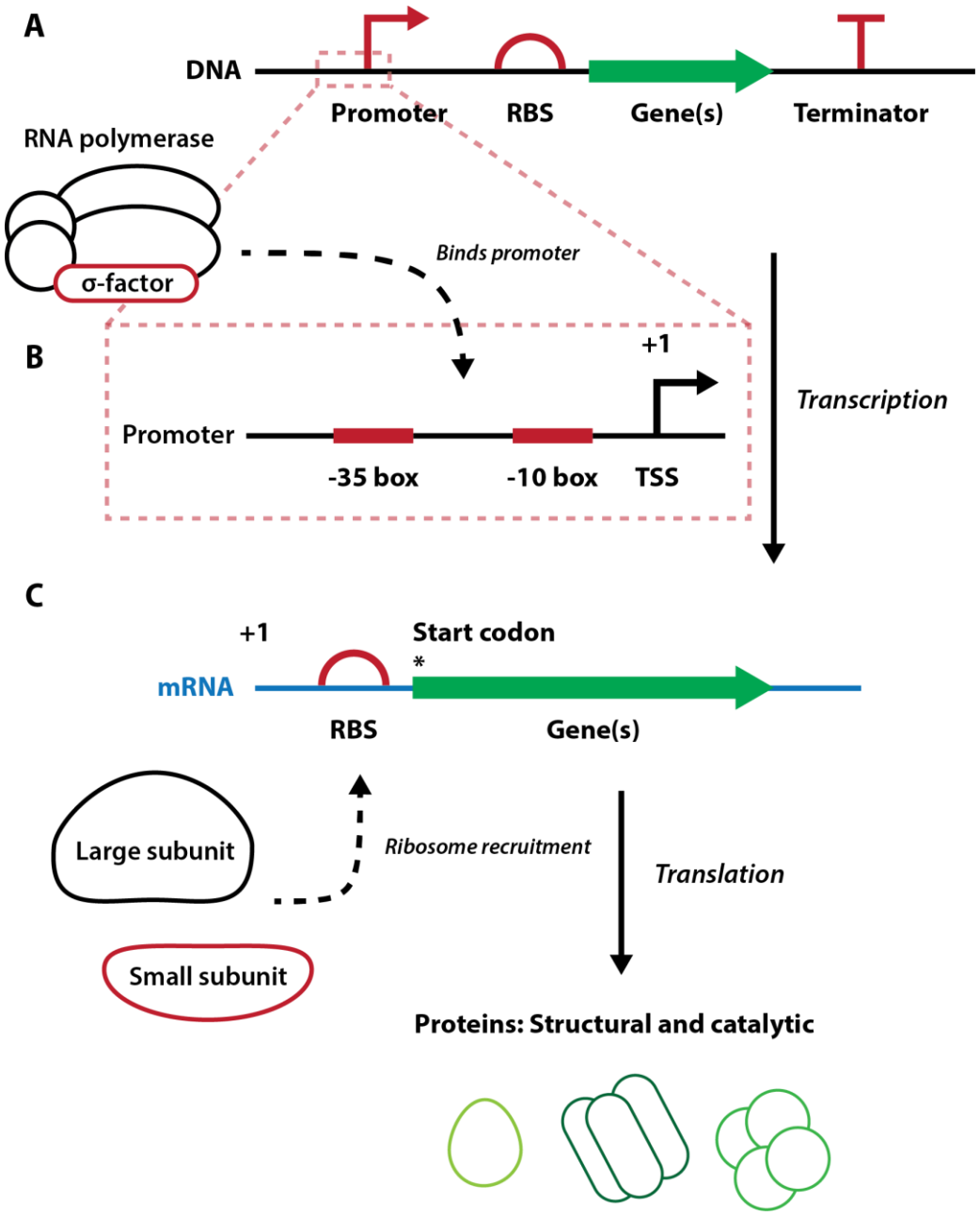

Figure 1.1 Gene expression in prokaryotes

DNA encodes (A) genetic components that allows for (B) transcription and (C) translation. Transcription and translation are major determinants of what proteins are present in a cell, and thereby determine phenotype.

1.1.4 Modern and emerging microbial platforms for biocatalyst development

Genetic tools have continued to improve, allowing scientist to harness microbial diversity for the production of sustainable and novel chemicals. With increasingly sophisticated techniques and instrumentation, the genomes, proteomes, and metabolomes of microorganisms are routinely examined to understand microbial physiology. System-level views of biology have allowed scientists to study the dynamics of gene expression, protein interactions, and to map regulatory and metabolic networks. Metabolic engineering has increasingly used these data to guide advanced genetic manipulation aimed at harnessing microorganism for the sustainable, economic, and reliable production of chemicals and biomolecules. This has resulted in extraordinary successes, such as microbial biocatalysts for the production of 1,4-butanediol (47) and artemisinin (48). However, as biocatalysts have become progressively more intricate, the majority are being assembled in model microorganisms, such as *E. coli* and *Saccharomyces cerevisiae*. These model organisms allow scientists to harness a wealth of tools, techniques, and knowledge that enables advanced genome engineering (49-52), the creation of detailed metabolic models (53), and the simple implementation of -omic technologies. These resources have increased the pace of design-build-test–learn cycles, and therefore, driven the proliferation of biocatalysts using model hosts.

A lack of these tools has hindered, but not prevented the development of biocatalysts using some non-model organisms. Biocatalysts developed in *Pseudomonas putida* (54-56) and *C. glutamicum* (57-60) have shown the potential of non-model hosts. These projects have also highlighted the need to develop well established, characterized, and robust genetic tools that can

be used to reduce the trial-and-error and genetic uncertainty in design-test-build cycles in non-model microbes (61-63). This remains one of the biggest challenges in working with non-model microbes, let alone engineering them into tunable biocatalysts, and as such, many novel and interesting biocatalysts have yet to be explored (41, 64-66).

1.1.5 Genome editing techniques for engineering biocatalysts

The ability to rationally and specifically modify the DNA of microbial genomes is critical to engineering biocatalysts. Strains are engineered through the insertion, deletion, or substitution of genomic DNA, which allows for the introduction, removal, or modification of genetic functionality. In bacteria, targeted genome modifications is routinely accomplished through two-step allelic exchange using homologous recombination and counter-selection tools, such as *Kan^R-sacB* cassettes (Figure 1.2) (67, 68). In two-step allelic exchange, a bacterium is transformed with a non-replicative suicide vector containing DNA sequences homologous to the recipient genome. The homology allows for the recombination events of the first and second cross-over, selected for using the *Kan^R* and *sacB* markers, respectively, in the case of *Kan^R-sacB* cassettes. Based on the design of the cassette, DNA can be inserted or deleted from the recipient genome. Two-step allelic exchange is reliable, robust, and has been used in a wide range of bacterial species (69-72). However, this method is slow, labor-intensive, and not amenable to high-throughput automation, limitations that have caused researchers to explore other options.

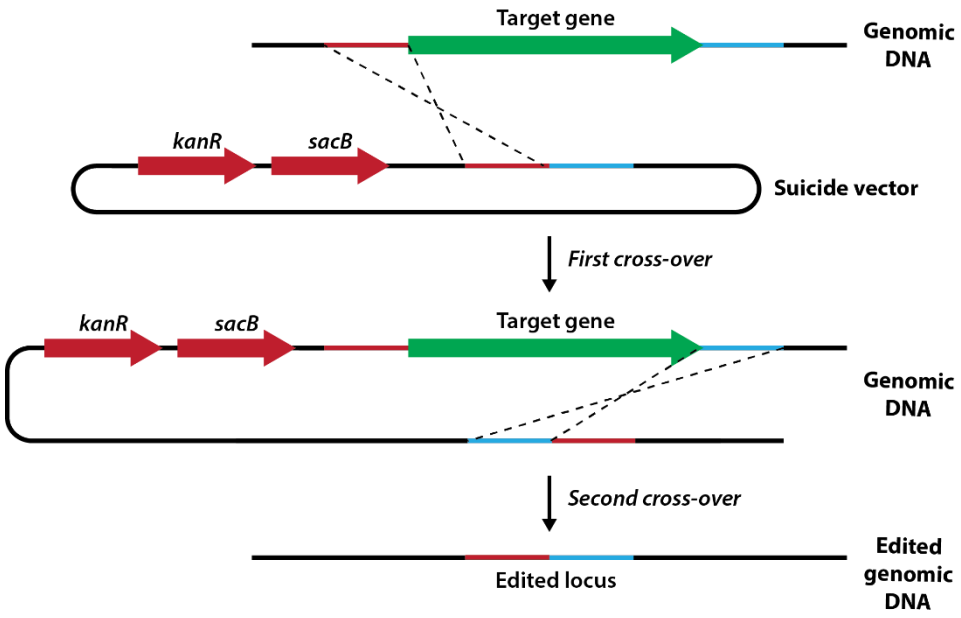

Figure 1.2 Two-step allelic exchange using *Kan*^{R}*-sacB* cassettes

The recombination between homologous regions (red and blue) on the genome and suicide vector introduce the *Kan*^{R}*-sacB* cassette into the recipient genome, and is selected using the *Kan*^{R} marker. A second cross-over event removes the *Kan*^{R}*-sacB* cassette and results in genome editing, and is selected using the *sacB* marker. The initial cross-over event can occur at either homologous region.

To enable high-throughput genome editing, new tools have been developed, such as recombineering, multiplexed automated genome engineering (MAGE), and clustered regularly interspaced short palindromic repeats (CRISPR) based methods (Figure 1.3) (73, 74). These new tools have become available by coupling advances in basic biology with well-characterized genetic components. Recombineering takes advantage of phage-derived recombinases to mediate homologous recombination at greatly increased efficiencies (75-77). This increased efficiency allows the direct insertion of DNA bearing selection-markers into the genome with minimal effort, adding functionality or disrupting native genes. For example, Recombineering enabled the

creation of the Keio strain collection, in which all non-essential *E. coli* genes were disrupted (78). The disadvantage of recombineering is the requirement for insertion of a selectable marker into the genome, which makes it difficult to generate scar-less deletions or to create multiple gene disruption within a single strain. Recombineering is further complicated by the necessity to express recombinases which may not be active in all bacterial species (79). MAGE is an extension of recombineering, in which recombinases are used to incorporate chemically-modified oligonucleotides into the DNA replication fork (80, 81). MAGE enables the simultaneous modification of multiple genetic loci, and has been used for massive-scale genome editing and tuning metabolic pathways (81-83). However, the full potential of MAGE requires specialized automation equipment, efficient recombinases, and the ability to transform oligonucleotides into a host at high-efficiencies. These limitations have largely prevented its use outside of *E. coli* (84, 85).

CRISPR-Cas9 is a bacterial adaptive viral-defense system that has been adapted to modify genomic DNA in a targeted manner (86, 87). CRISPR uses a nuclease to create double-stranded cuts in DNA at a site complementary to a guide RNA. This results in the induction of DNA repair mechanisms that can disrupt native genes or allow for efficient homologous recombination at the break site. The guided nature of CRISPR-Cas9 has also allowed for the modification of the Cas9 enzyme for gene knockdowns, in which a catalytically-dead Cas9 variant binds to DNA, preventing transcription of the targeted gene (88). CRISPR-Cas9 based systems can also be used in a high-throughput fashion for rapid genome engineering (89, 90). While all these tools have rapidly accelerated the creation of microbial biocatalysts, they have largely been confined to

well-studied model organisms, as these tools require well characterized promoters to reliably and predictably drive heterologous gene expression in the host.

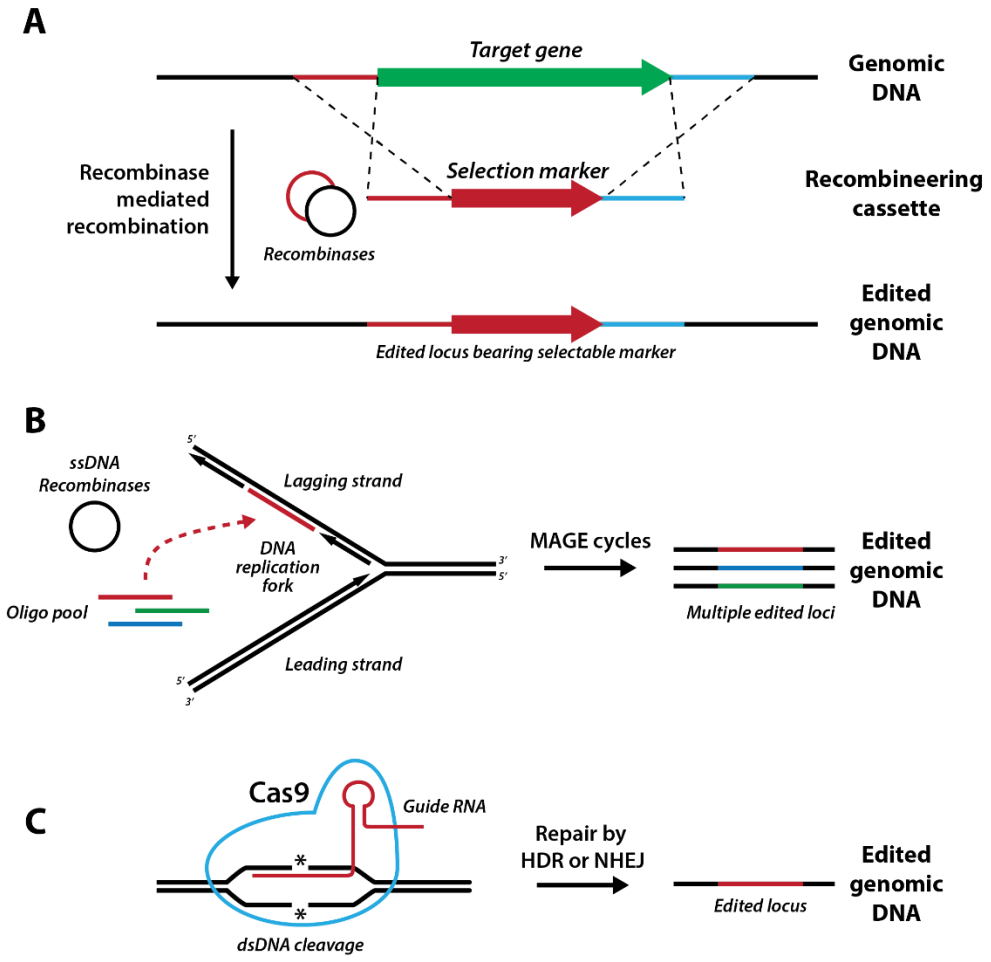

Figure 1.3 Advanced genome-editing techniques

Advanced genome-editing techniques have greatly accelerated biocatalyst development. (A) Recombineering uses phage-derived recombinases to mediate efficient homologous recombination. (B) Multiplexed automated genome engineering (MAGE) uses ssDNA recombinases to incorporate chemically modified oligos into the DNA replication fork. (C) Clustered regularly interspaced short palindromic repeats (CRISPR)-Cas9 uses a guide RNA to target the Cas9 nuclease to a genomic locus. Once Cas9 introduces double stranded DNA breaks, they are repaired by either non-homologous end joining (NHEJ) or homology directed repair (HDR), resulting in editing of the genome locus.

1.1.6 Promoters for engineered biocatalysts

Well-characterized promoters are essential to engineering biocatalysts (91, 92). By controlling the transcription of genes, characterized promoters allow for effective metabolic engineering and for the implementation of advance genome editing techniques. In bacterial physiology, promoters can be broadly separated into two classes: constitutive promoters, which are always active, and whose strength is primarily determined by the affinity of the promoter sequence for RNA polymerase (93); and regulated promoters, in which spatiotemporal activation and/or the strength of the promoter is influenced by transcription factors that respond to environmental stimuli (94, 95). Inducible promoters are the most commonly used regulated promoters, and are activated and/or repressed depending on the presence or absence of inducer molecules (96).

Constitutive promoters are preferred in the engineering of industrial biocatalysts (97). While regulated promoters have been successful in some applications, particularly the production of high-value recombinant proteins (98), they present challenges in other applications. Specifically, many inducible promoters display biphasic expression patterns and are not titratable at the cellular level, leading to variable expression within a population; which is further exacerbated by the heterogeneous environments found within industrial-scale bioreactors (99). Furthermore, the addition of inducer molecules to industrial-scale bioreactors can be cost-prohibitive. Finally, exquisite control of transcription factor expression is needed in the implementation of robust inducible promoters systems (100). This requires complex genetic constructs that can hinder rapid prototyping of biocatalysts, and can lead to unforeseen changes in phenotype as regulatory networks increase in complexity. These factors all contribute to the complications of using

inducible promoters in industrial biocatalysts. Consequently, for industrial applications, robust constitutive promoters with predictable promoter strengths are often preferred when tuning the flux of engineered metabolic pathways (101-103).

Inducible promoters are primarily used to drive heterologous gene expression in genetic tools. Promoters, such as P_{lac} (104) and P_{tet} (105), from the *E. coli* operons for lactose utilization and tetracycline resistance, respectively, have been extensively characterized and modified for use in molecular biology (106, 107). In model organisms, genetic tools take advantage of these highly characterized inducible promoters for reliable gene expression. In order to expand the repertoire of genetic tools in non-model organisms, scientists have adapted well-characterized inducible systems, exemplified by the plethora of tetracycline-responsive promoters adapted for use in divergent bacterial species (108-111). Tetracycline-responsive promoters have *tetO* operator sequences located at the -35 and -10 nucleotide sequences. In the absence of tetracycline, these operator sequences allow the *tet* repressor protein (TetR) to bind the promoter, preventing the recruitment of RNA polymerase. Upon binding tetracycline, the conformation of TetR changes, lowering the repressor's affinity for *tetO*, and releasing it from the promoter, and allowing transcription to occur. Due to the robust and titratable nature, TetR has been used to create hybrid-inducible promoters by adding *tetO* sequences to strong constitutive promoters (108). Furthermore, key amino acid residues within the TetR repressor have been mutated to reverse the activation and repression activities, further increasing the utility of *tetR*-based systems (112). The creation of well-characterized promoters in non-model organisms greatly increases our ability to engineer non-model organism into biocatalysts.

1.1.7 Non-model bacteria as chassis for engineered biocatalysts

As the biological limitations of model-organisms, such as *E. coli*, are realized, non-model bacteria are being increasingly explored as chassis for next-generation biocatalysts. The biological capabilities of non-model bacteria offer biocatalytic advantages over traditional hosts. The use of non-model bacteria can reduce bioprocess costs through the utilization of low-cost carbon sources that model organisms cannot metabolize, such as lignin-derived aromatics, methane, carbon dioxide, hydrocarbons, and industrial environmental pollutants (113-118). Other differences in metabolism that can benefit bioprocesses include: the efficient, simultaneous assimilation of multiple carbon sources (119); and the rapid replenishment of NADPH reducing equivalents (120, 121), which is the rate-limiting step in many biosynthetic pathways (122). Furthermore, non-model bacteria can possess inherent thermo-, halo-, or solvent-tolerance that can contribute to biocatalyst viability in industrial processes (117). Finally, many non-model bacteria contain biosynthetic pathways for the production of industrially relevant molecules, such as acids and alcohols, lipids, surfactants, biopolymers, and secondary metabolites (115, 117, 123). Despite the challenges in manipulating non-model bacteria, these biological capabilities make them attractive chassis for next-generation biocatalysts.

1.2 *Rhodococcus*

Rhodococcus is a genus of aerobic, non-spore forming, mycolic acid-containing bacteria within the phylum Actinobacteria. The genus belongs to the suborder Corynebacterineae and is closely related to *Mycobacterium* and *Corynebacterium*. As described in more detail below, *Rhodococci* are distinguished by the presence of a unique outer membrane (124), catabolic versatility (125-

128), and are oleaginous (129-131). The term oleaginous refers to the ability to synthesize and store large amounts of neutral lipids. In addition, many rhodococci have large genomes, exemplified by the 9.7 Mb genome of *Rhodococcus jostii* RHA1 (RHA1 hereafter) (126). These features have contributed to the use of rhodococci as biocatalysts for the industrial production of acrylamide, as well as research into their use for the transformation of bioactive steroids, desulfurization of petroleum, and production of biofuel (132).

1.2.1 Physiology

A defining feature of Corynebacterineae is their mycolic acid-containing outer membrane. The mycolic acids are partially anchored through ester bonds to arabinogalactan units that are part of the cell wall (124). Mycolic acids are long-chain lipids containing a long β-hydroxy moiety and a shorter α-alkyl side chain. The β-hydroxy portion of mycolic acids can be further modified through methylation, epoxidation, and hydroxylation (124). In rhodococci, mycolic acids are between 30 and 54 carbons atoms in length and contain up to 2 double bonds (124, 133, 134). The presence of this mycolic acid-containing membrane is hypothesised to contribute heavily to the physiological properties of members of the suborder (124), such as resistance to chemical damage, solvents, dehydration, hydrophilic antibiotics, and biocides (135, 136). This in turn likely contributes to their ability to assimilate toxic and hydrophobic substrates (128).

The large genomes of rhodococci provide broad genetic capabilities that facilitate the assimilation of diverse and otherwise recalcitrant carbon sources (125-128). Notable growth substrates include sterols, alkanes, halogenated substrates, heterocycles, polycyclic aromatics, and lignin-derived compounds. It is the presence of large numbers of catabolic enzymes, such as

oxygenases, which allow rhodococci to utilize these compounds. For example, the RHA1 genome encodes for more than 200 oxygenases, including 25 cytochromes P450 (126).

The highly oleaginous nature of rhodococci is exemplified by RHA1 and *Rhodococcus opacus* PD630 (PD630 hereafter), which accumulate up to 70% of their cellular dry weight (CDW) as neutral lipids under conditions of nitrogen limitation and other stress (129-131). These neutral lipids are primarily triacylglycerides (TAGs) stored in lipid droplets (LDs) within the cytoplasm (137) and have considerable potential as sustainable alternatives to oleochemicals currently derived from petroleum or palm oil (138-140). As described in Section 1.4 below, much work has been done to understand the biology of rhodococcal lipid accumulation. However, there have been few attempts to engineer rhodococcal metabolism to take advantage of this remarkable potential.

1.2.2 Phylogeny

The phylogeny of the *Rhodococcus* genus has been the subject of much debate (141-144). However, an extensive analysis based on 400 broadly conserved genes determined that the *Rhodococcus* genus is polyphyletic as currently defined, and should be consolidated into a monophyletic grouping by classify *R. equi* within the *Prescottella* genus (142). Despite the debate on the overall phylogeny of the genus, seven distinct phylogenetic groupings have consistently been described (141, 142). Notable species of five of these clades are: *R. erythropolis*, studied for its ability to desulfurize petroleum (145); *R. rhodochrous*, used as a biocatalyst for the production of acrylamide (146); *R. fascians*, a group of phytopathogens that causes leafy gall disease (147); *R. equi*, an intracellular pathogen that causes disease in

domesticated animals and immunocompromised humans (148); and PD630 (149) and RHA1 (129), two closely related oleaginous strains.

1.2.3 Biocatalytic potential and state of genetic tools

Industrial interest in rhodococci has traditionally focused on their ability to catabolize and transform a wide range of compounds. Beginning in 1985, *Rhodococcus sp*. N-774 was used industrially to produce acrylamide through the biotransformation of acrylonitrile (146). This success led to research that identified *R. rhodochrous* J1 as a superior biocatalyst; which is still used to produce more than 30,000 tonnes of acrylamide annually (150). Rhodococci have also been investigated as platforms for the biotransformation and production of high-value steroids (132), even though this process has yet to be implemented on the industrial scale (151). Due to the difficulties in manipulating rhodococci, biotransformation research has focused on bioprocess development and strain selection to achieve greater biocatalyst efficiencies. In the future, advanced genetic tools and well-characterized promoters will allow for the design of greatly improved rhodococcal biocatalysts.

Rhodococcal physiology offers significant advantages to industrial biocatalysts. Rhodococci can utilize a wide range of low-cost growth substrates that can decrease bioprocess costs. The mycolic acid-containing membrane of rhodococci provides a robust barrier that can protect biocatalysts from the harsh-conditions found in industrial bioprocesses. Finally, the large genomes of rhodococci contain significant amounts of untapped genetic potential, both for the transformation of substrates and for the biosynthesis of secondary metabolites or oleochemicals. Indeed, there is considerable interest in harnessing rhodococci to produce neutral lipids for

biofuels (138-140). However, the poor economics of biodiesel currently prevents the development and adoption of industrial-scale processes (152, 153). An alternate approach would be to harness the biosynthetic potential of rhodococci to produce higher-value lipids.

Rhodococcal genetic tools are in their infancy. The first useful *Rhodococcus-E. coli* shuttle vector was created in 1988 (154) and was followed by a series of similar vectors in the 90s (155, 156). More recent genetic tools include: Kan^R-*sacB* cassettes for unmarked deletions (71); protein expression vectors, such as the pTip plasmids (157); and integrative vectors based on site-specific phage recombinases (158, 159). While basic genetic tools have been available, only recently has interest in the ability of rhodococci to accumulate neutral lipids and catabolize lignin-derived aromatics created interest in the development of advanced tools and better-characterized promoters. These tools will allow for rapid iterations of design-build-test–learn cycles that will drive the advancement of rhodococcal biocatalysts.

1.3 Bacterial carbon storage

An important characteristic of bacteria is the ability to survive rapidly shifting, often stressful, environmental conditions. To this end, many bacteria accumulate carbon stores as energy reservoirs to survive periods of environmental or nutritional stress, such as nitrogen limitation. Carbon can be stored in multiple forms, such as glycogen, polyhydroxyalkanoates (PHAs), TAGs, and wax esters (WEs) (129). Interestingly, many of these carbon storage compounds are industrially useful, making bacteria an attractive source of these molecules.

1.3.1 PHAs

PHAs are polyesters comprising repeating hydroxyalkanoates units. In bacteria, PHAs primarily consist of 3-hydroxybutyrate or mixtures of 3-hydroxybutyrate and 3-hydroxyvalerate, and are stored in the cytoplasm within protein-coated inclusion bodies (160). PHAs are assembled from hydroxyalkanoate CoA-thioesters by PHA synthases, and liberated through hydrolysis by PHA depolymerases. 3-Hydroxybutyryl-CoA and 3-hydroxyvaleryl-CoA are synthesized step-wise through (a) the condensation of acetyl-CoA or propionyl-CoA, respectively, with acetyl-CoA, catalyzed by a β-ketothiolase, and (b) a subsequent reduction, catalyzed by 3-hydroxyacyl-CoA dehydrogenase (Figure 1.4) (161).

RHA1 has three clusters of genes predicted to encode PHA synthases and depolymerases (129). However, PHAs represent only a minor form of carbon storage under nitrogen-limited growth, accumulating 2 to 8 percent of CDW (129). In specialized bacteria, such as *Cupriavidus necator* (formerly *Alcaligenes eutrophus*) (162) or *Bacillus megaterium* (163), PHAs accumulation can reach greater than 80 percent of CDW during growth on unbalance nutrients (162). Due to the ability of bacteria to efficiently accumulated PHAs, there is considerable industrial interest in their use as biodegradable thermoplastics and components of advanced biomaterials (160, 164).

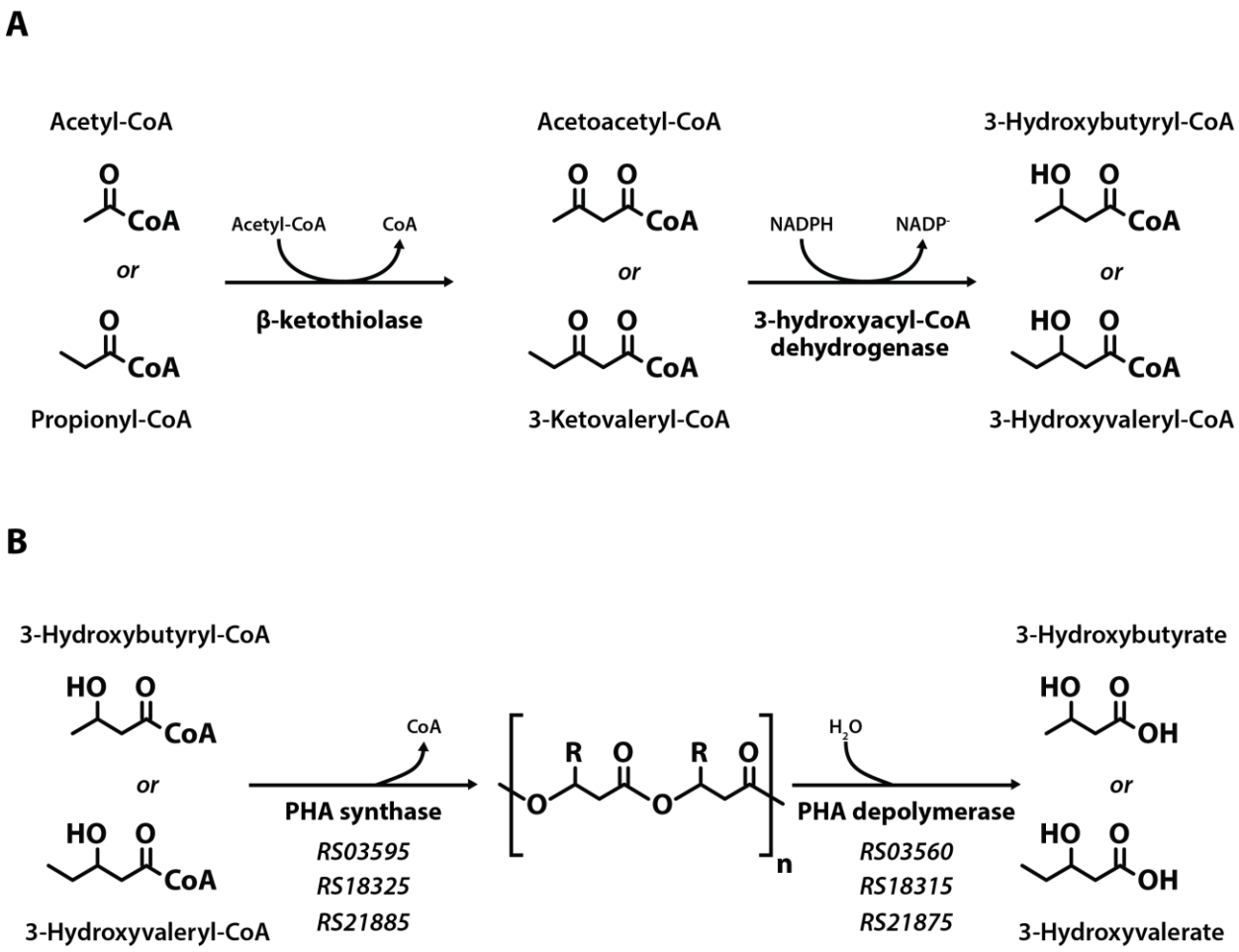

Figure 1.4 PHA synthesis in RHA1.

(A) Synthesis of 3-hydroxyacyl-CoA monomers. (B) Synthesis and hydrolysis of PHA1 polymer. RHA1 genes predicted to be involved in PHA synthesis are highlighted below their respective activities.

1.3.2 TAGs

TAGs are composed of three acyl-chains esterified to a glycerol backbone. In multicellular life, TAGs are predominantly stored within lipid bodies found within the cytosol of specialized storage cells. In prokaryotes, lipid bodies are found within the cytosol. In both cases, suites of enzymes regulate the flow of carbon into and out of these organelles (165, 166). TAG synthesis is a stepwise process in which acyl-CoA molecules are added to a glycerol backbone in reactions catalyzed by acyltransferases, releasing free CoA. Acyl-CoA substrates are primarily generated through lipid synthesis. The glycerol backbone is derived from 3-phosphoglycerol, generated through the NADPH-dependent reduction of dihydroxyacetone phosphate by glycerol-3-phosphate dehydrogenase. TAG biosynthesis in rhodococci is reviewed in greater detail in Section 1.4.

Microorganisms able to accumulate TAGs to greater than 20% of their CDW are defined as oleaginous (167). However, many natural and engineered oleaginous microorganisms reach TAG contents of greater than 60% of CDW (168, 169). Due to this remarkable biosynthetic capacity, there is considerable interest in using oleaginous microorganisms to produce sustainable neutral lipids to replace oleochemicals currently derived from palm oil and petroleum (138-140).

1.3.3 WEs

WEs are neutral lipids consisting of an esterified fatty alcohol and fatty acid. Found throughout the domains of life, WEs perform a variety of functional and structural roles (48, 170-173). In some oleaginous bacteria, WE are a form of carbon storage (174, 175); and are synthesized

through the esterification of a fatty alcohol with an acyl-CoA in a reaction catalyzed by a bifunctional WE synthase/acyl-CoA:diacylglycerol acyltransferase (WS/DGAT) (Figure 1.5) (176, 177). Acyl-CoA substrates for WE synthesis are predominantly provided through lipid synthesis. When not available exogenously or generated as intermediates in the degradation of alkanes, fatty alcohols are synthesized *de novo* from acyl-CoAs produced by fatty acid synthases (175, 178).

Fatty alcohols are produced through the reduction of activated fatty acids. In bacteria, the latter is usually a fatty acyl-CoA, and its reduction is accomplished by either a single bifunctional enzyme or consecutive reactions catalyzed by two enzymes (Figure 1.5). The two-enzyme pathway was first described in the WE-accumulating bacterium *Acinetobacter calcoaceticus* BD413. In this bacterium, an NADPH-dependant fatty acyl-CoA reductase (FAR), encoded by *acr1*, performs the two-electron reduction of the acyl-CoA to a fatty aldehyde. The second enzyme, responsible for reducing the fatty aldehyde to a fatty alcohol, has yet to be identified (179). *Marinobacter aquaeolei* VT8 accomplishes the same process using a FAR that catalyzes two successive two-electron reductions of the acyl-CoA to the corresponding fatty alcohol. *M. aquaeolei* VT8 contain two FAR-encoding genes with this activity, *maqu_2220* and *maqu_2507* (180, 181). *Mycobacterium tuberculosis*, which accumulates WEs to ~4% of total neutral lipids alongside TAGs during periods of stress (182, 183); contains both enzyme types: *fcr1* (*Rv3391*), a homolog of *maqu_2507*; and *fcr2* (*Rv1543*), a homolog of *acr1* (183). Maqu_2507 and Fcr1 contain two NADPH-binding domains. Interestingly, the C-terminal domain of these enzymes is homologous to the NADPH-binding domain of Acr1 and Fcr2.

Rhodococci produce WEs under lipid-accumulating conditions when supplied with exogenous fatty alcohols or hydrocarbons (129). Moreover, transient *de novo* production of WEs was reported in RHA1 by Barney *et al* (184). However, because this phenomenon has not been further investigated, the capacity of rhodococci to produce WEs *de novo* is unclear. Due to excellent physicochemical properties, including exceptional thermal and oxidative stability, WEs are valued for use in lubricants and cosmetics (185). Indeed, WEs were historically harvested from the head cavities of sperm whales. However, with the ban of whaling, new sources of low-cost WEs are needed. Harnessing the biosynthetic potential of rhodococci to produce WEs would create a sustainable and economic source of these high-value oleochemicals.

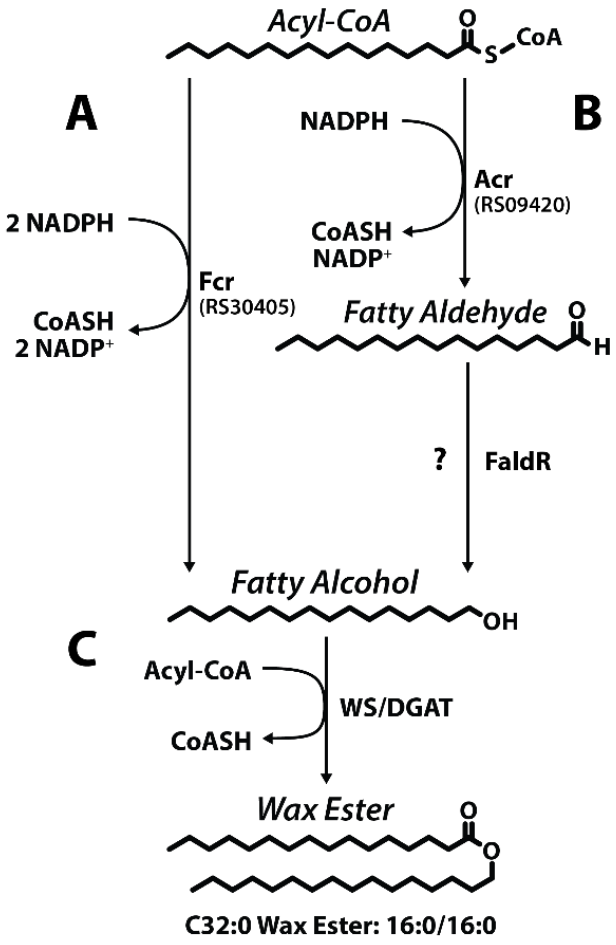

Figure 1.5 Bacterial WE biosynthesis pathways.

Fatty alcohols are generated through two successive reactions catalyzed by either a single two-domain enzyme (A) or two enzymes (B). Fatty alcohols and an acyl-CoA are esterified to form WEs (C). The enzymes are: Fcr, alcohol-forming fatty acyl-CoA reductase; Acr, aldehyde-forming fatty acyl-CoA reductase; FaldR, fatty aldehyde reductase; WS/DGAT, WE synthase/acyl-CoA:diacylglycerol acyltransferase. RS30405 and RS09420 are homologs identified in RHA1.

1.4 TAG biosynthesis in *Rhodococcus*

The biology of lipid accumulation in oleaginous rhodococci has been studied as a model for prokaryotic lipid accumulation. The insights gained from this research are critical to engineering of rhodococcal metabolism for the production of sustainable oleochemicals.

1.4.1 Fatty acid biosynthesis

Rhodococci and other Corynebacterineae have a unique fatty acid synthase (FAS) complex for the *de novo* synthesis of fatty acids (125, 186, 187). In *E. coli* and most bacteria, fatty acid biosynthesis occurs at a FASII complex, a loosely associated complex of seven proteins that synthesize fatty acids for membrane biogenesis (188). However, in Corynebacterineae, fatty acid synthesis takes place at a FASI complex. FASI complexes are distinct from FASII as they comprise a single large polypeptide containing all the machinery required for the elongation of an acyl-chain. Remarkably, they are reminiscent of the FASI complexes found in fungi and animals (186). In rhodococci, the FASI polypeptide is over 3100 amino acid residues in length, and is composed of six enzymatic domains and one non-enzymatic domain (Figure 1.6). From N- to C-terminus, these domains are: acetyl transferase (AT), enoyl reductase (ER), dehydratase (DH), malonyl palmityl transferase (MPT), acyl carrier protein (ACP), keto reductase (KR), and keto synthase (KS). In the cell, FASI complexes are arranged in large homohexamers. Interestingly, fatty acid synthesis by FASI is considered to be more efficient than that of FASII (188), which likely contributes to the lipid-synthesizing ability of rhodococci. Furthermore, in *Rhodococcus*, the end product of FASI-dependent lipid synthesis are acyl-CoAs, which can be fed directly into neutral lipid synthesis, rather than acyl-ACPs produced in *E. coli*. Finally,

rhodococci are relatively unique even among Corynebacterineae, as they routinely synthesize odd-chain lipids through their FASI complex during growth. These many unique features have interesting implication for the use of rhodococci as biocatalysts in the production of sustainable oleochemicals.

The first committed step of *de novo* lipid biosynthesis is the formation of malonyl-CoA through the ATP-dependant carboxylation of acetyl-CoA, catalyzed by acetyl-CoA carboxylase (ACC) (Figure 1.6) (131, 186). Malonyl-CoA is the common extender unit, used by the FAS complex to add two-carbon atom to a growing acyl chain. Fatty acid synthesis is initiated at the FASI complex by the acyl-transferase activity of the AT domain. For lipids of even and odd chain lengths, the AT domain transfers acetyl-CoA, or propionyl-CoA, respectively, to the ACP domain (187). This initial acyl-chain is then extended by the FASI complex through sequential rounds of elongation. In brief, the extender unit, malonyl-CoA, is transacylated to the FAS complex by the action of MPT. The FAS bound malonyl moiety in then transferred to the enzyme bound acyl-ACP in a decarboxylating condensation reaction, catalyzed by the KS domain, forming a 3-ketoacyl-ACP which has been extended by 2 carbon atoms. The 3-ketoacyl intermediate then undergoes reduction to a 3-hydroxyacyl-ACP, catalyzed by the NADPH-dependant KR domain. The 3-hydroxyacyl intermediate is dehydrated by the DH domain to form 2,3-*trans*-enoyl-ACP. Finally, the enzyme bound enoate is reduced back to an acyl-chain, catalyzed by the NADH-dependant ER domain. Overall, each addition of two carbon atoms consumes a molecule each of acetyl-CoA, ATP, NADPH and NADH. Sequential cycles of elongation continue until the acyl-ACP reaches a length between 14 and 18 carbon atoms (125, 131). At termination, the MPT domain of FASI transfers the acyl-chain to a molecule of free

CoA (187), resulting in the acyl-CoA that is used for membrane biogenesis and the synthesis of neutral storage lipids.

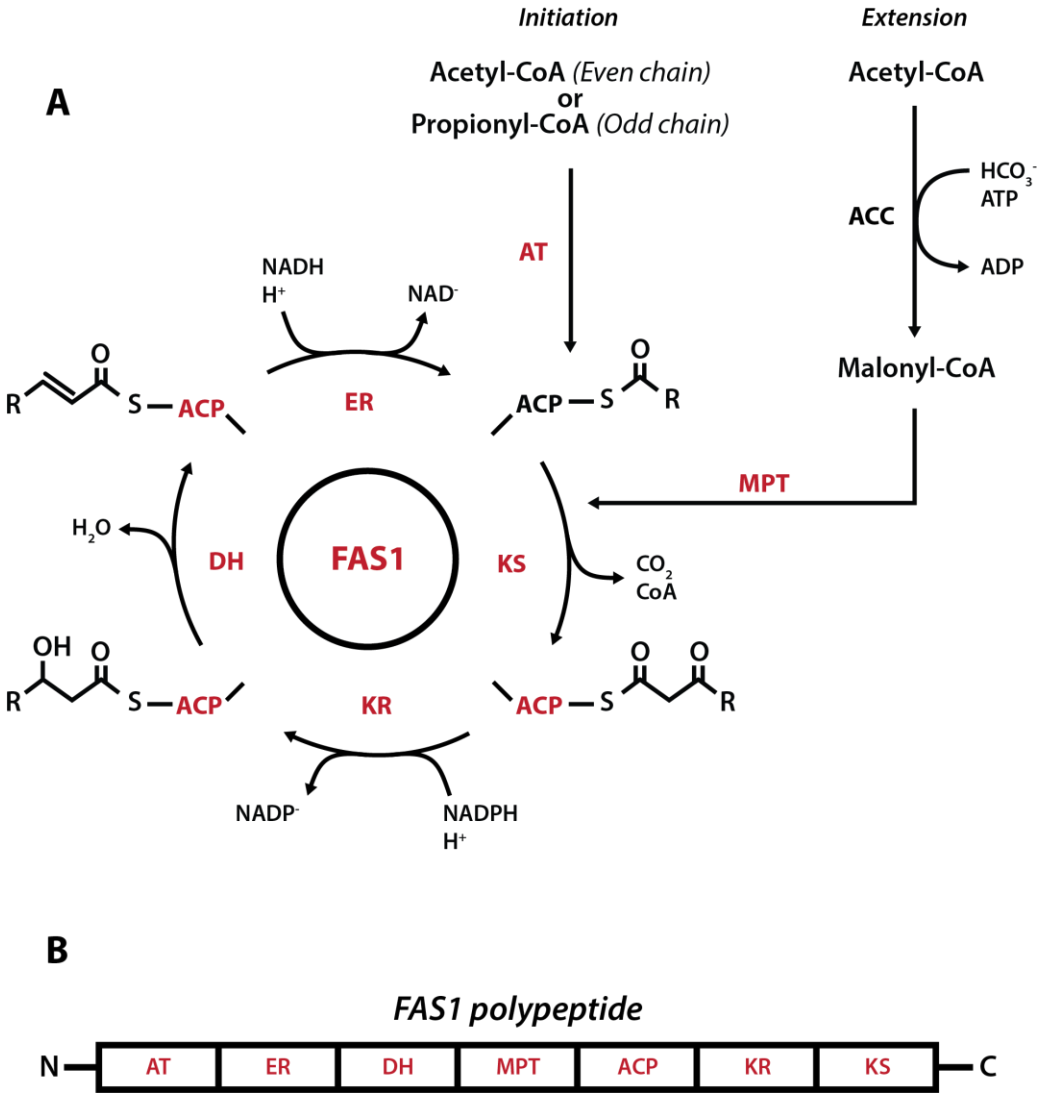

Figure 1.6 Fatty acid synthesis at the FAS1 complex.

(A) Elongation and initiation during fatty acid synthesis and (B) domain structure of the FAS1 polypeptide. Enzymatic domains of FAS1 are highlighted in red: AT, acetyl transferase; ER, enoyl reductase; DH, dehydratase; MPT, malonyl palmityl transferase; ACP, acyl carrier protein; KR, keto reductase; and KS, keto synthase. ACC, acetyl-CoA carboxylase.

1.4.2 TAG biosynthesis

In *Rhodococcus*, TAGs and phospholipids are thought to be synthesized through the Kennedy pathway (Figure 1.7) (131, 189). The Kennedy pathway involves two sequential acylations of glycerol-3-phosphate with acyl-CoA to produce phosphatidic acid (PA), catalyzed by glycerol-3-phosphate *O*-acyltransferase (GPAT) and 1-acylglycerol–3-phosphate *O*-acyltransferase (AGPAT). PA represents the branching point in the production of membrane phospholipids or TAGs. To create phospholipids, the phospho-headgroup is modified to create the range of membrane lipids. To create TAGs, PA is dephosporylated in a reaction proposed to be catalyzed by a type 2 phosphatidic acid phosphatase (PAP2) (182) to produce diacylglycerol (DAG), which is then acylated with acyl-CoA by a WS/DGAT, to produce TAG. While the Kennedy pathway has been well characterized in other organisms, in rhodococci the occurrence of multiple homologs of Kennedy pathway enzymes complicates the definitive characterization of this pathway.

Enzymes of the Kennedy pathway are highly redundant in rhodococci. For example, the genomes of PD630 and RHA1 contain seventeen and sixteen *atf* genes, respectively, that are predicted to encode WS/DGATs (125, 129, 190). Although some of these homologs have been genetically and biochemically characterized (131, 165, 190, 191), the precise roles of the different WS/DGATs in WE and TAG biosynthesis remains largely unknown. Furthermore, in RHA1 alone there exists: eight AGPAT homologs; and seven putative PA phosphatases: four PAP2s and three HAD-type hydrolases. Interestingly, only one GPAT can be found within the genome of RHA1.

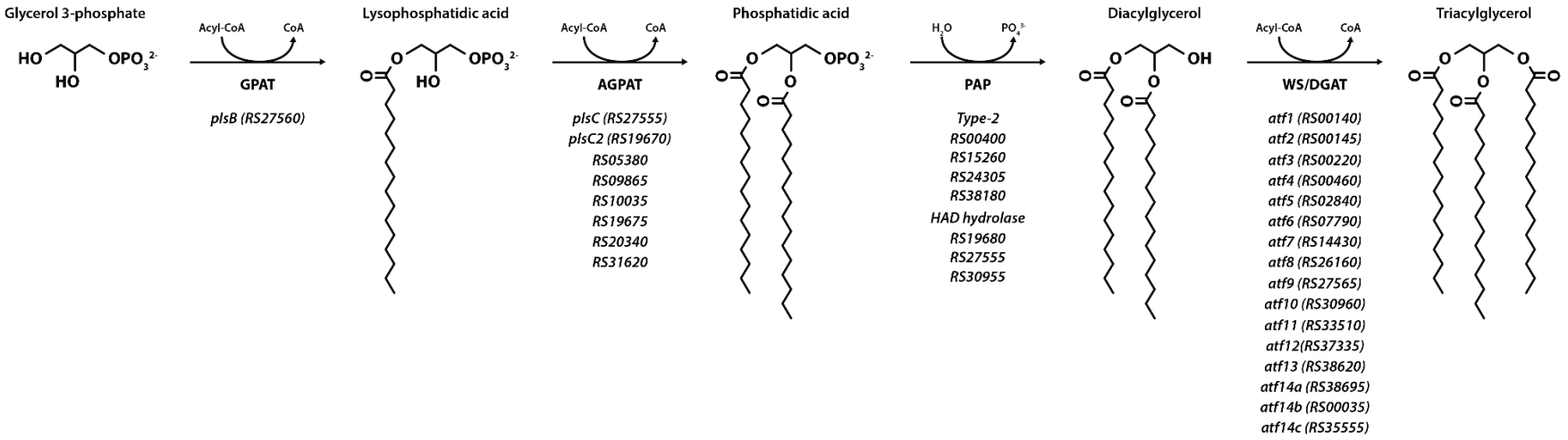

Figure 1.7 The Kennedy pathway in RHA1.

RHA1 genes predicted to encode enzymatic steps in TAG synthesis are highlighted beneath their respective activity. GPAT, glycerol-3-phosphate acyl transferase; AGPAT, acylglycerol-3-phosphate acyl transferase; PAP, phosphatidic acid phosphatase; DGAT, diacylglycerol acyl transferase.

This multiplicity of enzymes and the lack of biochemical or molecular genetic characterization has complicated functional assignment of the TAG biosynthetic enzymes. Indeed, deletions of the single GPAT (*plsB*) in RHA1 was non-lethal, which is surprising as this gene should be essential for membrane biogenesis (192). Furthermore, the predicted role of the PAP2s in lipid accumulation could not be confirmed in transcriptomic and genetic studies of RHA1, which prompted the suggestion that HAD-hydrolases, encoded in operons together with acyltransferases, may function as phosphatidic acid phosphatases (131). However, a triple deletion mutant of the three genes showed no obvious defect to TAG accumulation (Round & Eltis, unpublished data).

1.4.3 The lipid droplet

In *Rhodococcus*, TAGs are stored in intracellular LDs (106) located within the cytoplasm. Like eukaryotes, these LDs are composed of a hydrophobic core of TAGs surrounded by a phospholipid monolayer (193). In eukaryotes, LDs are bound by proteins such as oleosins and perilipins that play roles in the biogenesis and structure of LDs (166, 194). In *Rhodococcus*, proteomic studies have revealed large numbers of proteins that are associated with LDs, including: dynamin-, SNARE-, and apolipoprotein-like proteins putatively involved in biogenesis and structure (165, 195). In RHA1, Ro02104 (herein MLDS), an apolipoprotein homolog, was identified as a major constituents of the LD proteome. Gene deletion studies subsequently showed that MLDS is important in LD maturation and stability (195). A homolog in PD630, LPD06283 plays a similar role (165). Separately, *in vivo* and *in vitro* work identified a

heparin-binding hemagglutinin homolog (53) in PD630 that is involved in the assembly and maturation of LDs (196). The number of metabolic enzymes associated with the LD suggests that they constitute important metabolic centers for rhodococci (165, 195), facilitating the shuffling of lipids between utilization and storage, allowing the bacterium to sequester intracellular energy reserves as needed.

The exact mechanisms of LD formation is unknown. Using time-course microscopy, Wältermann et al posited that lipid body formation begins on the cytoplasmic face of the membrane with the formation of lipid-prebodies, that are eventually remodeled into discrete LDs that mature in the cytoplasm (193). However, dynamin- and SNARE-like proteins were identified on rhodococcal LDs (165), leading Yong et al to suggest that these proteins may aid in the budding of LDs from the cell membrane as they do in other organisms (197, 198).

Beyond functioning as a reservoir for energy and carbon, LDs bind DNA, protecting it from environmental insults. MLDS contains a C-terminal DNA binding domain that mediates interaction between LDs and genomic DNA. This interaction acts to protect the DNA, increasing the bacterium's resistance to DNA damage from nutrient or UV stress (199). LDs can even alter DNA transcription through regulatory proteins and transcription factors bound to them (165, 195). This is exemplified by RHA1_ro02105 (MLDSR) which was found to both positively and negatively regulate the production of MLDS and in a manner controlled by the presence of LDs (199). Overall, LDs are central to the growth and survival of rhodococci.

1.5 Creating a rhodococcal biocatalyst for the production of oleochemicals

Rhodococci have an established history of industrial use, but genetic engineering of genus members has lagged behind other industrial microorganisms. As the limitations of current model organisms are realized, bacteria such as *Corynebacterium glutamicum* and *Pseudomonas putida* are being established as next generation industrial biocatalysts (117). Despite innate advantages offered by its biology, *Rhodococcus* has not garnered the same attention in either academia or industry.

The overall objectives of this thesis are to characterize WE biosynthesis in *Rhodococcus* and to explore the genus's potential as a biocatalyst for the production of these high-value oleochemicals. These objectives were pursued through three specific aims that focused on production of WEs in RHA1: (1) to identify key WE biosynthetic enzymes; (2) to expand the genetic tools available in rhodococci; and (3) to apply these genetic tools to develop a rhodococcal biocatalyst for the production of high-value WEs.

In Section 3.1, I establish the ability of WT RHA1 to produce WEs, and identify key enzymes involved in WE accumulation. Expanding on the observations of Barney *et al.* (184), WE accumulation in RHA1 was investigated under different growth conditions. A fatty acyl-CoA reductase (FcrA) encoded by the RHA1 genome was identified, purified, and characterized with respect to its ability to transform various substrates. Finally, a deletion mutant and an FcrA overproduction strain were generated to examine the role of this fatty acyl-CoA reductase in WE synthesis.

With the ability of RHA1 to produce WEs established, in Section 3.2, I expanded the genetic tools available in rhodococci. I created pSYN, a modular integrative-vector, and employed this vector to identify and characterize P_{10}, a strong constitutive promoter active in *Rhodococcus*. To create promoters suited for microbial engineering, various strength minimal promoters were created from P_{10}. Finally, the utility of pSYN for engineering rhodococcal biocatalysts was demonstrated. RHA1 was transformed with pSYN to stably express a single copy of *fcrA* under the control of different strength constitutive promoters and strains were examined for the ability to accumulate WEs.

In Section 3.3, I characterized the ability of WSs to modulate WE accumulation, to understand and improve WE accumulation in the rhodococcal biocatalyst. I used gene deletions to investigate the role of the highly redundant rhodococcal *atf* genes in WE accumulation. Due to challenges in identifying a rhodococcal WS, pSYN-*fcrA* was employed to screen characterized WSs for the ability to increase WE accumulation, identifying *ws2* as an effective WS in RHA1. To generate strains suitable for industrial applications, cassettes for the co-expression of chromosomally integrated *fcrA* and *ws2* were created and transformed into RHA1. Resulting strains were characterized for the ability to produce WEs.

Overall, this study provides insight into the biosynthesis of WEs in rhodococci and provides a suite of tools to develop the biocatalytic potential of rhodococci, particularly for the production of high-value oleochemicals. In accelerating the engineering of rhodococcal biocatalysts for WE production, this work contributes to the development of novel bioprocesses for an important

class of oleochemicals that may ultimately allow us to phase out their unsustainable production from sources such as petroleum and palm oil.

Chapter 2: Material and Methods

2.1 Reagents

Enzymes for cloning were purchased from New England Biolabs unless otherwise noted. Primers were ordered from Integrated DNA Technologies. Chemicals were of at least reagent grade unless otherwise noted. Where indicated, specialty WEs were purchased from Nu-Chek Prep. Buffers were prepared using water purified on a Barnstead NANOpure UV apparatus to a resistivity of greater than 17 MΩcm.

2.2 Strains and culture conditions

Table 2.1 Bacterial strains used in this study.

Strains	Use	Reference
***Escherichia coli* strains**		
E. coli DH5α	Propagation of DNA	n/a
E. coli S17.1	Conjugation of pK18-derived plasmids into RHA1	n/a
E. coli NEB® 10-beta	Cloning pMiniT plasmids	(New England Biolabs)
***Rhodococcus* strains**		
R. jostii RHA1	Wild-type, protein expression, WE accumulation	(126)
RHA1 Δ*fcrA*	The role of *fcrA* in WE accumulation	This study
RHA1 Δ*atf8*	Role of RHA1 WS/DGATs in WE accumulation	(131)
RHA1 Δ*atf3*		(Diaz, Eltis *et al*., unpublished)
RHA1 Δ*atf6*		
RHA1 Δ*atf9*		
RHA1 Δ*atf10*		
RHA1 Δ*atf8atf10*		
RHA1 Δ*atf6 atf9*		
RHA1:T1/M6		This study

RHA1:T1/T1	RHA1 strains carrying *fcrA* and *ws2* co-expression cassettes driven by different strength promoters. (e.g., T1/T2 designates the strain in which: *fcrA* and *ws2* expression are driven by P_{T1} and P_{T2}, respectively)	
RHA1:T1/T2		
RHA1:T2/M6		
RHA1:T2/T1		
RHA1:T2/T2		

2.2.1 Culture conditions

E. coli strains were grown in LB broth at 37 °C, 200 rpm. RHA1 was grown at 30 °C while shaking at 200 rpm. For protein production and promoter characterization, RHA1 was grown in LB. For lipid production, RHA1 was grown in M9 minimal medium supplemented with trace elements, thiamin, and 4 g/L glucose as growth substrate (200, 201). In carbon-limited (C^-) media, the M9 medium contained 1 g/L ammonium chloride. Nitrogen-limiting (N^-) media, contained 0.05 g/L ammonium chloride, as previously described (131). For promoter characterization on different carbon sources, RHA1 was also grown in C^- M9 minimal medium with 20 mM benzoate or 10% APL as growth substrate. To test the ability of RHA1 *atf* mutants to accumulate WEs when grown on fatty alcohols, cells were grown in N^- M9 minimal medium, with 0.4% (w/v) hexadecanol as growth substrate, solubilized in 2% (v/v) DMSO.

2.2.2 Culture media supplements

For solid medium, LB broth was supplemented with Bacto agar (1.5% [w/v]; Difco). Media were further supplemented with 100 μg/mL ampicillin (*E. coli* carrying pTip-derived plasmids), 50 μg/mL kanamycin (*E. coli* carrying pK18-derived plasmids), 34 μg/mL chloramphenicol (RHA1 carrying pTip-derived plasmids), 10 μg/mL neomycin (RHA1 carrying pK18-derived plasmids),

or 30 μg/mL apramycin (*E. coli* and RHA1 carrying pSET152-derived or pSYN-derived plasmids) as appropriate.

2.3 DNA manipulation, plasmid construction, and gene deletion

DNA was isolated, manipulated, and analyzed using standard protocols (201). *E. coli* and RHA1 were transformed with DNA by electroporation using a MicroPulser with GenePulser cuvettes (Bio-Rad). The nucleotide sequence of key constructs was verified by sequencing (GENEWIZ).

Table 2.2 Plasmids used in this study

Plasmid	Description / Use	Reference
pTipQC2	*Rhodococcus* expression vector	(157)
pTip-*fcrA*-His_6	FrcA overproduction for purification and characterization	This study
pTip-*fcrA*	FrcA overproduction for WE accumulation	
pK18mobsacB-Δ*fcrA*	Kan^R-*sacB* suicide vector for deletion of *fcrA*	
pTip-*mCherry*	Cloning intermediate in the production of pSYN-*mCherry*	
pSET152	Integrative vector	(158, 202)
pSYN-*mCherry*	Modular integrative vector. Promotor-less backbone carrying mCherry. Promoter characterization	This study
pSYN-$P_{\#}$-*mCherry*	pSYN-*mCherry* variants carrying promoter regions. Promoter characterization	
pSYN-$P_{M\#}$-*mCherry*	pSYN-*mCherry* variants carrying minimal P10 promoters. Promoter characterization	
pSYN-P_{nit}-*mCherry*	pSYN-*mCherry* vector series (with various promoters). Promoter characterization	This study
pSYN-P_{M6}-*mCherry*		
pSYN-P_{T1}-*mCherry*		
pSYN-P_{T2}-*mCherry*		
pSYN-P_{nit}-*fcrA*	pSYN-*fcrA* vector series (with various promoters). WE accumulation	This study
pSYN-P_{M6}-*fcrA*		
pSYN-P_{T1}-*fcrA*		
pSYN-P_{T2}-*fcrA*		
pUC57-*ws1*	Synthesized WSs. Cloning intermediates	GENEWIZ
pUC57-*ws2*		

pUC57-*atfA*		
pUC57-*aftA2*		
pTip-*ws1*	Overproduction of WSs to promote WE accumulation	This study
pTip-*ws2*		
pTip-*atfA*		
pTip-*aftA2*		
pSYN-P_{M6}-*ws2*	pSYN-*ws2* series (with various promoters). Cloning intermediates for cassette assembly	This study
pSYN-P_{T1}-*ws2*		
pSYN-P_{T2}-*ws2*		
pLB	Integrative recipient vector for *fcrA* and *ws2* co-expression cassettes	This study
pMiniT	Cloning of TSS junction amplicons	(NEB)

Table 2.3 Primers used in this study

Name	Use	Sequence (5' to 3')
Cloning Primers		
fcrA-His$_6$_fwd	Generation of pTip-*fcrA*-His_6	TTTAAGAAGGAGATATACATATGGCCACCTACCTCGTCACCG
fcrA-His$_6$_rev		ATGGTGATGGTGATGCTCGAGGCTGCTGCCCTGGAAATACAAGTTTTCTCTGCCGCTGCTCCAGTGGGTGCCGGGCAC
*fcrA*_fwd	Generation of pTip-*fcrA*	TTTAAGAAGGAGATATACATATGGCCACCTACCTCGTCACC
*fcrA*_rev		GTGCCGGTGGGTCGACTAGTCACCAGTGGGTGCCGGG
Δ*fcrA*-up_fwd	Generation of pK18mobsacB-Δ*fcrA*	TGAGGTGCGAGGACGTGGATCTCGGCTG
Δ*fcrA*-up_rev		CGGGTACCGAGCTCGAATTCGTCTCCGCGCCATCACGC
Δ*fcrA*-down_fwd		GCTATGACATGATTACGAATTCGGCCGGGGTGCGGGTCA
Δ*fcrA*-down_rev		ACGTCCTCGCACCTCAGCACACACCGGAACCC
*mCherry*_fwd	Generation of pTip-*mCherry*	CTTTAAGAAGGAGATATACATATGGTGAGCAAGGGCGAG
*mCherry*_rev		CACGGGTGCCGGTGGGTCGACTAGTCACTTGTACAGCTCGTCCATG
MOD-MCS_fwd	Generation of pSYN-*mCherry*	GGCTGCAGGTCGACTCTAGAGCGGCCGCATCGATCATTGATATCGTCTAGAAATAATTTTGTTTAACTTTAAG
MOD-MCS_rev		GCGTTGGCCGATTCATTAATACTAGAGTCCCGCTGAGG
UL1-*frcA*-UL2_fwd	Amplification of *fcrA* cassette with universal linkers UL1 and UL2	CATTACTCGCATCCATTCTCAGGCTGTCTCGTCTCGTCTCGGCGCGCCGTTTTCCCAGTCACGACGTT
UL1-*frcA*-UL2_rev		GCTTGGATTCTGCGTTTGTTTCCGTCTACGAACTCCCAGCGAGTCAGTGAGCGAGGAAGC
UL2-*ws2*-ULX_fwd		GCTGGGAGTTCGTAGACGGAAACAAACGCAGAATCCAAGCGTTTTCCCAGTCACGACGTT

UL2-*ws2*-ULX_rev	Amplification of *ws2* cassette with universal linkers UL2 and ULX	GGTGGAAGGGCTCGGAGTTGTGGTAATCTATGTA TCCTGGTTAATTAAGAGTCAGTGAGCGAGGAAGC
Promoter amplification primers		
P_{nit}_fwd	Amplification of P_{nit} promoter	GGTCGACTCTAGAGCGGCCGCTCACTCTTCTGCT CGGCC
P_{nit}_rev		AACAAAATTATTTCTAGACGATATCGCCGTCCAT TATACCTCCTCACGTGACGTGAG
P_{T1}_fwd	Amplification of P_{T1} promoter	GGTCGACTCTAGAGCGGCCGCACCGCTCTGGTCA GCGAC
P_{T1}_rev		AACAAAATTATTTCTAGACGATATCCTTGCGACG AAAGGAACTC
P_{T2}_fwd	Amplification of P_{T2} promoter	GGTCGACTCTAGAGCGGCCGCACCGCTCTGGTCA GCGAC
P_{T2}_rev		AACAAAATTATTTCTAGACGATATCGAAAGGAAC TCTACAACAGCGAC
P_{M200}_fwd	Amplification of P_{M200} promoter	CTGCAGGTCGACTCTAGAGCGGCCGCCTCCTCCT GGCGAGCCGATC
P_{M200}_rev		ACAAAATTATTTCTAGACGATATCGGCAGTTCAT CCTCTCCCGC
Promoter region primers		
P1_fwd	Amplification of P_1 promoter region	GGTCGACTCTAGAGCGGCCGCGAGTCCGAGGAA GGTCGAC
P1_rev		AACAAAATTATTTCTAGACGATATCTTCGCTCGC CTCGACGC
P2_fwd	Amplification of P_2 promoter region	GGTCGACTCTAGAGCGGCCGCGTAGGCGGGGGT CGATCC
P2_rev		AACAAAATTATTTCTAGACGATATCTGGTGACCA TCAACCCTCC
P3_fwd	Amplification of P_3 promoter region	GGTCGACTCTAGAGCGGCCGCTACGTGCGGGCGT TCC
P3_rev		AACAAAATTATTTCTAGACGATATCGCTTCGGCG CCCGGGGA
P4_fwd	Amplification of P_4 promoter region	GGTCGACTCTAGAGCGGCCGCATGCCGATACTCC CTGAATATCGATCC
P4_rev		AACAAAATTATTTCTAGACGATATCGGGCCGGAG CGGGTTTCA
P5_fwd	Amplification of P_5 promoter region	GGTCGACTCTAGAGCGGCCGCCCGTCCGAGTTCG CGTA
P5_rev		AACAAAATTATTTCTAGACGATATCGTTGCGAAT CTGGTCGTG
P6_fwd	Amplification of P_6 promoter region	GGTCGACTCTAGAGCGGCCGCACCAGATAGCCG GTCCC
P6_rev		AACAAAATTATTTCTAGACGATATCTGCCATTGC CCATGACCA
P7_fwd	Amplification of P_7 promoter region	GGTCGACTCTAGAGCGGCCGCTTCCTTCGACCAG TTCGG
P7_rev		AACAAAATTATTTCTAGACGATATCGATCGGGAT CGACTTCCC
P8_fwd	Amplification of P_8 promoter region	GGTCGACTCTAGAGCGGCCGCACTGATGTCTCCG GGCT
P8_rev		AACAAAATTATTTCTAGACGATATCTCGGAGTAG TGAACGAAG
P9_fwd	Amplification of P_9 promoter region	GGTCGACTCTAGAGCGGCCGCGAGCGCAGATCA ACGTCG
P9_rev		AACAAAATTATTTCTAGACGATATCGTCCCTTGA CGACGATCTC
P10_fwd	Amplification of P_{10} promoter region	CTGCAGGTCGACTCTAGAGCGGCCGCACCGCTCT GGTCAGCGAC
P10_rev		CAAAATTATTTCTAGACGATATCCGGAGCGGGTT TCACTAC

P11_fwd	Amplification of P_{11} promoter region	GGTCGACTCTAGAGCGGCCGCGTGTGTCCAGGACGTCGG
P11_rev		AACAAAATTATTTCTAGACGATATCGTTAACAACCGCCCTGCTC
P12_fwd	Amplification of P_{12} promoter region	GGTCGACTCTAGAGCGGCCGCTTCGGGCAGGGCCGTGCG
P12_rev		AACAAAATTATTTCTAGACGATATCGTCGAGCCGCAGATCCCATG
P13_fwd	Amplification of P_{13} promoter region	GGTCGACTCTAGAGCGGCCGCGGCGCTGTGCGAGAAGTAC
P13_rev		AACAAAATTATTTCTAGACGATATCACTCTTCGATATCGCGCC
P14_fwd	Amplification of P_{14} promoter region	GGTCGACTCTAGAGCGGCCGCCTCGACCAGCAGTCGC
P14_rev		AACAAAATTATTTCTAGACGATATCGTCGTCACGACCTTCCTGATC
P15_fwd	Amplification of P_{15} promoter region	GGTCGACTCTAGAGCGGCCGCTTGCCGTTGACCGCGGCG
P15_rev		AACAAAATTATTTCTAGACGATATCATTCCTTCTGCTCACCCTTGATGGTGC
P16_fwd	Amplification of P_{16} promoter region	GGTCGACTCTAGAGCGGCCGCGAGCTGCCGAGGGGGACG
P16_rev		AACAAAATTATTTCTAGACGATATCCGTGTCGGGAATGACCAG
P17_fwd	Amplification of P_{17} promoter region	GGTCGACTCTAGAGCGGCCGCTCGCGCTCGGCGGTGGC
P17_rev		AACAAAATTATTTCTAGACGATATCCTTGGGGCCCAACGTCACC
P18_fwd	Amplification of P_{18} promoter region	GGTCGACTCTAGAGCGGCCGCTGATGAACCACACCCCCG
P18_rev		AACAAAATTATTTCTAGACGATATCCACCGTCAGACCACGGTATTC
P19_fwd	Amplification of P_{19} promoter region	GGTCGACTCTAGAGCGGCCGCAAGCCGCCCGCAAGGCCG
P19_rev		AACAAAATTATTTCTAGACGATATCTGGTGATGGCCGCGGTCAG
P20_fwd	Amplification of P_{20} promoter region	GGTCGACTCTAGAGCGGCCGCTTCCGAGGTCGTCGATCAG
P20_rev		AACAAAATTATTTCTAGACGATATCGTGATGCTTGTCGTGATG
Minimal promoter primers		
PM1_fwd	Amplification of P_{M1} promoter	CTGCAGGTCGACTCTAGAGCGGCCGCACCGCTCTGGTCAGCGAC
PM1_rev		AACAAAATTATTTCTAGACGATATCTCGTCTTGCCTGCCCGG
PM2_fwd	Amplification of P_{M2} promoter	CTGCAGGTCGACTCTAGAGCGGCCGCACCGCTCTGGTCAGCGAC
PM2_rev		AACAAAATTATTTCTAGACGATATCACATCAACCCTTGCCC
PM3_fwd	Amplification of P_{M3} promoter	GGTCGACTCTAGAGCGGCCGCTGACACGTCCCCATCGTG
PM3_rev		CAAAATTATTTCTAGACGATATCCGGAGCGGGTTTCACTAC
PM4_fwd	Amplification of P_{M4} promoter	GGTCGACTCTAGAGCGGCCGCAACCCACTCGCCCCTGCC
PM4_rev		CAAAATTATTTCTAGACGATATCCGGAGCGGGTTTCACTAC
PM5_fwd	Amplification of P_{M5} promoter	GGTCGACTCTAGAGCGGCCGCTTTCGTCGCAAGGAAAGAG
PM5_rev		CAAAATTATTTCTAGACGATATCCGGAGCGGGTTTCACTAC

PM6_fwd	Amplification of P_{M6} promoter	CTGCAGGTCGACTCTAGAGCGGCCGCACCGCTCTGGTCAGCGAC
PM6_rev		AACAAAATTATTTCTAGACGATATCGGCAGTTCATCCTCTCCC
PM7_fwd	Amplification of P_{M7} promoter	CTGCAGGTCGACTCTAGAGCGGCCGCACCGCTCTGGTCAGCGAC
PM7_rev		AACAAAATTATTTCTAGACGATATCGAACTCTACAACAGCGACACCTC
PM8_fwd	Amplification of P_{M8} promoter	CTGCAGGTCGACTCTAGAGCGGCCGCACCGCTCTGGTCAGCGAC
PM8_rev		AACAAAATTATTTCTAGACGATATCTGGAGTCGGTTGACCAG
PM9_fwd	Amplification of P_{M9} promoter	CTGCAGGTCGACTCTAGAGCGGCCGCACCGCTCTGGTCAGCGAC
PM9_rev		AACAAAATTATTTCTAGACGATATCCGTCGACGTCGCCGGGT
ARF-TSS primers		
*mCherry*_RT	*mCherry* specific RT primer	Phosph-CGCCCTCGATCTCGAACT
*mCherry*_Inv1	Inverse PCR primers for TSS junction amplification	ATGGAGGGCTCCGTGAAC
*mCherry*_Inv2		GCAAAGGCTGGGACGTTAGTG
PCR screening / Sequencing primers		
pSYN_fwd	pSYN sequencing and screening primers	GTTTTCCCAGTCACGACGTT
pSYN_rev		GAGTCAGTGAGCGAGGAAGC
pLB_fwd	pLB sequencing and screening primers	GGCGATTAAGTTGGGTAACG
pLB_rev		AACCGTATTACCGCCTTTGA
pTip_fwd	pTip sequencing and screening primers	GCAGCGTGGACGGCG
pTip_rev		CACCGGCACCCGCAGCGA
pMiniT_fwd	pMiniT sequencing and screening primers	ACCTGCCAACCAAAGCGAGAAC
pMiniT_rev		TCAGGGTTATTGTCTCATGAGCG

2.3.1 Cloning of FcrA

To produce a C-terminal His_6-tag FcrA, RHA1_RS30405 was amplified from RHA1 genomic DNA using Phusion Polymerase™ and the *fcrA-His*$_6$ primer pair (Table 2.3). The resulting amplicon was inserted into pTip-QC2 linearized with Nde1 and Xho1 using Gibson Assembly to produce pTip-*fcrA*-His_6. Tagless FcrA was cloned as above using the *fcrA* primer pair to produce pTip-*fcrA*.

2.3.2 Deletion of *fcrA*

The Δ*fcrA* mutant was constructed using a *sacB* counter selection system (71). Two 500 bp flanking regions of RHA1_RS30405 were amplified from RHA1 genomic DNA using the upstream and the downstream primer pairs. The resulting amplicons were inserted into pK18mobsacB linearized with EcoR1 using Gibson Assembly, resulting in pK18mobsacB-Δ*fcrA*. Kanamycin-sensitive/sucrose-resistant colonies were screened using PCR and the gene deletion was confirmed by sequencing.

2.3.3 Construction of pSYN

A promoter-less pSYN containing the mCherry reporter was constructed. The mCherry gene was amplified from pMS689mCherry using the *mCherry* primer pair. The amplicon was inserted into Nde1/Spe1-linearized pTipQC2 using Gibson Assembly to yield pTip-*mCherry*. A modular expression cassette, including the RBS, reporter, and terminator, was then amplified from pTip-*mCherry* using the MOD-MCS primer pair. The amplicon was inserted into Not1/Ase1-linearized pSET152 using Gibson Assembly to yield pSYN-*mCherry*.

2.3.4 Cloning promoters into pSYN

The P_{nit} promoter was amplified from pTipQC2 using the P_{nit} primer pair. The amplicon was inserted into Not1/EcoRV-linearized pSYN-*mCherry* using Gibson Assembly, resulting in pSYN-P_{nit}-*mCherry*. Putative promoter regions were amplified from RHA1 genomic DNA using primer pairs listed in Table 2.3 and assembled into pSYN-*mCherry* as described to generate the pSYN-$P_{\#}$-*mCherry* series of plasmids. Minimal P_{10} promoters were amplified from pSYN-P_{10}-

mCherry using primer pairs listed in Table 2.3 and assembled into pSYN-*mCherry* as described to generate the pSYN-$P_{M\#}$-*mCherry* series of plasmids.

2.3.5 Subcloning *fcrA* into pSYN

To insert *fcrA* into pSYN vectors containing various promoters (P_{nit}, P_{M6}, P_{T1}, P_{T2}), pSYN-*mCherry* vectors were digested with Nde1/Spe1 to remove the *mCherry* gene. Similarly, pTip-*fcrA* was digested with Nde1/Spe1 to generate the subcloning fragment. Resulting fragment and linearized vectors were assembled using T4 ligase, resulting in the pSYN-*fcrA* plasmid series.

2.3.6 Subcloning synthesized WSs into pTip

WSs were codon-optimized using the COOL webserver (203) and synthesized (GENEWIZ). Sequences can be found in Appendix A. pUC57 plasmids containing synthesized WSs were digested with Nde1/Spe1 and ligated into Nde1/Spe1-linearized pTipQC2 as described above.

2.3.7 Subcloning *ws2* into pSYN

To insert *ws2* into pSYN vectors containing various promoters (P_{M6}, P_{T1}, P_{T2}), pTip-*ws2* first was digested with Nde1/Spe1 to generate the *ws2* fragment. Similar to above, pSYN-*mCherry* vectors were digested with Nde1/Spe1. Resulting fragment and linearized vectors were ligated as described.

2.3.8 Construction of pLB

The pLB recipient vector was designed by synthesizing a DNA fragment containing UL1 and ULX universal linker sequences (204), *asc1* and *pac1* restriction sites, and Gibson-Assembly overlaps corresponding to the pSET152 (Appendix A). This DNA fragments was cloned into Not1/Ase1-linearized pSET152 using Gibson Assembly to yield pLB.

2.3.9 Assembly of *fcrA* and *ws2* tandem co-expression cassettes

Fragments containing the *fcrA* expression cassette were amplified from pSYN-*fcrA* vectors containing various promoters (P_{M6}, P_{T1}, P_{T2}), using the UL1-*frcA*-UL2 primer pair containing UL1 and UL2 universal linker sequences. Fragments containing the *ws2* expression cassette were amplified from pSYN-*ws2* vectors containing various promoters (P_{M6}, P_{T1}, P_{T2}), using the UL2-*ws2*-ULX primer pair containing UL2 and ULX universal linker sequences. Resulting fragments were inserted into Asc1/Pac1-linearized pLB using Gibson Assembly to generate nine cassette variants.

2.3.10 Generation of RHA1 strains harboring tandem co-expression cassettes

Gibson Assembly reactions containing the assembled co-expression cassettes were dialyzed and transformed into RHA1 by electroporation. Resulting apramycin-resistant colonies were screened by PCR, and transformants containing cassettes were streaked to obtain isolated colonies on LB agar. A single colony for each candidate was inoculated into LB media and grown for 48 hours, resulting cultures were used to create freezer stocks, stored at -80 °C in 20% glycerol, and for isolation of genomic DNA. Genomic DNA was isolated as described (205).

Resulting DNA was used to sequence confirm the tandem co-expression cassettes had been assembled properly and were free of mutations.

2.4 Protein production and purification

2.4.1 FcrA

RHA1 freshly transformed with pTip-*fcrA* were grown overnight in LB. These cultures were used to inoculate 1 L fresh LB medium to an optical density at 600 nm (OD_{600}) of 0.05. Cultures were grown to an OD_{600} ~0.8, the expression of *fcrA* was induced with 10 µg/mL of thiostrepton, and cultures were incubated for a further 24 h. Cells were harvested by centrifugation and stored at -80 °C.

Cells from 2 L of culture were suspended in 40 mL of lysis buffer (50 mM Na-phosphate, pH 8.5, 500 mM NaCl, 2.5 mM imidazole) containing cOmplete Mini EDTA-Free protease inhibitors (Roche Diagnostics). The cell suspension was split between four 15 mL conical tubes each containing ~1 mL 0.1 mm zirconium/silica beads and ~1 mL 0.5 mm glass beads (BioSpec Products) and subjected to three rounds of bead-beating at 5-6 m/s using a FastPrep®-24 (MP Biomedicals) with 5 min on ice between rounds. The lysate was centrifuged (4000 × g for 5 min) to remove unbroken cells. The supernatant lysate was removed and stored on ice. The pellets were suspended in 5 mL lysis buffer and subjected to another three rounds of bead-beating. The supernatants were combined and further clarified by ultracentrifugation (40,000 × g for 60 min) and passage through a 0.22 µm filter.

The clarified lysate was incubated with 5 mL Ni Sepharose 6 fast flow resin (GE Healthcare Bio-Sciences) for 3 h. After incubation, the resin was poured into a column, then washed with 50 mL lysis buffer, 50 mL lysis buffer containing 50 mM imidazole, and 15 mL lysis buffer containing 75 mM imidazole. FcrA was eluted with 15 mL lysis buffer containing 250 mM imidazole. FcrA-containing fractions, as judged by SDS-PAGE, were pooled, exchanged into 50 mM Na-phosphate, pH 8.5, 500 mM NaCl, and concentrated to ~10 mg/mL using an Amicon Ultra-15 centrifugal filtration unit (Merck KGaA) equipped with a 30 kDa cut-off membrane. Protein was flash frozen as beads in liquid nitrogen and stored at -80 °C. Protein concentration was determined by Micro BCA (Thermo Fisher Scientific, Rockford, IL) and by absorbance at 280 nm.

2.4.2 WSs

RHA1 freshly transformed with pTip vectors containing WSs were grown overnight in LB. These cultures were used to inoculate 50 mL fresh LB medium to an OD_{600} of 0.05. Cultures were grown to an OD_{600} ~0.8, the expression of the WSs were induced with 10 µg/mL of thiostrepton, and cultures were incubated for a further 24 h. Cells were harvested by centrifugation and stored at -80 °C.

Cells pellets from 50 mL cultures were suspended in 1.5 mL of buffer (50 mM Na-phosphate, pH 7.5, 300 mM NaCl) and subjected to three rounds of bead-beating in 2mL screwcap tubes, as previously described. Resulting lysates were centrifuged (4000 × g for 5 min) to remove unbroken cells. Remaining lysate was removed and clarified by centrifugation (16,000 × g for 60 min). The soluble supernatant of the lysate (soluble fraction) was removed and stored on ice. The

remaining pellet was solubilized in buffer contain urea (50 mM Na-phosphate, pH 7.5, 300 mM NaCl, 8 M urea) and centrifuged (16,000 × g for 60 min). The solubilized supernatant (insoluble fraction) was removed and stored on ice. Presence of the expressed WSs in the soluble or insoluble fractions was assessed by SDS-PAGE.

2.4.3 Mass spectrometry of purified FrcA

Purified FcrA (~4 µg/mL in 5% acetonitrile, 0.1% formic Acid (v/v)) was injected onto a 5 mm C4 column connected to a Waters Xevo GS-2 QTof mass spectromter via a NanoAquity UPLC system operated at 20 µL/min. Samples were eluted in a 40 µL gradient of 5-100% acetonitrile at 20 µL/min. MS spectra were summed and deconvoluted using Waters' MaxEnt algorithm.

2.5 FcrA activity assays

2.5.1 Spectrophotometric assays

FcrA activity was evaluated using two spectrophotometric assays (181). Assays were performed at 25 °C in 1 mL 20 mM MOPS, 80 mM NaCl, pH 7.0 (I = 0.1 M) containing 5 µM acyl-CoA or 60 µM aldehyde, and 200 µM NADPH. Reactions were initiated by the addition of FcrA to a final concentration of 0.1 to 2 µM. In one assay, the oxidation of NADPH was followed at 340 nm (ε = 6.3 mM mM^{-1} cm^{-1} (206)). In the second assay, the reaction mixture also contained 0.1 mg/mL 5,5'-dithiobis-(2-nitrobenzoic acid) (DTNB), and the formation of NTB^{2-} was followed at 412 nm (ε = 14.15 mM^{-1} cm^{-1} for NTB^{2-} (207)). Reaction rates were calculated from progress curves using Cary WinUV Kinetics Application (Agilent). The pH-dependence of the reaction

was evaluated using the DTNB assay and a series of 20 mM Good's buffers (MES, MOPS, HEPPS, or TAPS), 80 mM NaCl (I = 0.1 M), pH 6 to 9.

2.5.2 *In vitro* fatty alcohol production

To analyze fatty alcohols produced *in vitro*, quenched reactions of 2 mL were extracted with 5 mL of 2:1 chloroform:methanol (v/v). The organic phase was collected, washed once with 1:1 H_2O:methanol, and three times with H_2O. The organic phase was removed and dried under nitrogen stream. The extract was suspended in pyridine and derivatized with tetramethylsilane for 1 h at 60 °C. Derivatized extracts were analyzed by gas chromatography-mass spectrometry (GC/MS) as described below.

2.6 Production of neutral lipids and WEs

Fresh media were inoculated to an OD_{600} of 0.1 using washed RHA1 cells harvested from cultures grown overnight in C^- media. For analyses of C^- cultures, cells were harvested during exponential growth, approximately 24 h after inoculation. For analyses of N^- cultures, cells were harvested after approximately 72 h (131). To induce nitric oxide (NO) stress, cells were grown in C^- media to an OD_{600} of 0.5-0.6 at which point SNP was added to the cultures to a concentration 1 mM at two-hour intervals for six hours. NO-stressed cells were harvested two hours after the final addition of SNP. For RHA1 transformed with pTip-*fcrA*, or empty pTipQC2, cultures were grown as above, except that when they reached an OD_{600} between 0.6-1.0, thiostrepton was added to 10 µg/mL. For RHA1 co-transformed with pSYN-P_{M6}-*fcrA* and pTip vectors containing

WSs, cultures were induced at an OD_{600} between 0.3-0.5. Cells were pelleted at 4,000 × *g* for 30 min at 4 °C, washed with distilled water, and stored at -80 °C.

2.7 Lipid extraction and thin layer chromatography (TLC)

Frozen cell pellets were lyophilized for 24 to 48 h using a FreeZone 2.5 liter benchtop freeze dryer (LABCONCO). Dried cells were suspended in water and sonicated to lyse cells. Myristyl myristate (Nu-Chek Prep) and/or ethyl myristate (Sigma) was added as a standard. In Section 3.1, total lipids were extracted from lysate using 2:1 chloroform:methanol with 1% acetic acid (208). The organic phase was collected, and dried using a rotary evaporator (Buchi) and/or nitrogen gas. Dried extracts were suspended in chloroform and stored at -20 °C. In Sections 3.2 and 3.3, total lipids were extracted MTBE/methanol/water (10:3:2.5, v/v/v) (209). Lipid extracts were analyzed using silica-TLC and a mobile phase of 90:6:1 v/v of hexane/diethyl ether/acetic acid. Lipids were visualized by staining with 10% cupric sulphate in 8% aqueous phosphoric acid (v/v) and charring for 5 min at 200°C.

2.8 Isolation, fractionation, and gravimetric quantification of neutral lipids

Neutral cellular lipids were purified using flash chromatography. Total lipid extracts were applied to a column of silica resin (10 mg lipids per 300 mg resin (210)) equilibrated with 5 column volumes (CV) of chloroform. Neutral lipids eluted with 5 CV of chloroform, were dried as described above, and quantified by weight using an AT200 analytical balance (METTLER). The neutral lipids were suspended in hexanes and fractionated using silica equilibrated with 5 CV of hexanes. Neutral lipid extracts were applied to the column and the hydrocarbon fraction

was eluted with 10 CV of hexanes, the WE fraction with 10 CV of 98:2 v/v of hexanes/diethyl ether, and the remaining TAGs and neutral lipids with 10 CV of chloroform. The fractions were dried, weighed, and suspended in chloroform for storage at -20 °C.

2.9 GC/MS analyses

Analyses were performed using an Agilent 6890n gas chromatograph system fitted with an HP-5 MS 30 m × 0.25 mm capillary column (Hewlett-Packard) and an Agilent 5973n mass-selective detector. The GC was operated at an injector temperature of 300 °C, a transfer line temperature of 320 °C, a quad temperature of 150 °C, a source temperature of 230 °C, and a helium flow rate of 1 mL/min. Samples of 1 µL were injected in splitless mode. For fatty alcohol analyses, the temperature program of the oven was 40 °C for 2 min, increased to 160 °C at a rate of 40 °C per min, then increased to 240 °C at a rate of 5 °C per min, and finally increased to 300 °C at a rate of 60 °C per min and held for 5 min. The mass spectrometer was operated in electron emission scanning mode at 40 to 800 m/z and 1.97 scans per second. For WE analysis, the temperature program of the oven was 40 °C for 2 min, increased to 180 °C at a rate of 40 °C per min, and then increased to 320 °C at a rate of 2.5 °C per min and held for 20 min. Derivatized fatty alcohols and WEs were identified using Chemstation E.02.02.1431 (Agilent) and the NIST08 Library. The identity of fatty alcohols was further verified using similarly derivatized authentic fatty alcohols. WEs were further identified by comparison to an authentic stearyl stearate standard and were quantified using a standard curve generated using palmityl myristate (Nu-Chek Prep).

2.10 Determination of promoter strengths

RHA1 was freshly transformed with pSYN-*mCherry* vectors containing a promoter or promoter region and were grown overnight in LB. These cultures were used to inoculate 5 mL fresh LB medium to an OD_{600} of 0.1. Cultures were grown to early stationary phase, ~24 hours. Subsequently, 100 µL of culture was transferred to a black clear-bottom 96-well plate (Corning), diluted 1:2 with dH_2O (to an OD_{600} of ~ 0.6 on the microplate reader), Next, mCherry fluorescence (at an excitation: 587 nm and emission: 610 nm) and optical density at 600 nm was measured in an Infinite F200 Pro microplate reader (Tecan). Promotor strength was determined by normalizing mCherry fluorescence against optical density. To investigate promotor strengths at different growth phases, fluorescence was measured at early exponential (OD_{600} ~0.8), mid exponential (OD_{600} ~4), and early stationary (OD_{600} ~10). To investigate the effect of carbon source on promoter strength, cells were grown in M9 media supplemented with different carbon sources as described in Section 2.2.2, and fluorescence was measured in early stationary phase.

2.11 Transcription start site (TSS) determination

TSSs were determined using the ARF-TSS method (211). RHA1 was freshly transformed with pSYN-*mCherry* vectors containing promoters and were grown overnight in LB. These cultures were used to inoculate 5 mL fresh LB medium to an OD_{600} of 0.1. Cultures were grown overnight to mid exponential phase (OD_{600} ~4). Cells were pelleted at 4,000 × *g* for 5 min at 4 °C, flash frozen in liquid nitrogen, and stored at -80 °C. RNA was isolated using Trizol (Thermo Fisher Scientific) and DNA was removed using TURBO™ DNase (Thermo Fisher Scientific) as previously described (131). The resulting RNA was quantified using a Nanodrop 1000 (Thermo

Fisher Scientific) and stored at -80 °C. The integrity of the RNA was assessed using agarose gel electrophoresis.

cDNA was generated by reverse transcription from the above RNA. Briefly, reaction mixtures contained 5 µg RNA, 0.25 µM of the 5' phosphorylated primer *mCherry*_RT (Table 2.3) and 200 U SuperScript IV Reverse Transcriptase (Thermo Fisher Scientific) were incubated at 50 °C for 10 min, as per manufacturer instructions. RNA was removed from the completed reaction by the addition of 10 µL of 3 M NaOH and incubating at 70 °C for 30 min. The cDNA-containing mixture was then neutralized using 5 µL of 6 M HCl and purified using the NEB Monarch PCR purification kit. Forty µg of cDNA, supplemented with 10% DMSO, was ligated overnight at room temperature using T4 RNA ligase 1. The TSS junction was amplified from circularized cDNA using GoTaq DNA Polymerase (Promega) and the *mCherry*_Inv primers (Table 2.3). The resulting amplicons were cloned into pMiniT using a PCR cloning kit (NEB) and transformed into *E. coli* NEB-10β. Resulting colonies were screened by PCR. Transformants containing plasmids with inserts were inoculated into LB and grown overnight. Plasmid DNA was isolated from resulting cultures, and sequenced to determine TSSs.

2.12 Characterization of RHA1 strains containing *frcA* and *ws2* co-expression cassettes

2.12.1 Screening of growth characteristics and WE accumulation

Single colonies of RHA1 strains harboring co-expression cassettes were inoculated into 5 mL of C^- media and grown overnight. These cultures were used to inoculate 50 mL of fresh C^- or N^- media to an OD_{600} of 0.05. To assess WE accumulation, these strains were grown as described

for C^- and N^- media (Section 2.2.1). Total lipids were extracted using MTBE, and WEs were quantified using GC/MS. Growth rates and lag phases were quantified in C^- media using a Bioscreen C automated plate reader (Growth Curves AB). Specifically, RHA1 strains were grown overnight in C^- M9 medium. These cultures were used to inoculate a Bioscreen C microplate with 200 µL of fresh C^- M9 medium at an OD_{600} of 0.05. Plates were grown in the Bioscreen for 48 hours at 30 °C, with maximum shaking, and OD_{600} was measured every hour. Resulting growth curves were plotted in Excel (Microsoft), and growth rate and lag phases were determined using DMFit v 3.5 (212).

2.12.2 Determination of dry biomass and WE yields

RHA1 strains harboring co-expression cassettes were prepared as above. These cultures were used to inoculate 300 mL of fresh C^- or N^- media to an OD_{600} of 0.05. RHA1 strains were grown and harvested as described (see 2.6). In parallel, 500 µL of the resulting culture supernatant was filtered, and stored at -20 °C for glucose quantification. Lipids were extracted using MTBE, purified using flash chromatography, and gravimetrically quantified as described in Section 2.8. To calculate dry biomass and lipid yields, the glucose concentration in the cultures was determined at inoculation and harvest, using an Amplex Red Glucose/Glucose Oxidase Assay Kit (Thermo Fisher Scientific).

Chapter 3: Results

3.1 FcrA promotes WE accumulation in RHA1

Among the best-studied oleaginous bacteria, rhodococci have considerable potential for the sustainable production of lipid-based commodity chemicals such as WEs. However, many aspects of lipid synthesis in these bacteria are poorly understood. While *M. tuberculosis* has been observed to produce de novo WEs under conditions of stress (6, 7), the capacity of rhodococci to produce WEs via a de novo route is unclear. This work aims to study the production of WEs in RHA1 and identify key enzymes involved in WE biosynthesis, in order to facilitate the development of this genus for the production of high-value neutral lipids.

3.1.1 Identification and characterization of WEs in RHA1

Based on the ability of mycobacteria to produce WEs (182, 183) and the similar physiologies of mycobacteria and rhodococci, I hypothesized that the latter also produce WEs when supplied with a growth substrate other than a fatty alcohol or hydrocarbon (129). To test this hypothesis, I grew RHA1 on glucose minimal medium (C- media), extracted the neutral lipids from exponentially growing cells, and fractionated them using flash chromatography. Initial GC/MS analyses revealed that cells contained saturated WEs ranging from 31-34 carbons in length, with C32 species being the most abundant (Figure 3.1A). Using electron ionization mass spectrometry, I analyzed the WEs using the $RCOOH_2^+$ and $RCO^-H^{+\bullet}$ ions of their saturated and unsaturated fatty acid components, respectively (213). For example, the length of the fatty acyl component of the C32 WEs varied from 14 to 18 carbons, as seen from the $RCOOH_2^+$ ions with

m/z values of 229, 243, 257, 271, 285, respectively (Figure 3.1B). These ions indicate that ~70% of the C32 WEs were C16:C16 species, while the remainder were a mixture of species varying from C14:C18 to C18:C14. Finally, using the highly abundant C16 ion, which is more abundant than the corresponding WE molecular ion, I was able to identify additional WEs with 29, 30, and 35 carbon atoms that were not apparent in the total ion trace (Figure 3.1C). In summary, the most abundant WEs in exponentially growing cells contained 32 carbons (Figure 3.2A). Moreover, C16 was the most abundant WE fatty acyl moiety in the detected WEs (Figure 3.2B). No unsaturated fatty acids were detected under these conditions. Quantification by GC/MS revealed that the cells contained 2.2 ± 0.2 µg of WEs/g CDW. Interestingly, the cells contained lower amounts of WEs (0.6 ± 0.2 µg/g CDW) when grown in N- media and examined in stationary phase (Table 3.1), conditions under which they accumulate TAGs to over 50% of their CDW (129). WEs produced in N- media were similar in length and composition to those in C- media (Figure 3.2).

Table 3.1 WE levels in RHA1 strains under different growth conditions.

	Growth condition and WE content[a]		
RHA1 strain	**N^- (stationary)**	**C^- (exponential)**	**SNP-treated (exponential)**
WT	0.6 ± 0.2	2.2 ± 0.3	3.0 ± 0.3
Δ*fcrA*	0.7 ± 0.1	3.2 ± 0.5	0.5 ± 0.1

[a]Experimental values represent µg WE / g CDW. Values represent the mean of biological duplicates, error is given as standard deviation.

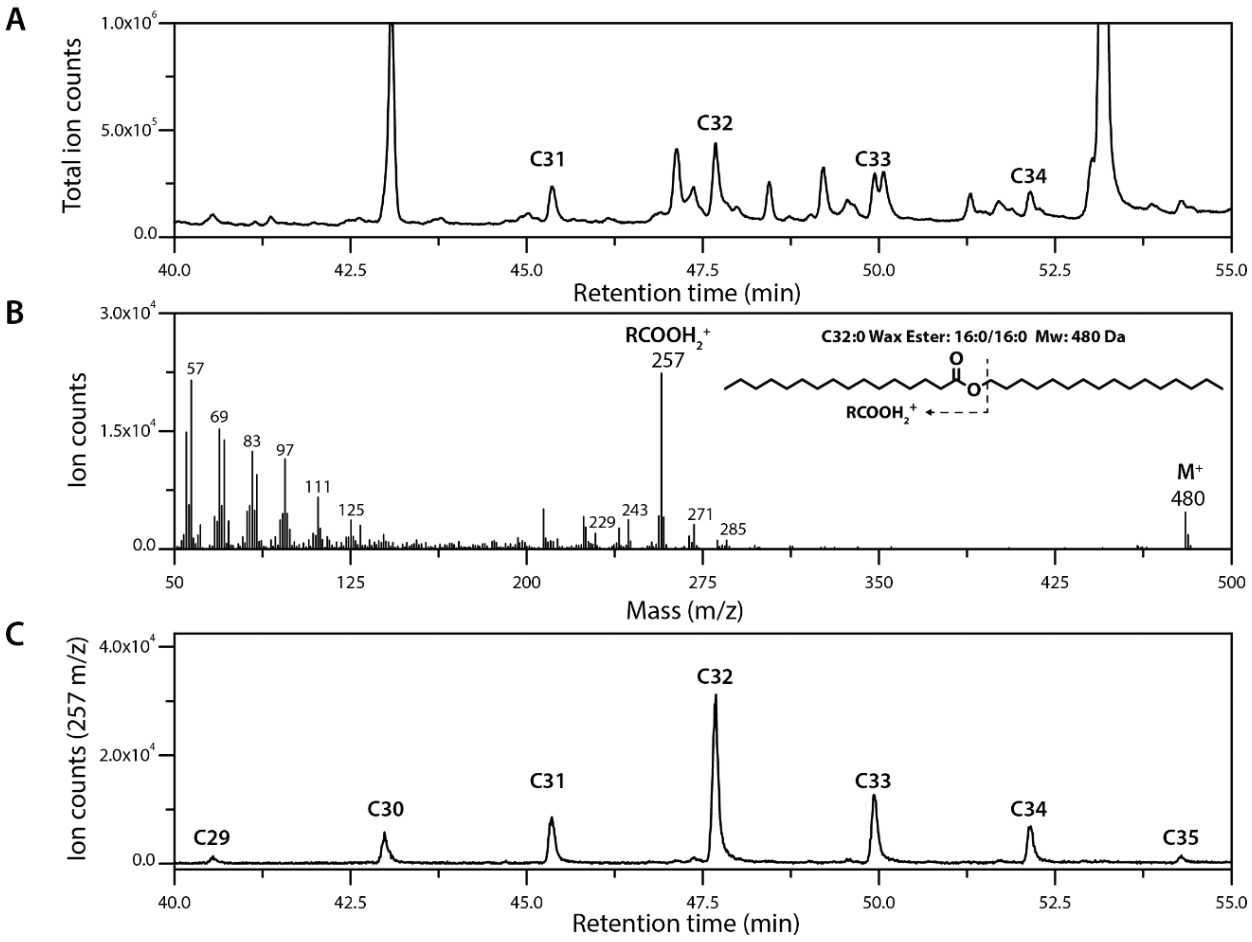

Figure 3.1 Analyses of WEs in RHA1.

(A) GC/MS chromatogram of WE-containing lipid fraction. Identified WEs are labeled according to total number of carbon atoms. (B) Mass spectrum of the detected C32 WEs. Molecular ion and major fatty acyl fragments labeled. (C) WEs detected using the C16 $RCOOH_2^+$ ion (m/z = 257), the most abundant ion fragment associated with the WEs. Cells were grown on glucose and neutral lipids were extracted and fractionated using flash chromatography.

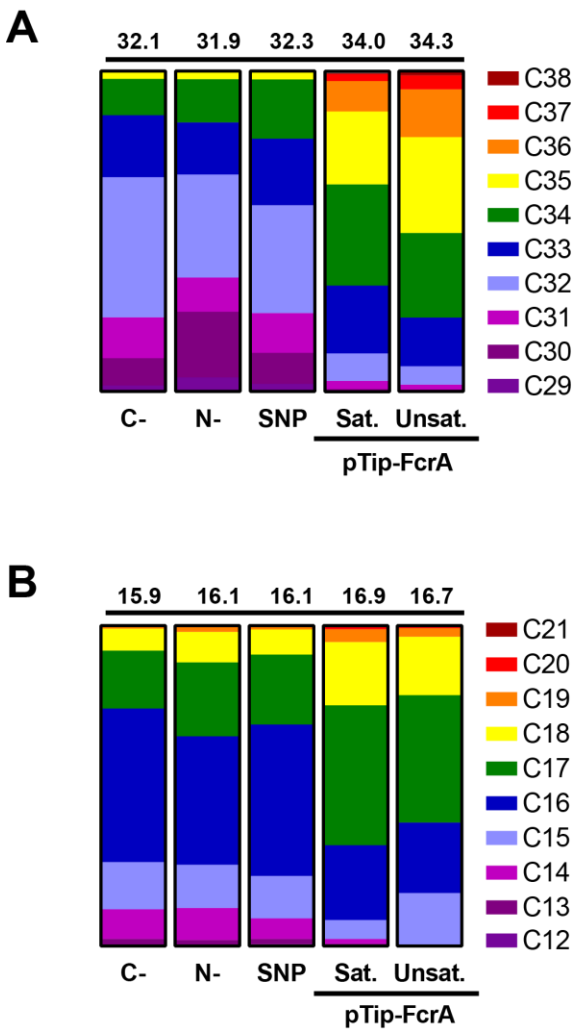

Figure 3.2 WE content of RHA1 under different conditions.

(A) Distribution of WE chain lengths detected. (B) Distribution of acyl-chain lengths of detected WEs. The numerical values displayed above each column indicate weighted mean chain lengths. Values were obtained from biological duplicates, errors ranged from 0.06 to 1 %. Conditions were: C-, carbon-limited (exponential); N-, nitrogen limited (stationary); SNP, SNP-treated RHA1; pTip-FcrA, RHA1 overproducing FcrA in N^- media. Sat. and Unsat. indicated saturated and unsaturated WEs/acyl-chains, respectively.

3.1.2 Bioinformatic identification of FcrA

Having identified WEs in RHA1, I searched the strain's genome for homologs of *fcr1* or *fcr2* of *M. tuberculosis*, which encode FARs (183). Using BLAST, I identified RHA1_RS30405 and RHA1_RS09420 as reciprocal best hits of Fcr1 and Fcr2, respectively. *RS30405* encodes a protein of 664 amino acid residues, identified here as FcrA, that shares 56% and 43% amino acid sequence identities with Fcr1 and Maqu_2507 from *M. aquaeolei* VT8, respectively. The three enzymes share a similar two-domain structure in which each domain contains a predicted nucleotide-binding site (Figure 3.3). *RS30405* is conserved in all rhodococci whose genomes have been sequenced. *RS09420* encodes a protein of 280 amino acids that shares 48% and 46% amino acid sequence identities with Fcr2 and Acr1 from *A. calcoaceticus*, respectively, as well as 46% identity with the second nucleotide-binding domain of FcrA.

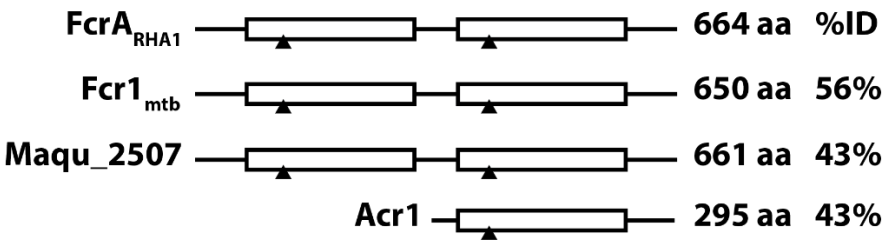

Figure 3.3 Bacterial fatty acyl-CoA reductases.

Domain structure of bacterial FARs. White boxes represent NADPH-binding domains, conserved nucleotide-binding residues are highlight with black triangles. Amino acids length and percent identity (%ID) to FcrA from RHA1 are reported.

To gain further insight into the physiological role of the identified FARs in RHA1, I considered their transcript levels in previous RNA-seq studies aimed at understanding TAG biosynthesis (131). In N^- media, the transcript levels of both *fcrA* and *RS09420* were low, with reads per kilobase per million mapped reads (RPKM) values between 6 and 11 in exponential and stationary phase. Interestingly, *fcrA* appears to be more highly expressed in C^- media, with RPKMs of 19 ± 9 and 87 ± 6 in exponential and stationary phase, respectively. By contrast, *RS09420* transcript levels were also low in C^- media: the RPKM value was 9 ± 5 in exponential phase and no transcripts were detected in stationary phase.

The RNA-seq data also provides insight into the operon structures of *fcrA*. Thus, *RS30410*, located immediately upstream of *fcrA* and encoding a putative membrane protein, was not co-transcribed with *fcrA*. Interestingly, *RS30410* is conserved upstream of *fcrA* across the diverse phylogenetic clades of rhodococci (141), while the surrounding genomic context is not. By contrast, a homolog of *RS30410* is not present upstream of *fcr1* in mycobacterial species, suggesting that *RS30410* is not essential for the activity of *fcrA*. The low transcription levels for *RS09420* did not allow us to make meaningful observations about the structure of its transcript.

3.1.3 Production, purification, and characterization of recombinant FcrA

Further efforts were focused on exploring the function of FcrA as related two-domain enzymes completely reduce acyl-CoAs to fatty alcohols (181) and have been used in biotechnology applications (214, 215). To investigate the activity of FcrA, I produced it as a C-terminally His-tagged protein in RHA1 and purified it to greater than 95% apparent homogeneity (Figure 3.4A). To check for post-translational modification, purified FcrA was subjected to intact protein mass-

spectrometry. The molecular mass of FcrA-His_6 was 73627 Da, which corresponds to the predicted mass of the protein (73758 Da) based on its amino acid sequence less the N-terminal methionine (131 Da).

To evaluate the ability of FcrA to catalyze the transformation of acyl-CoAs to fatty alcohols, 1.4 µM FcrA was incubated with 400 µM NADPH and 100 µM oleoyl-CoA in 1 mL of reaction buffer (20 mM Tris-HCl, pH 7.0, 50 mM NaCl) for 20 h at room temperature. The reaction was quenched with 1 mL saturated NaCl and 100 µM of tetradecanol was added as a standard. Analysis of the extracted and derivatized reaction products by GC/MS revealed that FcrA converted oleoyl-CoA to oleyl alcohol (Figure 3.4B). No alcohol was detected in control reactions in which FcrA was omitted.

Using a spectrophotometric assay following either the production of 2-nitro-5-thiobenzoate (NTB^{2-}) or the consumption of NADPH, FcrA catalyzed the reduction of various acyl-CoAs. As with previously characterized FARs (181, 183), activity was maximal at pH 7.0. Moreover, no activity was detected when NADPH was substituted with NADH. Similar to Maqu_2507 (181), the rate of NADPH consumption was twice that of NTB^{2-} production, indicating that FcrA oxidizes two equivalents of NADPH for every molecule of CoA released. NTB^{2-} production was used to query a range of acyl-CoA substrates. Among the tested substrates, FcrA had highest specific activity for stearoyl-CoA (C18-CoA), reducing it at a rate of 45 ± 3 nmol/mg·min. The specific activity of FcrA dropped off with decreasing chain length of the acyl-CoA substrate (Table 3.2). By contrast, oleoyl-CoA (C18:1-CoA), a monounsaturated acyl-CoA, was reduced at a similar rate to stearoyl-CoA.

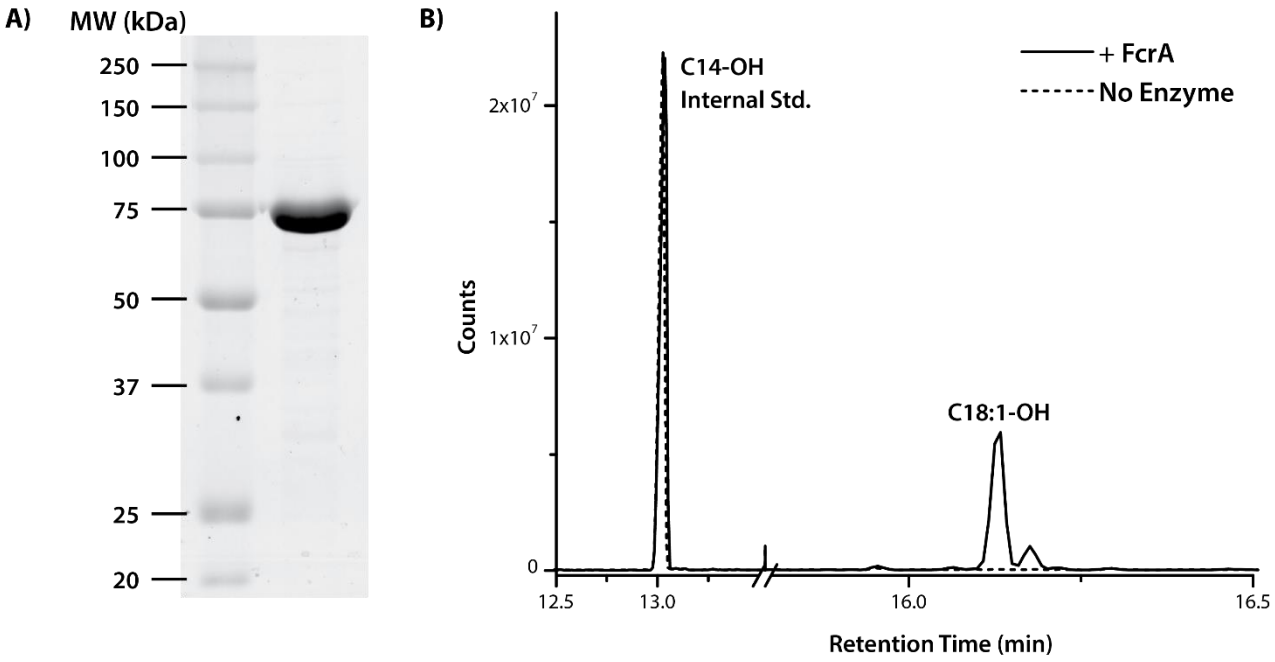

Figure 3.4 Purification and activity of recombinant FcrA.

(A) SDS-PAGE of 8 µg His_6-tagged FcrA purified from RHA1. (B) GC/MS trace of a reaction mixture containing 1.4 µM FcrA-His_6, 100 µM oleoyl-CoA and 400 µM NADPH (20 mM Tris-HCl, pH 7.0, 50 mM NaCl) incubated for 20 hours.

As previously characterized FARs are also able to reduce fatty aldehydes, a spectrophotometric assay was used to show that FcrA catalysed the reduction of fatty aldehydes in a NADPH-dependant manor. Like Maqu_2507 (181), the rate of aldehyde reduction for FcrA was approximately a 100-fold greater than acyl-CoAs. Among the tested aldehydes, FcrA had highest specific activity for dodecanal, reducing it at a rate of 5300 ± 300 nmol/mg·min. The specific activity of FcrA fell when the chain length of the aldehyde substrates was increased or decreased (Table 3.2).

Table 3.2 Specific activities of FcrA with various acyl-CoA and fatty aldehyde substrates.

Substrate	**Chain Length**	**Specific Activity**[a,b] (nmol/min/(mg protein))
Stearoyl-CoA	C18	45 ± 3
Oleoyl-CoA	C18:1	41 ± 1
Palmitoyl-CoA	C16	7.0 ± 0.1
Lauroyl-CoA	C12	1.5 ± 0.3
Decanal	C10	3300 ± 200
Dodecanal	C12	5300 ± 300
Cis-11-hexadecanl	C16:1	2800 ± 300

[a]Specific activity for acyl-CoA substrates was determined from $NTB2^-$ ion formation as detected at 412 nm.

[b]Specific activity for aldehyde substrates was determined from $NADP^+$ formation as detected at 340 nm. Values represent means determined from triplicate experiments, error is given as standard deviation.

FcrA of RHA1 had comparable activity to the other two-domain FARs that have been characterized to date, but had subtly different substrate preferences. For example, FcrA showed a strong preference for C18-CoAs, in contrast to Maqu_2507, which had highest activity for C16-CoA (181). Both enzymes showed decreased activity with shorter-chain acyl-CoAs. Monounsaturation of the acyl-CoA substrate appears to have no significant effect on activity of either of these two enzymes. In contrast, Fcr1 of *M. tuberculosis* had a strong preference for C18:1-CoA over saturated acyl-CoAs (183). Maqu_2507 and FcrA both reduced fatty aldehyde substrates at comparable rates, but maximal activity was again seen with subtly different substrates. Maqu_2507 had maximal activity with decanal (C10) while FcrA had maximal activity with dodecanal (C12). Interestingly, with both aldehyde and acyl-CoA substrates, the maximal rate seen with FcrA is with substrate chain-lengths two carbons longer than Maqu_2507.

3.1.4 WE production in a Δ*fcrA* mutant

Having established the identity of RS30405 as a fatty acyl-CoA reductase, I further investigated the physiological role of *fcrA* by deleting the gene in RHA1. Interestingly, the Δ*fcrA* mutant contained similar amounts of WEs as wild type (WT) RHA1 when grown in both C^- and N^- media, in exponential and stationary phase, respectively (Table 3.1).

In *M. tuberculosis*, a Δ*fcr1* mutant did not show a decrease in WEs when starved for both carbon and nitrogen, but did so under conditions of nitric oxide (NO) stress (183). Therefore, I sought to use sodium nitroprusside (SNP), to generate NO in RHA1 cultures and investigate whether WE production by *fcrA* is linked to the presence of reactive nitrogen species. When stressed with NO, WT cells growing exponentially on glucose minimal medium produced similar levels of WEs as non-stressed cells. The majority of the WE species observed in WT RHA1 are similar in chain length and composition to those seen under other growth conditions (Figure 3.2). However, trace amounts of unsaturated C32-34 WEs were detected in the SNP-treated cells. The production of WEs in response to NO stress was strikingly different in the Δ*fcrA* mutant (Figure 3.5), with a 6-fold reduction in accumulated WEs (Table 3.1).

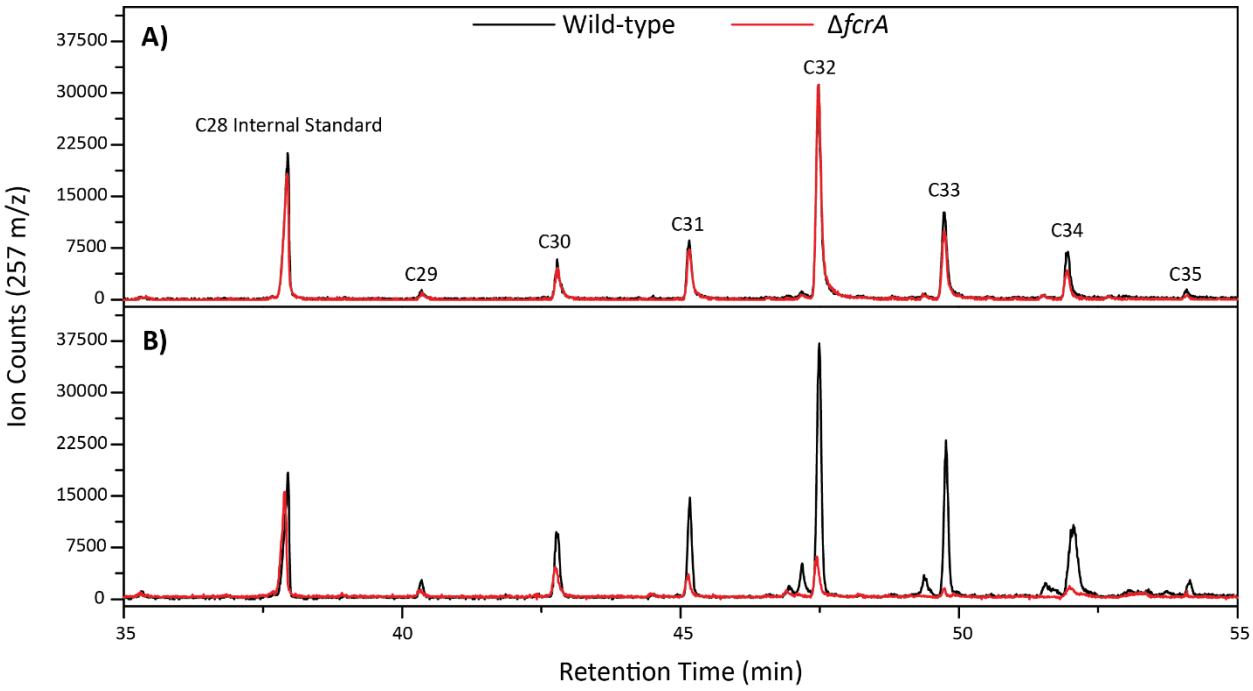

Figure 3.5 Comparison of WEs in wild-type RHA1 and Δ*fcrA* mutant.

Neutral lipids were extracted from exponentially growing cells in C^- media (A) without and (B) with SNP treatment, fractionated on silica resin, and examined by GC/MS. The C16 $RCOOH_2^+$ ion with an *m*/*z* of 257 was used to identify WEs. Similar trends were seen when other $RCOOH_2^+$ ions were examined.

3.1.5 Overexpression of *fcrA*

To investigate the potential of FcrA to promote WE accumulation, I overproduced a tag-less form of the enzyme in RHA1 using a pTip vector. This experiment was performed using N^- media, which promotes neutral lipid accumulation (129). Indeed, TLC analyses of cells overproducing FcrA indicated that they contained significant amounts of WEs under these conditions (Figure 3.6A). Thus, overproduction of FcrA resulted in the appearance of a large band that ran similarly to stearyl stearate. Gravimetric analysis indicated that the FcrA-overproducing strain accumulated WEs to 13 ± 5 % of CDW in N^- media. No significant

accumulation of WEs was observed during exponential or stationary phase in C^- media. These WEs ranged from 30 to 38 C atoms in length (Figure 3.6B). The WEs were on average a couple of carbon atoms longer than those in WT Cells (Figure 3.2A). Moreover, a significant portion (~20%) of the WEs were unsaturated. Analysis of the fragmentation ions further revealed that the most abundant saturated and unsaturated fatty acyl chain lengths were C17 (Figure 3.3B). Finally, only trace amounts (<1% of total) of unsaturated fatty alcohols were detected, signifying that the unsaturation was primarily located within the acyl moiety.

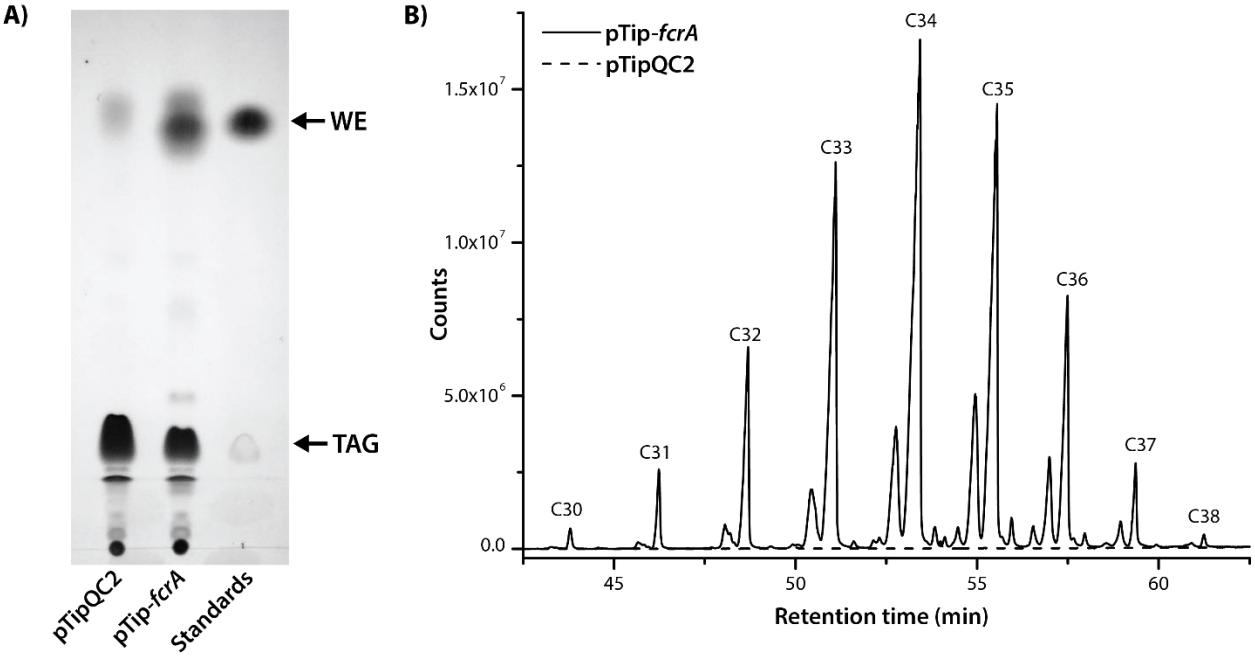

Figure 3.6 WE content of RHA1 overproducing FcrA.

(A) Total lipid extracts as visualized by TLC. Lanes were loaded with: 1, extract of RHA1 carrying an empty vector (pTipQC2); 2, extract of RHA1 overproducing FcrA (pTip-*fcrA*); and 3, stearyl stearate and glyceryl tripalmitate. (B) GC/MS analysis of WE fraction isolated from RHA1 overproducing FcrA from pTip-*fcrA*.

3.1.6 The role of FARs and WEs in bacterial physiology

While, purified FcrA catalyzed the reduction of various fatty acyl-CoAs to the corresponding fatty alcohol, the enzyme did not appear to contribute significantly to the synthesis of WEs under normal growth conditions. Specifically, the deletion of *fcrA* resulted in significantly lower production of WEs only under NO stress.

Our data indicate that, like *M. tuberculosis* and *M. aquaeolei* VT8, RHA1 has more than one WE biosynthesis pathway. Moreover, FcrA only contributes to WE biosynthesis under specific stresses. Thus, deletion of *fcrA* had no effect on WE synthesis during nutrient-limited growth, similar to the phenotypes of the *fcr1* mutant in *M. tuberculosis* (183) and the *maqu_2507* mutant in *M. aquaeolei* VT8 (174), a Gram-negative WE-accumulating bacterium isolated from an offshore oil-producing well. In further similarity to the phenotype of the *fcr1* mutant in *M. tuberculosis* (183), deletion of *fcrA* impacted WE synthesis in the presence of reactive nitrogen species. Consistent with the apparently minor role of FcrA in WE biosynthesis during exponential growth, the WE composition of RHA1 under these conditions did not reflect the substrate preference of FcrA. More specifically, FcrA had a preference for longer acyl-CoAs than the average chain length of the WE alcohols under these conditions. By contrast, the WE content of RHA1 cells was more reflective of FcrA's substrate preference in cells overproducing the enzyme in N^- media. That is, the WEs contained alcohols with longer chain lengths. Overall, this suggests that the two-domain FARs may be responsible for producing WEs only in response to specific stresses (183).

Aldehyde-forming fatty acyl-CoA reductases may play a larger role in WE synthesis in mycolic acid-producing Actinobacteria. For example, the *fcr2* mutant of *M. tuberculosis* contained lower amounts of WEs under all conditions examined. It seems reasonable that in RHA1, RS09420 plays a similar role. Both Fcr2 and RS09420 are homologs of Acr1 (179), the aldehyde-forming fatty acyl-CoA reductase of *A. calcoaceticus* BD413, and could therefore function as such. Sirakova *et al*. reported that Fcr2 generated fatty alcohols from acyl-CoA substrates (183). However, Fcr2 was characterized in *E. coli* lysate, which contains an unidentified enzyme that reduces fatty aldehydes to fatty alcohols (179). Indeed, the presence of this enzyme has been exploited to produce fatty alcohols in *E. coli* expressing *acr1* (140). Genetic and biochemical characterization of *RS09420* are required to definitively assign this gene's function.

3.2 Development of synthetic biology tools for rhodococci

The engineering of rhodococcal biocatalysts, whether to produce acrylamide, WEs or other commodity chemicals, requires tools to genetically manipulate strains effectively. In RHA1, WE accumulation was induced when FcrA was overproduced from a plasmid. However, plasmid-based expression systems are not suited for industrial biocatalysts. Their shortcomings include: instability, requiring the use of expensive antibiotics to maintain selection; metabolic burden, decreasing the efficiency of a bioprocess; and, often, the addition of chemical inducers to activate gene expression, many of which are cost-prohibitive at industrial scales (216-219). Instead, industrial settings favour biocatalysts constructed through the stable, chromosomal integration of genes controlled by constitutive promoters. The creation of viable industrial strains

has been stymied in part by the dearth of well-characterized genetic tools in rhodococci. In the following work, I developed such tools to accelerate the creation of rhodococcal biocatalysts. Specifically, I created pSYN, a modular integrative vector for *Rhodococcus*, and applied this tool to identify and characterize putative constitutive promoters. Finally, I demonstrated the utility of pSYN by constitutively expressing a chromosomal copy of *fcrA* to produce WEs.

3.2.1 Creation of pSYN, a modular integrative vector

An integrative vector was constructed to allow for rapid prototyping of RHA1 strains. Given the success of increasing WE production in RHA1 using FcrA overproduced from an inducible plasmid (220), I wanted to investigated WE production using a single constitutively-expressed copy of *fcrA* integrated into the RHA1 genome. To accomplish this, a tool that allowed for the robust integration and expression of single-copy heterologous genes in rhodococci was created. I constructed pSYN (Figure 3.7A), a modular integrative-vector based on the pSET152 backbone (158, 202). The pSET backbone contains ϕC31, a gene encoding a site-specific serine integrase, and its cognate *attP* site. Together, these enable the rapid and reliable insertion of the vector into the RHA1 genome at an *attB* site located within *RS20555*, encoding a pirin-like protein of unknown function. To create a vector useful in the engineering and characterization of biocatalysts, the pSYN multiple cloning site was designed with unique restrictions sites that enable genetic components such as promoters, ribosome binding sites, genes, and terminators to be easily swapped. This modularity allows the pSYN vector to be used in a variety of synthetic biology applications, such as the creation and characterization of single-copy promoters or gene libraries (Figure 3.7B).

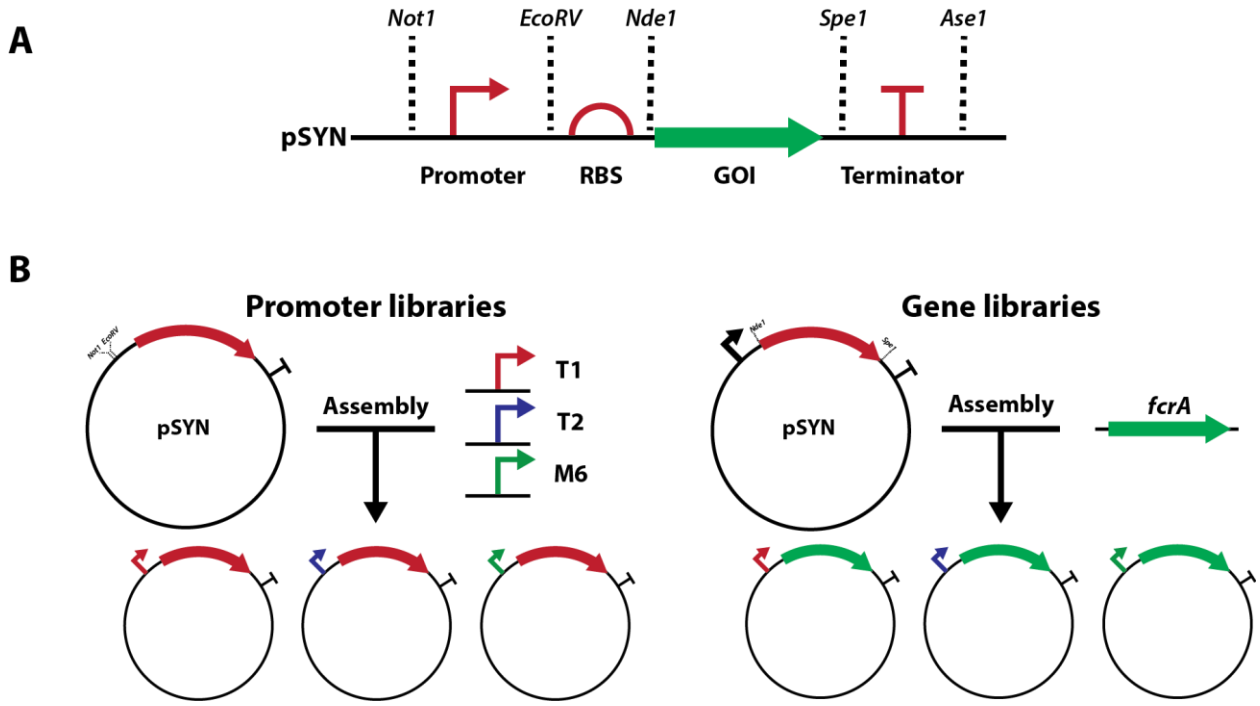

Figure 3.7 pSYN, a modular integrative-plasmid for engineering rhodococcal biocatalysts.

(A) The pSYN multiple cloning site was designed to be modular: the use of unique restriction sites allow genetic components to be easily swapped. (B) The pSYN vector facilitates the design and implementation of biocatalysts by enabling the creation and characterization of promoter and gene libraries.

3.2.2 Identification of P_{10} as a strong-constitutive promoter

To address the lack of characterized constitutive promoters in rhodococci, pSYN was used to validate putative strong constitutive promoters. Promoter candidates were identified by examining four sets of transcriptomic data of RHA1 in exponential or stationary growth phases, in C^- and N^- media containing benzoate as a sole carbon source (131). Twenty genes highly-transcribed under different growth phases and media conditions were selected (Table 3.3). Benzoate catabolic genes were avoided. Putative promoters were isolated by cloning 500-

nucleotide regions spanning the start codon of each gene: 100 bases downstream and 400 bases upstream. These regions were cloned into the NotI-EcoRV restriction sites of pSYN containing *mCherry* as a fluorescent reporter (Figure 3.8A). Constructs were transformed into RHA1, and promoter strengths were determined in early stationary phase by measuring fluorescence. Fluorescence was normalized to OD_{600} and the constitutive P_{nit} promoter (157). While the P_{nit} promoter, a constitutive variant of the inducible P_{tipA} promoter, was characterized using a multi-copy plasmid backbone, its strength has never been compared in single copy to other potential constitutive promoters. Of the 20 tested promoter regions, only P_{10} and P_2 yielded higher fluorescent signals than the P_{nit} promoter (Figure 3.8B), at 2.6- and 1.4-fold, respectively. This suggests that P_{nit} is a strong constitutive promoter.

P_{10}, the promoter region of *RS36130*, a MerR-family transcriptional regulator of unknown function located on the pRHL1 plasmid of RHA1, was further examined. First, the expression of P_{nit} was compared to P_{10}, and two medium-strength promoter regions, P_{15} and P_{18}, across three different growth phases: early exponential, mid exponential, and early stationary phase. Expression from P_{nit} and P_{10} was strong throughout exponential growth, and remained at a high level in stationary phase, as opposed to the medium-strength promoters, P_{15} and P_{18} (Figure 3.8C). To assess the effects of different media on promoter expression, RHA1 transformed with each of the P_{nit}-*mCherry* and P_{10}-*mCherry* constructs were grown to early stationary phase on minimal media supplemented with various carbon sources, including: glucose, in both C^- and N^- media; benzoate, an aromatic carbon source; and alkaline pretreated liquor (APL), a biomass derived source of sugars, aromatics, and simple acids (221). In all tested media, P_{10} was consistently 2.6- to 3-fold stronger then P_{nit} (Figure 3.8D). Together, these results suggest that

P_{10} is constitutive under the conditions tested, and stronger than the previously characterized P_{nit} promoter (157).

Table 3.3 Candidate genes for identification of strong constitutive promoters.

Name	Locus	Predicted product
P_1	RS04990	Quinolinate synthetase
P_2	RS05290	Division cluster transcriptional repressor
P_3	ro01178	Hypothetical protein
P_4	RS19805	MerR-family transcriptional regulator
P_5	RS19555	Bacterioferritin
P_6	RS19805	Membrane protein
P_7	RS20995	Transcriptional regulator
P_8	RS21170	Cold-shock protein
P_9	RS30940	Ribosomal subunit interface protein
P_{10}	RS36130	MerR-family transcriptional regulator
P_{11}	RS44810	Bacterial RNase P
P_{12}	RS11020	Hypothetical protein
P_{13}	RS30980	Stearoyl-CoA 9-desaturase
P_{14}	RS05505	Hypothetical protein
P_{15}	RS21725	CarD-family transcriptional regulator
P_{16}	RS30245	Co-chaperone GroES
P_{17}	RS10475	Molecular chaperone GroEL
P_{18}	RS09620	50S ribosomal protein L10
P_{19}	RS09350	Elongation factor Tu
P_{20}	RS19475	Superoxide dismutase

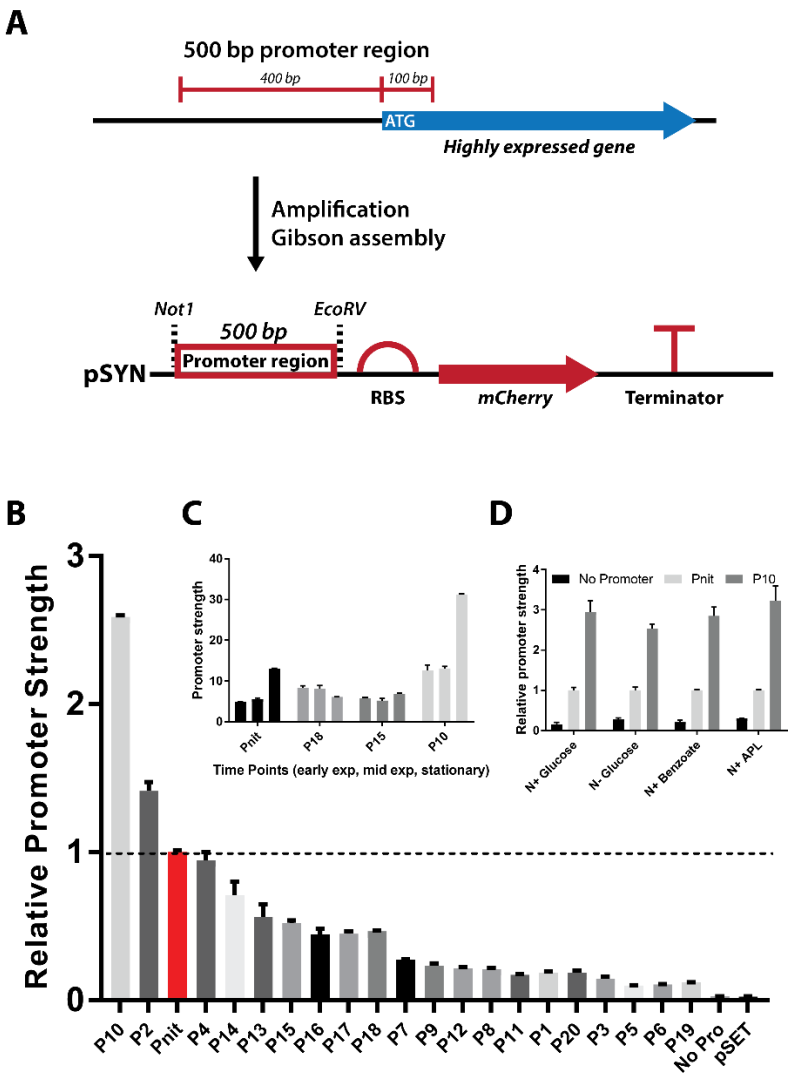

Figure 3.8 Characterization of constitutive promoters found in RHA1.

(A) 500 nucleotide promoter regions of highly expressed genes were cloned into pSYN carrying the gene encoding mCherry. (B) Relative promoter strength was determined by comparing fluorescence relative to OD_{600}, normalized against the strength of P_{nit}. (C) Strength of select promoters at various growth phases. (D) Relative promoter strengths in various media. Values represent the mean of biological duplicates, error is given as standard deviation.

3.2.3 Characterization of P_{10}

The 500 nucleotide fragment containing the P_{10} promoter is large and therefore not ideal for biocatalyst development. To further characterized P_{10} and create a smaller minimal promoter, truncations were performed to identify the core promoter sequence required for strong-constitutive expression (Figure 3.9A). Truncated promoter regions were tested as described above. It was determined that at least 200 bases could be truncated from the 5' end of the fragment and 150 bases could be truncated from the 3' end without significantly affecting the fluorescence signal (Figure 3.9B). This indicates that the core region of the promoter is located within a 150 base fragment. Interestingly, as the upstream regions were truncated, the expression of mCherry increased: the fluorescence of the P_{M6} construct (Figure 3.9A) was 6-fold stronger than P_{nit} and 2.5-fold stronger than P_{10}.

To further characterize P_{10}, the transcriptional start site (TSS) of P_{10} and P_{M6} were determined using the ARF-TSS method (211). In brief, ARF-TSS involves generating gene-specific cDNA with a phosphorylated primer that captures the 5' end of a transcript of interest. The cDNA is circularized, and the ligation junction is amplified using inverse-PCR. The junction is cloned, and the TSS is identified by sequencing. The TSS is the base located at the ligation junction formed between the gene-specific primer and the 3'-end of the cDNA (Figure 3.10A). Using the P_{M6} promoter, two TSSs were found. Of twenty-two sequenced colonies, ten mapped to a guanine residue 87 nucleotides upstream of the start codon, while nine mapped to a guanine residue 95 nucleotides upstream, herein TSS1 and TSS2, respectively (Figure 3.10B). Interestingly, when the ARF-TSS method was performed on the full length P_{10} promoter, only

TSS2 was reliably detected. Out of sixteen sequenced colonies, eleven mapped to TSS2, while only one mapped to TSS1. In both experiments, remaining colonies contained cDNA resulting from degraded mRNA.

Examining the nucleotide sequences at the TSSs revealed putative -10 and -35 boxes (Figure 3.10C). The -10 box located 7 nucleotides upstream of TSS2 conforms to the well characterized actinobacterial σ^A consensus sequence TANNNT (222), while the -10 box located 6 nucleotides upstream of TSS1 is less well conserved. Neither -10 box appears to have the upstream extended -10 motif TGG that is common in actinobacteria (222, 223). Only the putative -35 box of TSS1 conforms to the pseudo-consensus -35 sequence TTGNNN (222, 224). However, as the sequence and position of actinobacterial -35 boxes is highly variable (222), the -35 boxes cannot be definitively assigned.

The P_{M6} promoter was further truncated to the TSSs, yielding promoters P_{T1} and P_{T2}. These were approximately 3- and 5-fold weaker than P_{M6}, respectively. As bases downstream of the TSSs appear to be required for full activity, they were included in future constructs. A minimal 200 nucleotide promoter, herein P_{M200}, was created for future biocatalyst development. P_{M200} had comparable promoter strength to the full 350 base pair P_{M6} promoter (Figure 3.10D).

Overlapping promoters of the type observed for *RS36130* (*i.e.*, P_{10}) have been reported in bacteria and appear to be a mechanism of transcriptional regulation. The galactose regulon of *E. coli* provided the first well-studied example of overlapping promoters allowing differential transcription (225). The paradigm of overlapping promoters has since been reported in a range of *E. coli* genes, such as the flagellar class II operons (226), the *napF* operon (227), and the *focApfl*

operon (228). In actinobacteria, genome-wide TSS mapping has suggested that overlapping promoters are relatively common (229, 230). For example, in *M. tuberculosis*, 19% of the primary transcripts identified by differential RNA-Seq appeared to originate from more than one TSS (229) with the *recA* gene being a specific example (231).

The overlapping promoters of *RS36130* may enable the regulation of this MerR-family transcriptional regulator. While the original transcriptomic data do not resolve any complexity at the *RS36130* promoter (131), this idea is supported by the TSS analysis of P_{10} and P_{M6}, which have different strengths. More specifically, the P_{10} promoter fragment specified transcription from a single promoter, while the significantly stronger P_{M6} specified transcription from two. The 150-nucleotide truncation on the downstream end of the P_{M6} promoter region may have eliminated a regulatory element that suppresses expression from TSS1. Interestingly, two strong constitutive promoters extensively used in *Streptomyces*, SF14p and *ermE*p*, each have overlapping promoters (232, 233).

Subtle changes in the promoter region of P_{M6} greatly affected promoter strength. The ~5-fold decrease in the strength of P_{T2} can be attributed to the inactivation of the second promoter during truncation of P_{M6} to TSS2. However, the ~3-fold decrease in strength when P_{M6} was truncated to TSS1 is more difficult to explain. *RS36130* encodes for a MerR-family regulator of unknown function. Unlike prototypical promoters, which have a 17 ± 1-bp spacer sequence between the -35 and -10 hexameric sequences (234), MerR-regulated promoters have an extended 19- to 20-bp spacer (235). This extended spacer prevents efficient transcription in the absence of the MerR-regulator, which primarily acts as transcriptional activators by changing the DNA conformation

at the promoter to allow for efficient binding of RNA polymerase (235). These extended spacers are present in the promoters of *RS36130*. It is possible that Rs36130 regulates the transcription of its gene, as is the case for other MerR-family regulators, such as TipAL (236). Therefore, the truncation that created P_{T1} may alter the binding of Rs36130 that is presumably present in the host RHA1, decreasing its ability to act as an activator. A similar phenomenon was observed for the *merR* promoter of *E. coli*, where promoter activity decreased ~5-fold when the 3' end of the promoter was truncated to the TSSs (237). However, as nucleotide sequences downstream of TSSs have been known to interact with RNA polymerase, and thereby influence promoter strength (238), further work is required to elucidate the regulation of the *RS36130* promoter.

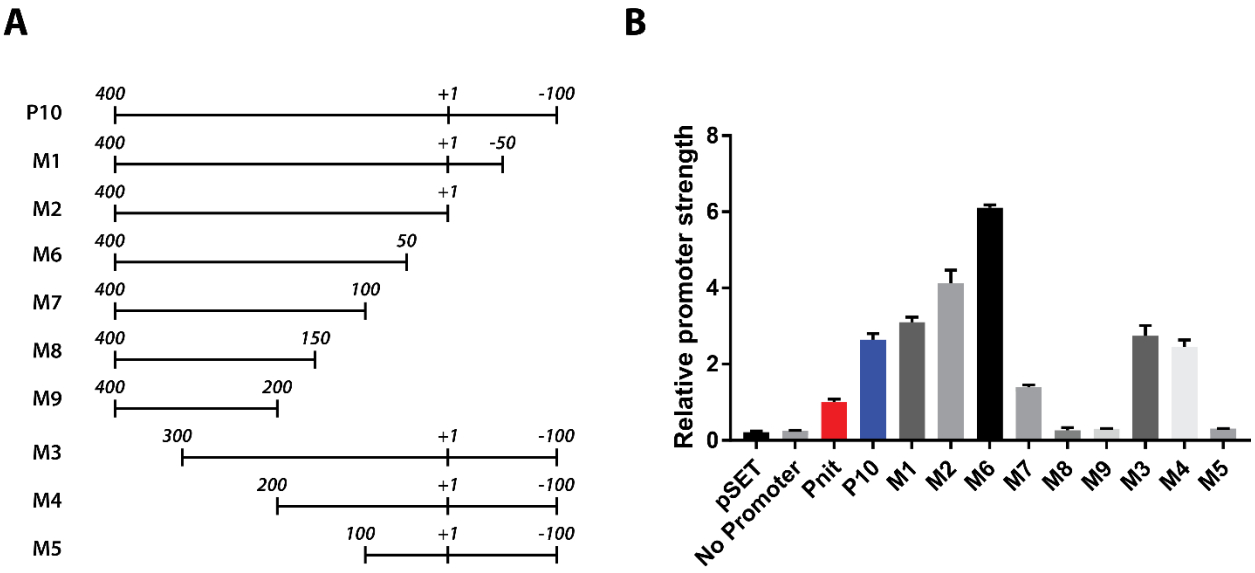

Figure 3.9 Characterization of minimal P_{10} promoters.

(A) Truncated P_{10} promoters. +1 represents the adenine in the start codon of *RS36130*. (B) Relative strengths of truncated promoters, normalized against the strength of P_{nit}. Values represent the mean of biological duplicates. Error is given as standard deviation.

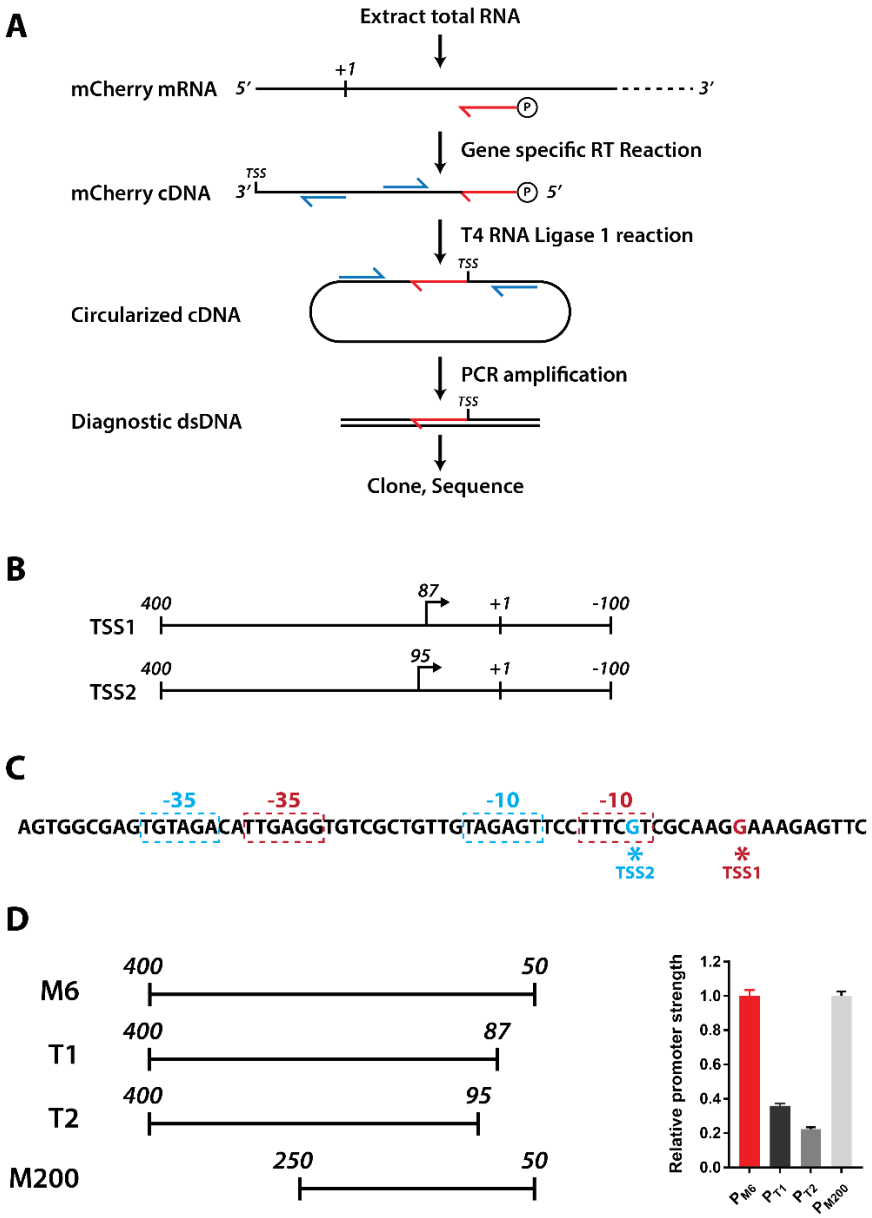

Figure 3.10 Transcriptional start sites of the P_{10} promoter.

(A) ARF-TSS work flow. (B) TSSs identified by the ARF-TSS method. +1 represents the adenine in the start codon of RS36130. (C) Putative -10 and -35 sequences for the identified TSSs. TSS1 in red, TSS2 in blue. (D) Promoters truncated to the TSSs of P_{10}, and a 200 nucleotide minimal promoter were created, cloned, and characterized. Promoter strength was assessed relative to the P_{M6} promoter. Values represent the mean of biological duplicates. Error is given as standard deviation.

3.2.4 Demonstration of pSYN for FcrA overproduction

To establish the utility of pSYN in engineering the metabolism of RHA1, *fcrA* was subcloned into pSYN vectors containing $P_{T1,}$ $P_{T2,}$ or P_{M6} constitutive promoters (Figure 3.11A). Constructs were transformed into RHA1 and resulting strains were grown on N^- media to induce lipid accumulation (Figure 3.11B). Lipids were extracted and analyzed by GC/MS. RHA1 strains constitutively expressing *fcrA* accumulated WEs (Figure 3.11C). Expression from the strongest promoters, P_{T1} and P_{M6}, resulted in approximately 3- and 5- fold higher WE content than the P_{nit} promoter, respectively. As constitutive expression of *fcrA* resulted in reduced biomass, I also considered the titre of WEs produced (Figure 3.11D). Both P_{T1} and P_{M6} resulted in a 3-fold increase in WE titre compared to the P_{nit} promoter.

Resulting WEs were 29 to 38 C atoms in length and had varying degrees of unsaturation (Figure 3.12). As previously reported (220), produced WEs were highly isobaric and contained mixtures of even and odd acyl chains. The chain length profile of WEs were similar to those produced by pTip-*fcrA*. However, under similar growth conditions, RHA1 transformed with pSYN-P_{M6}-*fcrA* produced approximately 3-fold more unsaturated WEs then *fcrA* expressed from a plasmid (approximately 60 vs 20%). Further, RHA1 containing the integrated *fcrA* produced significant amounts of diunsaturated WEs, amounting to 18% of total WEs and 30% of the unsaturated fraction. These values compare with 2% of total WEs in pTip-*fcrA*.

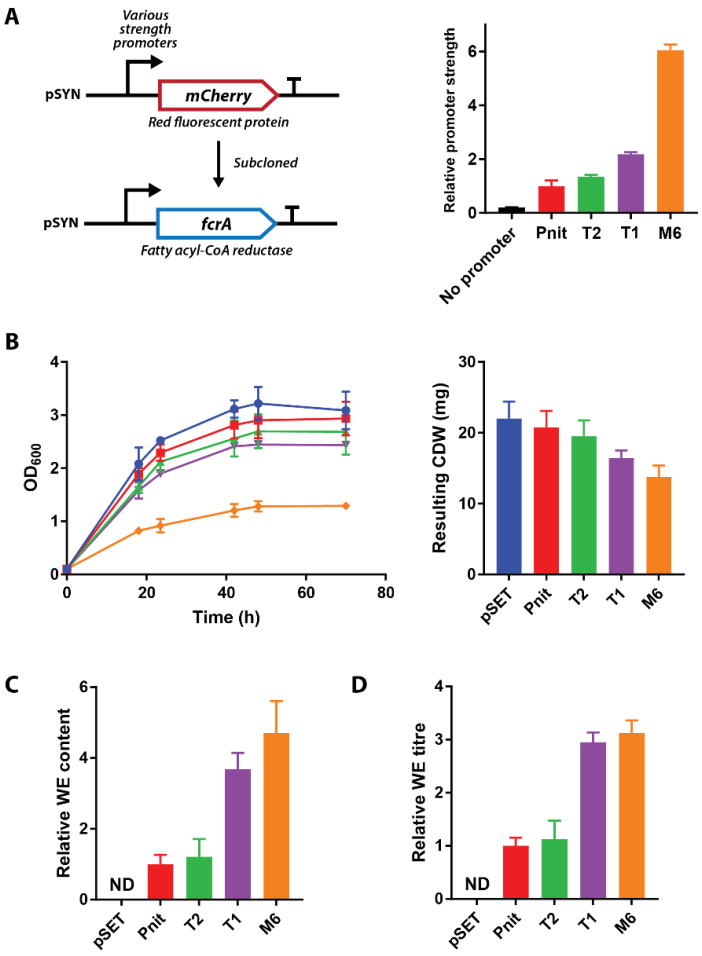

Figure 3.11 Constitutive overexpression of *fcrA* using pSYN.

(A) *fcrA* was subcloned into pSYN plasmids containing various strength constitutive promoters. (B) Growth of transformed strains in 50 mL of N^- media, and resulting CDW. Neutral lipids were extracted using MTBE, dried down under nitrogen, and resuspended in chloroform. Relative WEs content (C) and titre (D) was determined using GC/MS, and normalized against the P_{nit} promoter. Values represent the mean of biological duplicates. Error is given as standard deviation.

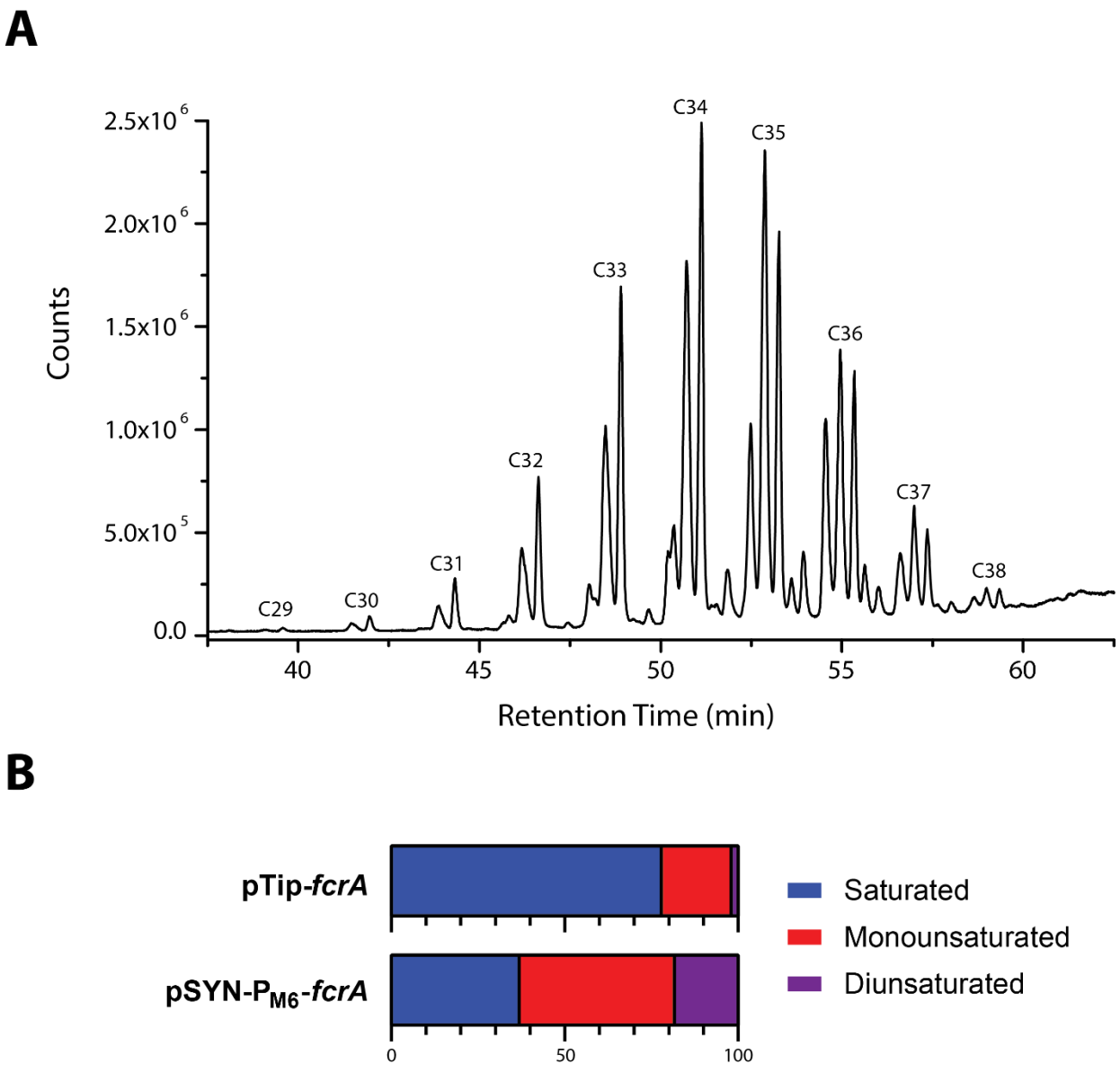

Figure 3.12 Profile of WEs produced in RHA1 containing an integrated, constitutively expressed copy of *fcrA*.

(A) GC/MS analysis of WEs isolated from RHA1:pSYN-P_{M6}-*fcrA*. (B) Distribution of WE unsaturation.

3.3 Identification and production of wax synthases in RHA1

Balancing metabolic pathways is critical to engineering biocatalysts able to convert feedstocks to products at industrially feasible yields, titers, and productivities (48, 239, 240). Among methodologies to achieve this balance, the "push-pull" strategy is a straightforward technique for improving metabolic flux (241). Using this strategy, gene expression is tuned at a minimal number of metabolic nodes, "pushing" carbon into the start of a metabolic pathway and "pulling" it out at the other end. Push-pull strategies improve metabolic flux by reducing feedback inhibition, and can improve biocatalyst performance and stability by reducing the accumulation of toxic intermediates. In section 3.1 and 3.2, I described "pushing" carbon into WE biosynthesis through the overproduction of FcrA, but relied on the activity of RHA1's endogenous WS/DGATs to perform the second step in WE biosynthesis, the esterification of fatty alcohol and acyl-CoA. To further increase WE accumulation, it would be advantageous to overproduce a WS/DGAT that has higher WS activity than DGAT activity, and thereby increase the "pull" of carbon into WEs. In the following work, the genetic tools I developed were applied to: identify wax synthases (WSs) able to increase WE accumulation in RHA1; co-express chromosomally integrated *fcrA* and WSs; and tune the expression of these enzymes to balance the WE biosynthetic pathway.

3.3.1 Identification of WSs in RHA1

RHA1 contains 16 WS/DGATs, any one of which might act as a WS (129, 131). To evaluate whether any of these has sufficient WS activity to contribute to WE accumulation, I examined the latter in previously constructed single and double *atf* mutants that have been implicated in

WE or TAG accumulation: Δ*atf3*, Δ*atf6*, Δ*atf8*, Δ*atf9*, Δ*atf10*, Δ*atf8*Δ*atf10*, and Δ*atf6*Δ*atf9*. Atf3 is the RHA1 homolog of $Atf1_{PD630}$, which has higher WS than DGAT activity (191). Consistent with this, partially purified Atf3 has *in vitro* WS activity (Round & Eltis, unpublished). During exponential growth, *atf6* and *atf9* are the most highly expressed WS/DGATs (131); and Atf6 has significant *in vitro* WS activity (184). Under lipid accumulating conditions, *atf8* and *atf10* are highly expressed (131). Finally, Atf3, Atf8, and Atf10 are associated with RHA1 LDs (195). Double mutants of the highly expressed *atf*s were selected to contend with the redundancy of lipid biosynthesis enzymes in RHA1. Mutant strains were grown under each of two conditions that promote WE production: growth on fatty alcohols (Figure 3.13); and while overproducing FcrA from a plasmid (Figure 3.14). WE accumulation was assessed using TLC. None of the mutants produced detectably lower amounts of WEs under either tested conditions. This suggests that none of the encoded enzymes functions as a WS.

Subsequently, a bioinformatic approach was attempted to identify RHA1 enzymes that may function as WSs. In this approach, four homologs possessing higher WS activity than DGAT activity were selected from WE-accumulating Gram-negative bacteria: *ws1* and *ws2* from *Marinobacter hydrocarbonoclasticus* DSM 8798 (242), *atfA* from *Acinetobacter calcoaceticus* ADP1 (176), and *atfA2* from *Alcanivorax borkumensis* (243). The amino acid sequences of these WSs were aligned with those of the RHA1 WS/DGATs and a phylogenetic tree was constructed. The characterized Gram-negative WSs clustered independently of RHA1 WS/DGATs (Figure 3.15), preventing the identification of a rhodococcal WS. Similar clustering was observed when WS/DGATs were aligned using their respective N- and C-terminal domains (244).

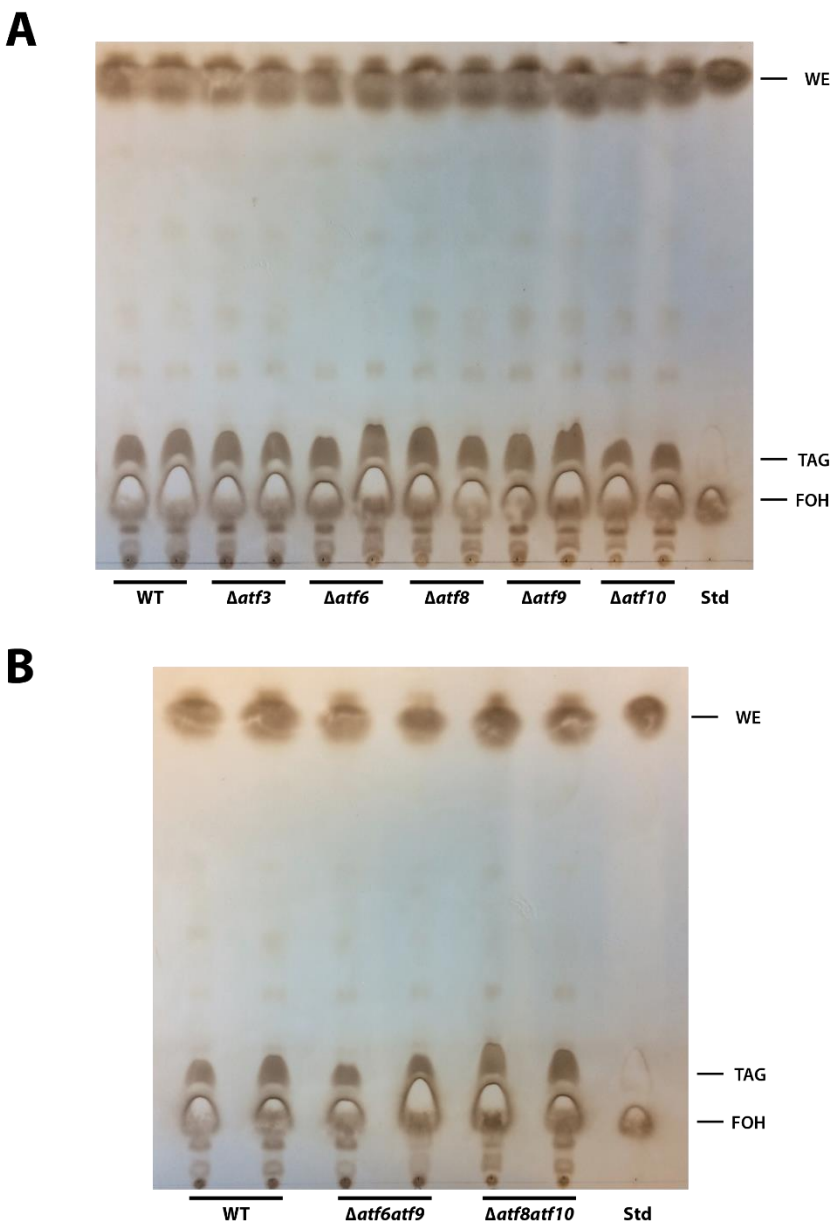

Figure 3.13 TLC analysis of WE accumulation in *atf* mutants during growth on fatty alcohols.

Neutral lipids produced by (A) single and (B) double *atf* deletion mutants during growth on fatty alcohols under lipid accumulating conditions (N^- media). Std - lane loaded with a mixture of stearyl stearate, glyceryl tripalmitate and hexadecanol.

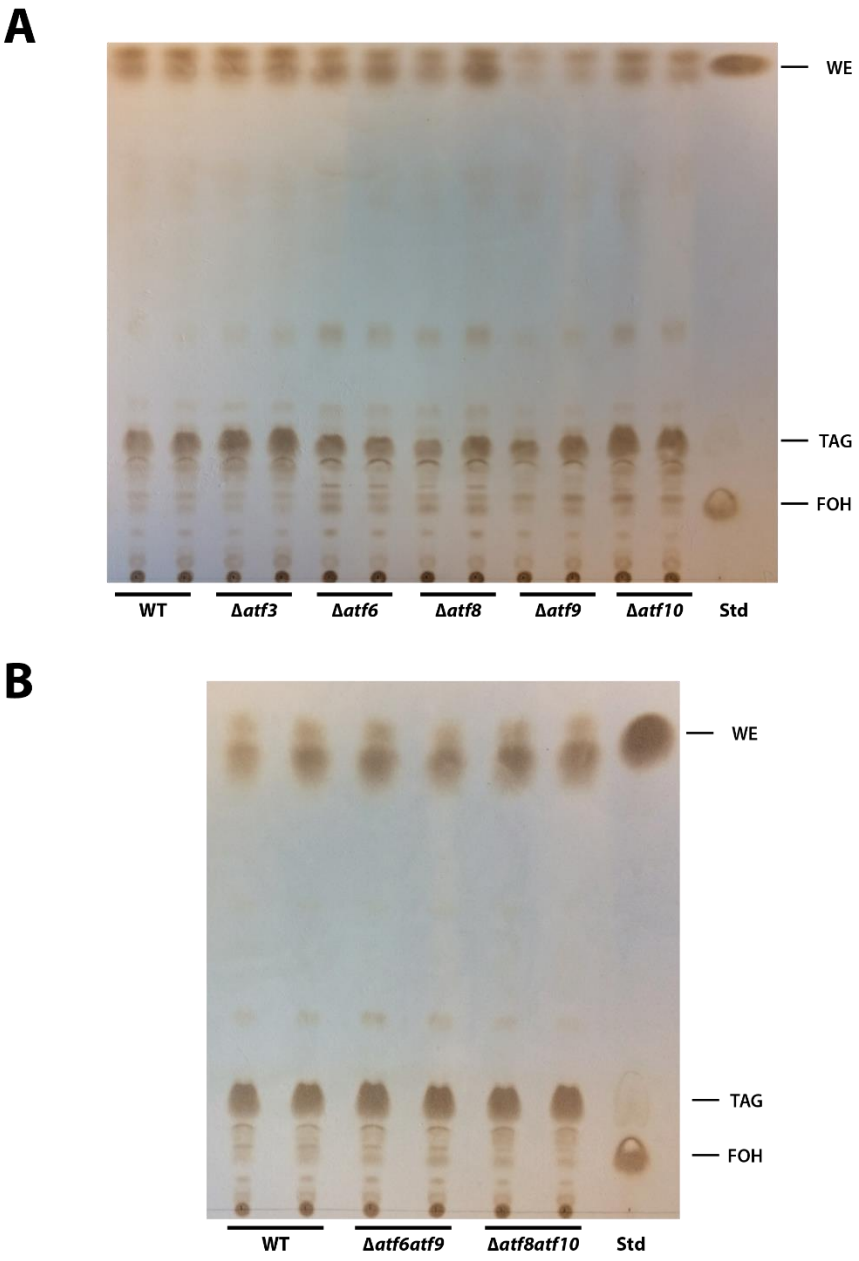

Figure 3.14 TLC analysis of WE accumulation in *atf* mutants during fcrA overproduction.

Neutral lipids produced by (A) single and (B) double *atf* deletion mutants overproducing FcrA (pTip-*fcrA*). Standard lanes contain stearyl stearate, glyceryl tripalmitate, and hexadecanol. Decrease in WEs in the Δ*atf9* single mutant is due to a loading of less sample, reflected in the decreased intensity of all lipid species.

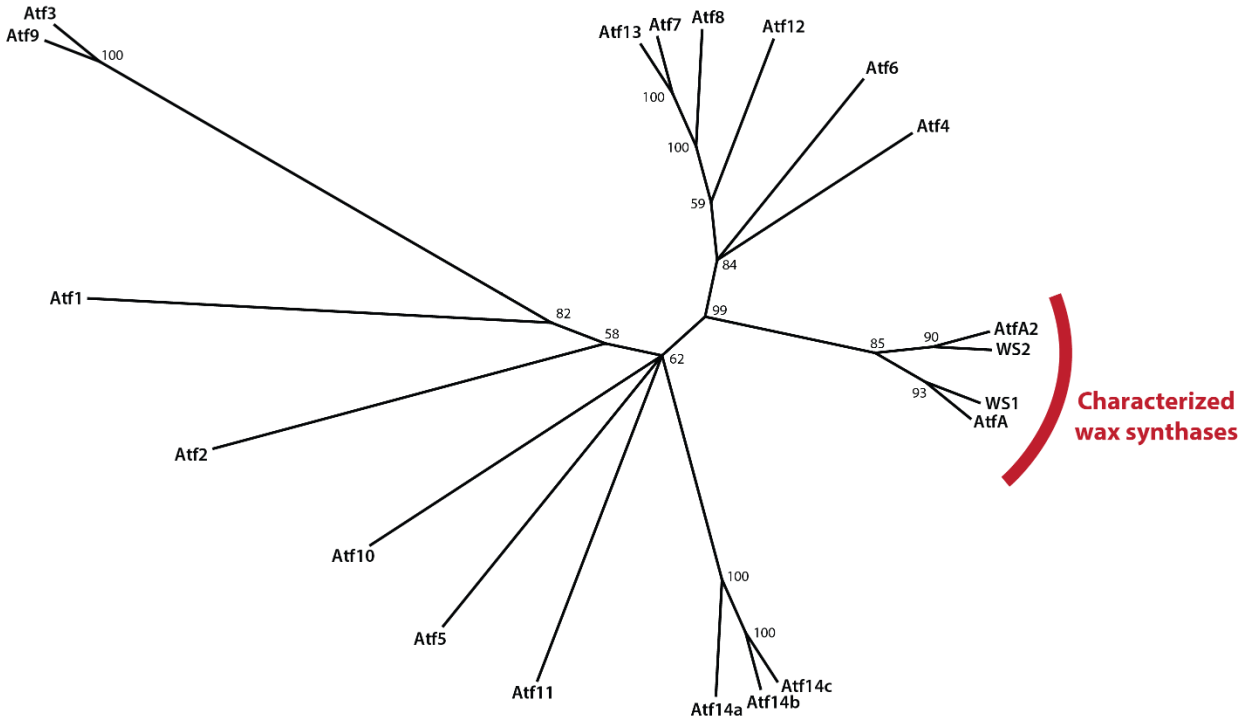

Figure 3.15 Bioinformatic analysis of RHA1 WS/DGATs and characterized WSs.

Amino acid sequences aligned with MUSCLE, unrooted tree assembled using UPGMA. Bootstrap values are displayed at branch points. Characterized WSs: WS1 and WS2 from *M. hydrocarbonoclasticus* DSM 8798, AtfA from *A. calcoaceticus* ADP1, and AtfA2 from *A. borkumensis*.

3.3.2 Co-expression of *fcrA* with characterized WSs.

As no rhodococcal WS was identified, characterized WSs (*ws1*, *ws2*, *atfA* and *atfA2*) were codon-optimized for expression in RHA1 using a codon-context approach (203), cloned into pTip vectors, and expressed in RHA1. In brief, amino acid sequences of 1545 highly expressed genes (approximately the 20th percentile of expressed genes) in RHA1 grown on minimal media

with glucose as sole carbon source (189), were collected and used to generate a codon context usage pattern. WS genes were then codon-optimized on the basis of codon context and 5' RNA folding instability using the COOL web server (203). Resulting sequences were synthesized, cloned into pTip vectors, and transformed into RHA1. To assess the ability of RHA1 to express synthesized WSs, recombinant RHA1 was grown in LB media, WS expression was induced, and SDS-PAGE was used to evaluate the levels of soluble and insoluble proteins in cellular lysate. All four WSs were produced and observed in the insoluble fraction, which includes membrane-associated proteins (Figure 3.16).

To assess the ability of the heterologously produced WSs to modulate WE accumulation, I co-transformed RHA1 with pSYN-P_{M6}-*fcrA* and pTip vectors containing each of the synthesized WS genes. Transformants were grown in C^- and N^- media, and WS expression was induced in early log phase. GC/MS analyses of the extracted lipids established that, as compared to RHA1:pSYN-P_{M6}-*fcrA* with an empty pTip vector, expression of *ws1* and *atfA* led to a 20-fold increase in WE content during exponential growth on C^- media, while expression of *ws2* led to a 60-fold increase and expression of *atfA2* did not increase WE content (Figure 3.17A). Under lipid-accumulating conditions (N^- media), the expression of *ws2* led to a 7-fold increase in WE content as compared to the empty vector control (Figure 3.17B).

Expression of WSs also resulted in a greater proportion of unsaturated WEs (Figure 3.17C). Thus, expression of *ws1*, *ws2*, or *atfA* during exponential growth in C^- media resulted in the production of WEs between 29 to 38 C atoms in length. Unsaturated WEs represented 45-55% of total WEs, with a ~4:1 mix of mono- and diunsaturated species. Under lipid-accumulating

conditions (N^- media), WE were also 29 to 38 C atoms in length. Expression of *ws2* increased the unsaturated fraction of WEs from approximately 60 to 80%, with a ~1:1 mix of mono- and diunsaturated species, as compared to the ~4:1 mix of the empty vector control. Interestingly, while expression of *atfA* or *ws1* did not increase WE content, they did increase the unsaturation of accumulated WEs, to 75 and 90%, respectively, and the mix of mono- and diunsaturated WEs, to ~2:3 and ~3:2, respectively. As only expression of *ws2* led to an increase in WE content in N^- media, it was chosen for further biocatalyst development.

The relative increase in unsaturated WEs in the strains producing heterologous WSs is consistent with the substrate preferences of those enzymes. For example, AtfA has a preference for long-chain acyl-CoAs and can incorporate both saturated and unsaturated species into the WE (177). Similarly, WS1 and WS2 have equal or higher activity towards unsaturated acyl-CoAs, and can even accept polyunsaturated species, such as linolenoyl-CoA (C18:3) (242). For the alcohol moiety, the WSs display a preference for long-chain alcohols, and are able to utilize a range of unusual substrates such as aromatic alcohols, long-chain diols, long-chain thiols, and isoprenoid alcohols (177, 242, 245, 246). Further, AftA has a slight preference for unsaturated C18:1 fatty alcohols over saturated C18:0 (177). However, the lack of commercially available unsaturated fatty alcohols has prevented a comprehensive analysis of WSs activity on a wider range of these substrates. Activity of these enzymes towards unsaturated fatty alcohols can be inferred from GC/MS analysis of *de novo* WEs accumulated in *Marinobacter* and *Acinetobacter*, in which 50 and 100%, respectively, of the alcohol moiety of WEs were unsaturated (184).

WS2 is a robust enzyme active in a range of hosts. In *E. coli*, heterologous expression of WS2 in a strain modified for fatty acid production led to the production of WEs (247). WS2 was expressed in a modified strain of *Saccharomyces cerevisiae* to produce alkyl esters of short chain fatty acids (248, 249), and resulted in higher yields than either AtfA or $Atf1_{PD630}$ (249). WS2 also facilitated the WE accumulation when heterologously produced in plants, such as *Nicotiana benthamiana* (215) and *Camelina sativa* (250). Interestedly, in *C. sativa*, expression of WS2 led to a 2.5-fold greater increase in WE content than did AtfA. Similar to RHA1, the WEs produced by both AtfA and WS2 in *C. sativa* contained greater proportions of unsaturated acyl- and alcohol-chains (~1.5 to 2-fold more than saturated species (250)).

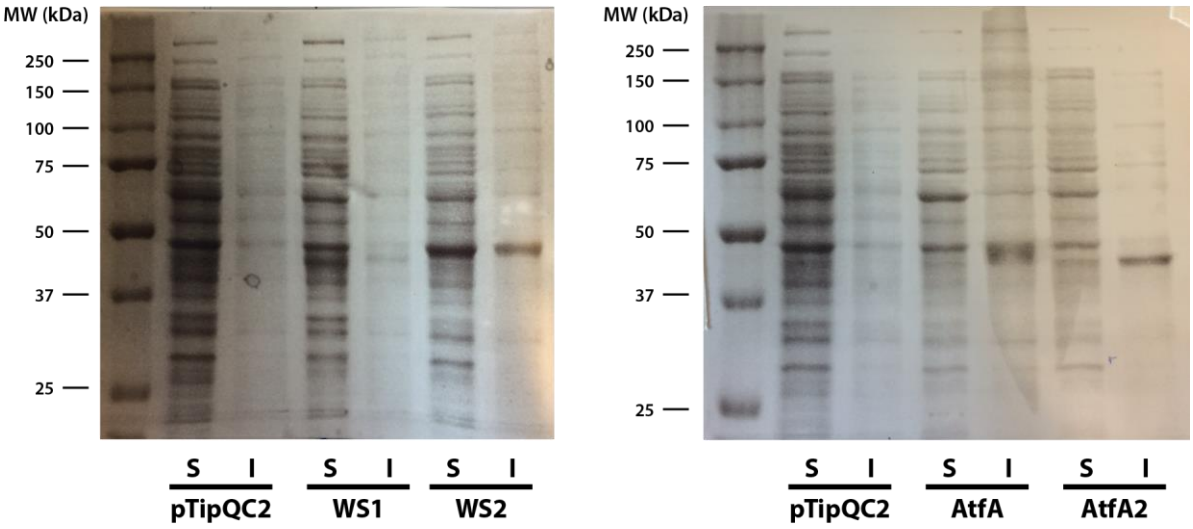

Figure 3.16 Expression of codon-optimized wax synthases.

Previously characterized WSs were codon optimized using a codon-context approach, cloned into pTip vectors, and expressed in RHA1, pTipQC2 was included as an empty vector control. Lane labels: S, soluble fraction; I, insoluble membrane fraction. Expected molecular weights: WS1, 51.5 kDa; WS2, 52.5 kDa; AtfA, 51.8 kDa; AtfA2, 49.8 kDa.

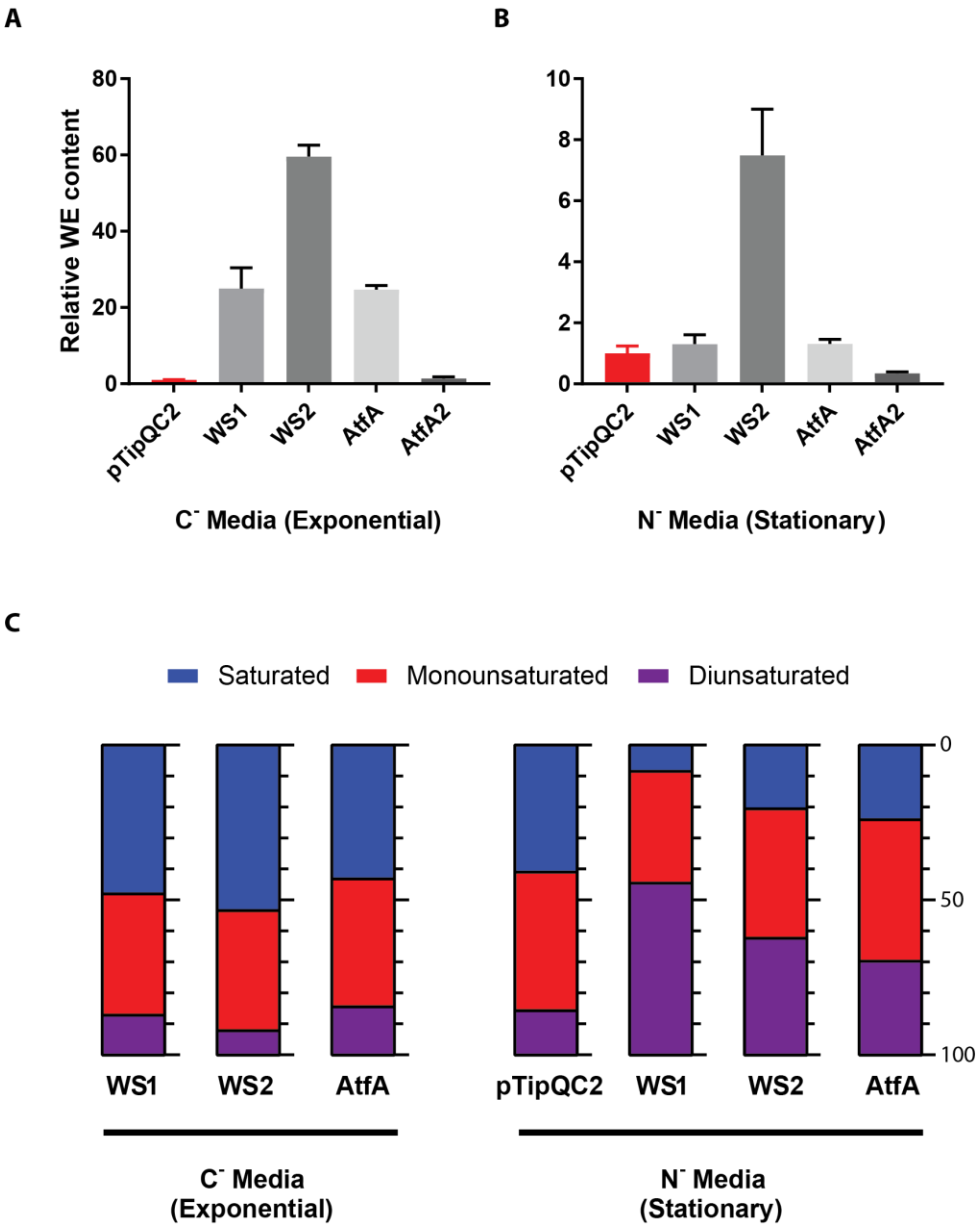

Figure 3.17 WE production in RHA1 expressing a chromosomally integrated *fcrA* and plasmid-borne WSs. Strains were assessed for WE content in (A) C^- and (B) N^- media. (C) Relative levels of saturated, monounsaturated and diunsaturated WEs. Lipids were extracted and analyzed by GC/MS. WE content was normalized against the strain control strain, expressing a chromosomally integrated *fcrA* and transformed with an empty vector (pTipQC2). Values represent the mean of biological duplicates. Error is given as standard deviation.

3.3.3 Genomic co-integration of *fcrA* and *ws2*

To create a biocatalyst suited for industrial applications, both *fcrA* and *ws2* were integrated into the RHA1 genome. Co-integration was accomplished by assembling a cassette of tandemly expressed genes in an integrative plasmid-backbone. Such cassettes allow for the independent expression of multiple genes each with their own standardized promoter, RBS, and terminator to facilitate the assembly and balancing of metabolic pathways (251). In brief, I used optimized universal-linkers designed by Torella *et al* (204) to create: (A) pLB, a pSET152-based plasmid in which two universal-linkers sequences flank restriction sites allowing for linearization of the backbone; and (B) a series of universal-linkers containing primers, designed to target regions flanking the expression cassette of pSYN. Cassette fragments containing *fcrA* and *ws2,* and flanked by appropriate universal-linkers, were amplified from pSYN and assembled in pLB using Gibson assembly (Figure 3.18A). Fragments were amplified from pSYN plasmids containing one of three constitutive promoters of different strength (P_{M6}, P_{T1}, and P_{T2}) in order to create nine expression cassette variants differing in the expression levels of *fcrA* and *ws2* (Figure 3.18B).

Initially, Gibson assembly mixtures were transformed into *E. coli* for screening and propagation using standard procedures. However, none of the resulting colonies contained inserts of the expected size. Sequencing a selection of plasmids revealed different truncations and mutations within the arrays, of the type associated with gene toxicity (252, 253). I hypothesized that toxicity was due to leaky expression of *fcrA* and *ws2* when the assembled expression cassettes were propagated at high-copies numbers in *E. coli*. To circumvent this toxicity, I directly

transformed the assembled plasmids into RHA1. Electroporation of Gibson assembly mixtures into RHA1 resulted in ~1 x 10^3 transformants per µg of vector, of which ~50% contained the full-length expression cassette as assessed by colony PCR. Correct assembly of gene cassettes was confirmed by sequencing. Arrays for six of the nine strains were created. I was unable to obtain transformants containing cassettes in which *fcrA* expression was driven by P_{M6}, the strongest constitutive promoter, as they proved genetically unstable. Herein, strains containing the genetic cassettes are named for the promoters driving *fcrA*/*ws2* expression (e.g., T1/T2 designates the strain in which: *fcrA* and *ws2* expression are driven by P_{T1} and P_{T2}, respectively).

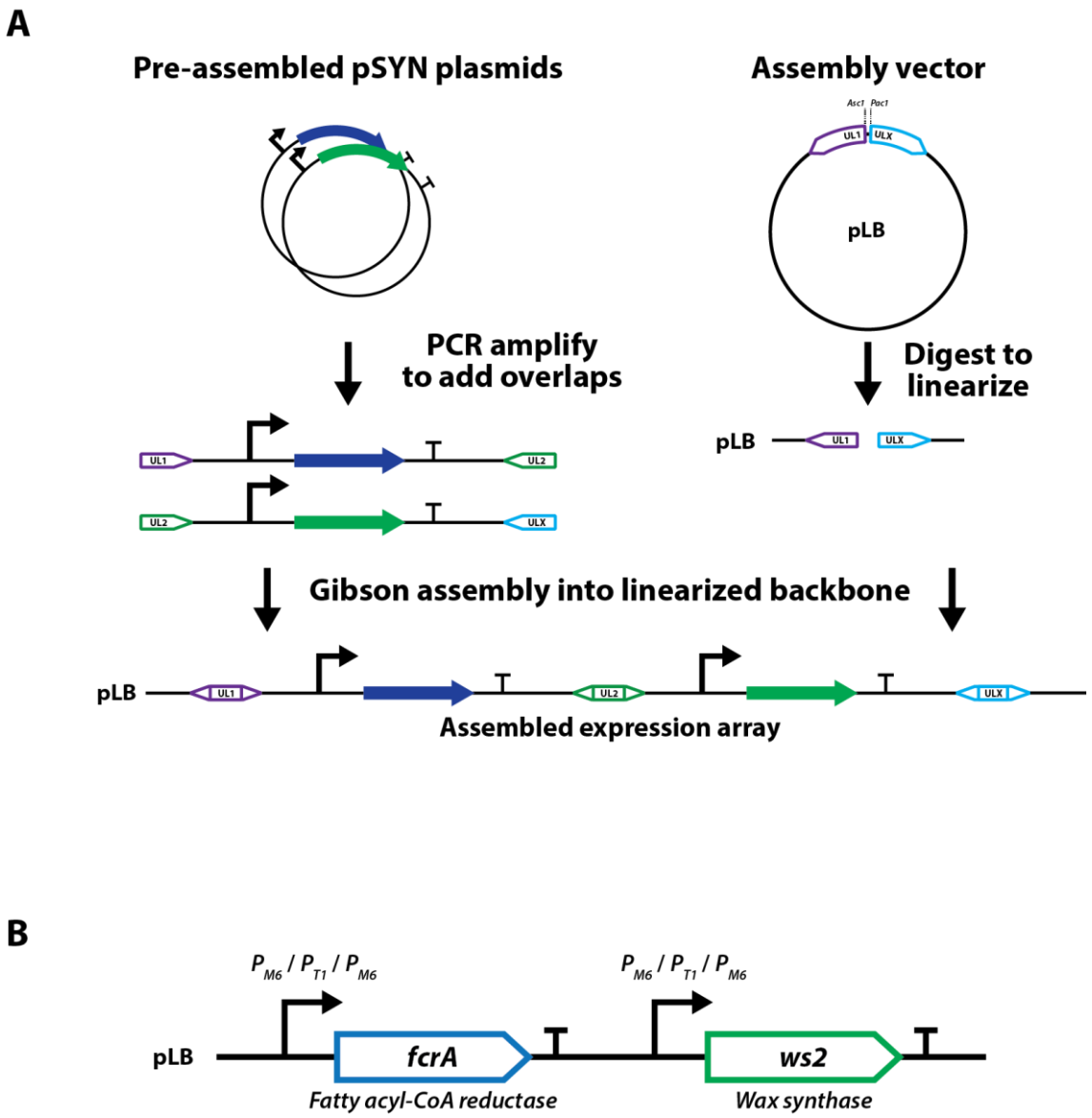

Figure 3.18 Assembly of *frcA* and *ws2* expression cassettes.

Gene arrays allow for the expression of multiple genes from standardized expression cassettes. (A) Design and assembly of gene expression arrays in *Rhodococcus* using unique linker sequences developed by Torella *et al* (204) (UL1, UL2, and ULX). (B) Array variants for integrated co-expression of *fcrA* and *ws2*.

3.3.4 Screening WE accumulating strains

RHA1 strains transformed with *fcrA* and *ws2* expression cassettes were screened for WE accumulation during exponential phase (C^- media) and under lipid-accumulating conditions (N^- media) (Figure 3.19). Similar to plasmid-based experiments, strains expressing chromosomal copies of *fcrA* and *ws2* accumulated WEs in exponential phase. WE were not detected in exponential phase for control stains containing either an empty pSET152 vector or a chromosomally integrated *fcrA* expressed constitutively by P_{M6}. During lipid accumulation, co-expression of *fcrA* and *ws2* led to a 3- to 12- fold increase in WE content, when compared to the control strain only expressing *fcrA*. As increased expression of *fcrA* and *ws2* resulted in decreased biomass, I also considered WE titres. Co-expression of *ws2* led to a 2.5- to 10-fold increase in WE titre.

Strains were also evaluated for metabolic burden, as manifested through reduction in exponential growth rate and increased lag phase (254). I evaluated these parameters in C^- media using an automated microplate reader. Strains containing a chromosomal copy of *fcrA* grew at 65% the rate of the empty vector control, while strains expressing both *fcrA* and *ws2* grew at 65 to 97% the rate of the control strain, despite accumulating WEs. Lag phase duration was dependent on the cumulative expression of *fcrA* and *ws2*. Strains expressing *fcrA* alone had lag-phases 1.9-fold larger than the empty vector control, while the co-expression strains had lag phases 1.2- to 2.2-fold higher than the control strain. The four co-expression strains containing combinations of P_{T1} and P_{T2} promoters (T1/T1, T1/T2, T2/T1, and T2/T2) had: a 7- to 12-fold increase in WE

content, an 8- to 10-fold increases in WE titre, and maintained growth rates 80 to 97% of the pSET152 control. Therefore, these four strain were chosen for further characterization.

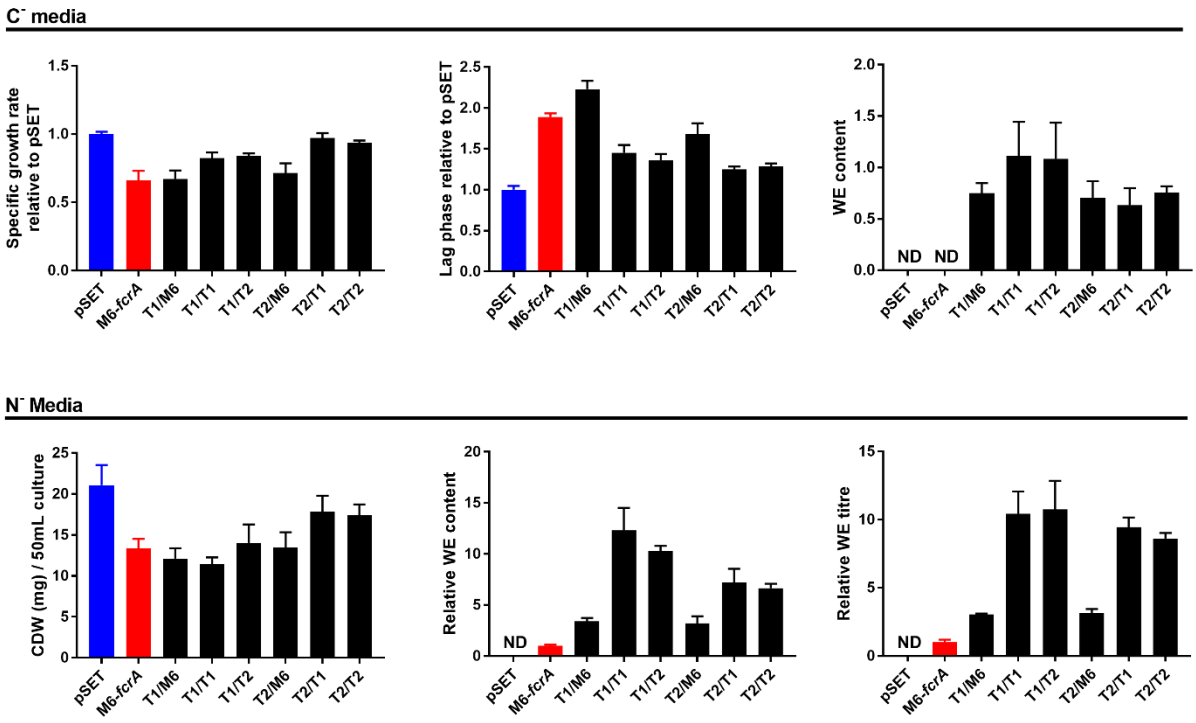

Figure 3.19 WE production and growth parameters of RHA1 strains containing chromosomally integrated *fcrA* and *ws2* expression cassettes.

Strains were screened in C- media for growth rate, lag phase and WE content. Strains were screened in N- media for biomass yield, WE content and WE titre. WEs were extracted and analyzed by GC/MS. Values represent the mean of biological triplicate. Error is given as standard deviation.

3.3.5 Characterization of WE accumulating strains

The four RHA1 strains transformed with expression cassettes containing combinations of P_{T1} and P_{T2} promoters were evaluated for biocatalyst performance (Table 4). Specifically, I examined growth rates, dry biomass yields, lipid yields, and lipid content in exponential growth and lipid-accumulating conditions. During exponential growth in C^- media, specific growth rates were between 0.20 and 0.22 h^{-1}, with biomass yields between 0.54 and 0.69 g per g glucose. Under these conditions, neutral lipid content was approximately 20% of CDW, with a yield of 0.12 to 0.16 g per g glucose. WEs represented 4 to 7% of CDW, with a yields of 0.03 to 0.04 g per g glucose. Under lipid accumulating conditions (N^- media), biomass yields were between 0.25 and 0.36 g per g glucose. Neutral lipid content was approximately 35% of CDW, with a yield of 0.09 to 0.14 g per g glucose, and WEs represented 11 to 16% of CDW, with yields of 0.04 to 0.05 g per g glucose. The WE species produced by T1/T1, the strain having the highest WE content under lipid accumulating conditions, and T2/T1, having the highest WE content in exponential growth, were nearly identical under lipid-accumulating conditions (Figure 3.20): WEs were 29 to 38 C atoms in length, of which 75% were unsaturated with a ~2:1 mix of mono- and diunsaturated species.

Table 3.4 Characterization of integrative co-expression strains that accumulate WEs.

C⁻ Media (Exponential)[a]						
RHA1 strain	**Specific growth rate** (h^{-1})[b]	**Y Biomass** (g / g glucose)	**Y Neutral lipids** (g / g glucose)	**NL content** (% CDW)	**Y WEs** (g / g glucose)	**WE content** (% CDW)
WT	0.25 ± 0.01	0.64 ± 0.11	0.19 ± 0.04	30 ± 2	---	---
T1/T1	0.20 ± 0.02	0.64 ± 0.09	0.13 ± 0.02	20.6 ± 0.4	0.027 ± 0.009	4 ± 1
T1/T2	0.20 ± 0.01	0.69 ± 0.12	0.16 ± 0.04	22 ± 4	0.038 ± 0.039	5 ± 5
T2/T1	0.21 ± 0.01	0.54 ± 0.07	0.12 ± 0.02	21.3 ± 0.5	0.038 ± 0.008	7 ± 1
T2/T2	0.22 ± 0.01	0.58 ± 0.11	0.13 ± 0.03	21.3 ± 0.5	0.028 ± 0.008	5 ± 1
N⁻ Media (Stationary)[a]						
RHA1 strain	---	**Y Biomass** (g / g glucose)	**Y Neutral lipids** (g / g glucose)	**NL content** (% CDW)	**Y WEs** (g / g glucose)	**WE content** (% CDW)
WT	---	0.37 ± 0.06	0.14 ± 0.02	39.0 ± 0.5	---	---
T1/T1	---	0.30 ± 0.02	0.11 ± 0.01	36.9 ± 0.2	0.047 ± 0.002	15.7 ± 0.4
T1/T2	---	0.25 ± 0.09	0.09 ± 0.04	36 ± 3	0.038 ± 0.013	15 ± 2
T2/T1	---	0.32 ± 0.03	0.13 ± 0.01	34 ± 1	0.034 ± 0.002	10.8 ± 0.2
T2/T2	---	0.36 ± 0.01	0.14 ± 0.01	36 ± 2	0.038 ± 0.002	10.6 ± 0.4

[a]Experimental values represent the mean of biological triplicate, error is given as standard deviation.

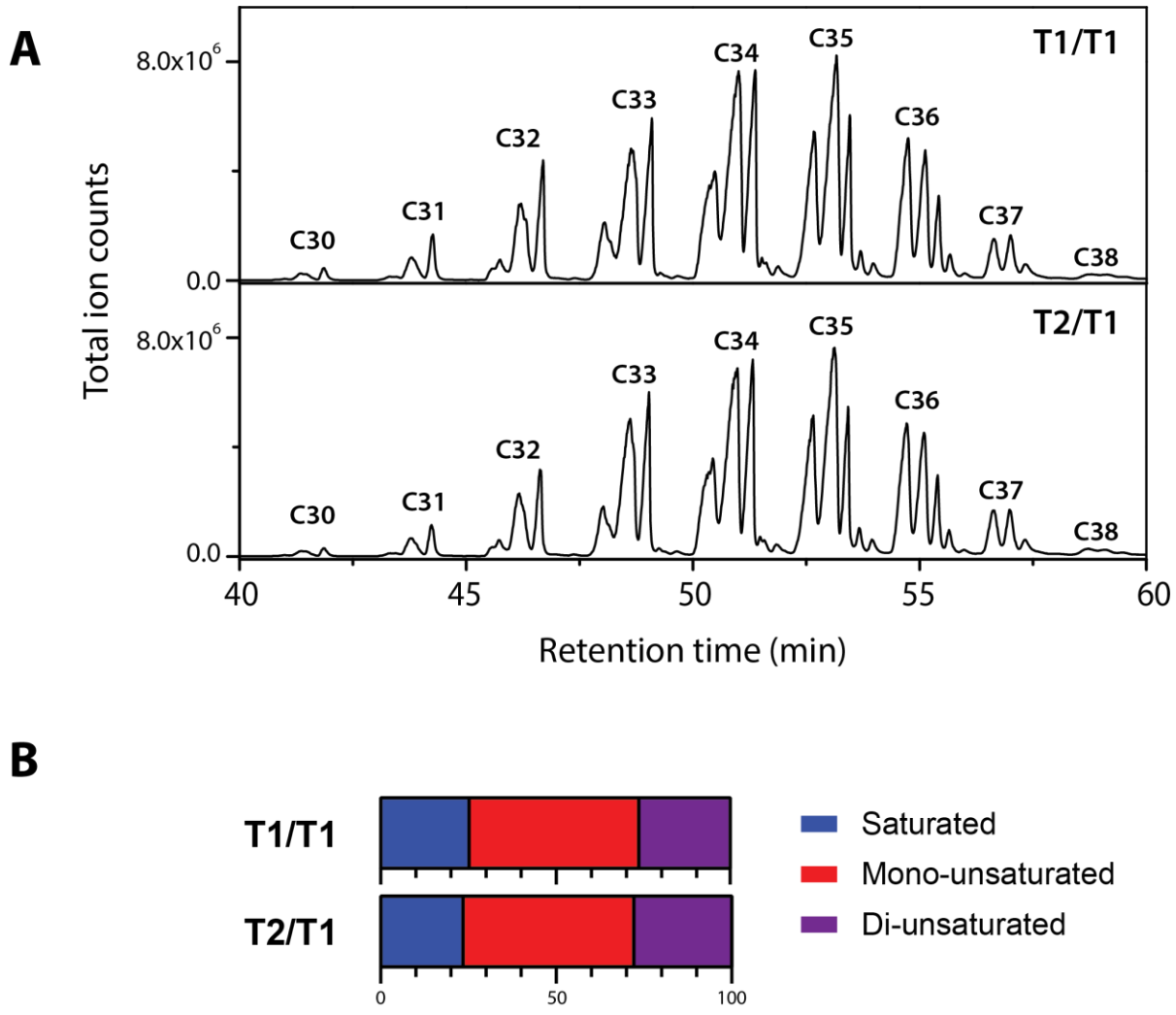

Figure 3.20 WE profile of T1/T1 and T2/T1 RHA1 strains containing chromosomal *fcrA* and *ws2*.

(A) GC/MS analysis of WEs isolated from RHA1 strains. (B) Distribution of WE unsaturation.

3.3.6 A rhodococcal biocatalyst for the production of WEs

In this study, I examined native and heterologous WSs that promote and modify WE accumulation in *Rhodococcus*. Using gene deletions, I determined that none of the RHA1 *atf* genes previously implicated in TAG or WE biosynthesis have a significant role in WE accumulation. This result suggests that the WE accumulation reported in Sections 3.1 and 3.2 is due either to the activity of an as-yet-to-be identified Atf functioning as a WS, or to the combined activities of multiple Atfs present in RHA1 (131). In the latter case, the redundancy of rhodococcal Atfs complicates the identification of these enzymes. Interestingly, a similar result was recently observed in PD630 (255), where deletion of $atf1_{PD630}$, previously shown to have greater WS than DGAT activity, did not affect WE accumulation. It is clear that further work is required to identify rhodococcal WSs, including targeted approaches to examine the expression of *atf*s under WE-accumulating conditions, and screening approaches using the WS overproduction techniques developed in Section 3.3.2. Furthermore, WE accumulation in *atf* mutants should be examined using quantitative techniques, such as GC/MS.

Despite failing to identify a rhodococal WS, this study established that WS2 functions as a wax synthase in RHA1, significantly contributing to the biosynthesis of WEs. More specifically, co-expression of *fcrA* and *ws2* increased WE accumulation during both exponential growth and under lipid accumulating conditions. Furthermore, expression of WSs resulted in WEs of increased unsaturation. Finally, an RHA1 strain co-expressing genomically integrated copies of *fcrA* and *ws2* resulted in a bacterium capable of accumulating WEs to greater than 15% of CDW with yields of 0.05 g per g glucose under conditions that promote lipid production.

Chapter 4: Conclusion

This research characterized the ability of *Rhodococcus* to accumulate WEs, resulted in the creation of genetic tools for this genus, and yielded a biocatalyst for the production of WEs. More specifically, examining WE accumulation in RHA1 led to the identification of a fatty acyl-CoA reductase (FcrA) encoded by the RHA1 genome. FcrA was biochemically characterized, and overproduced from a plasmid to promote WE synthesis. To facilitate the creation of rhodococcal biocatalysts, pSYN a modular integrative-vector was created and used to identify a series of strong constitutive promoters. Finally, to understand and improve WE accumulation in *Rhodococcus*, the ability of WSs to modulate WE accumulation was examined, identifying *ws2* as an effective WS in RHA1. A rhodococcal biocatalyst co-expressing *fcrA* and *ws2*, accumulated significant amounts of WEs. These contributions are discussed in more detail below.

4.1 The role of WEs in the physiology of mycolic acid-containing bacteria

This study presents evidence for the *de novo* synthesis of WEs in rhodococci from non-alkane substrates. Nevertheless, the amount of WEs found in RHA1 is significantly less than what has been reported in *M. tuberculosis*. More specifically, WEs comprised a larger portion of the neutral lipids in *M. tuberculosis* than in WT RHA1 under all the conditions we tested and, as quantified by [1-^{14}C]-oleate incorporation into neutral lipid pools after 6 h, were approximately 10,000-fold higher than in RHA1 under stress conditions (182, 183). It is unclear whether the WE content of *M. tuberculosis* is representative of mycolic acid-containing bacteria. For

example, WEs were not detected in *Mycobacterium smegmatis* under nitrogen-limited conditions by TLC (176), an observation that does not preclude their presence in the trace amounts reported here for RHA1. WEs have been suggested to contribute to dormancy and membrane permeability in *M. tuberculosis* (183). Interestingly, *M. tuberculosis* is one of the few mycobacterial species that does not produce mycolate-derived WEs (256), a class of lipids synthesized from keto-mycolic acids by a Baeyer-Villiger monooxygenase (257). These mycolate-derived WEs are integral components of the mycolic acid layer of mycobacteria (258) and appear to be replaced by methoxy-mycolates in *M. tuberculosis*. More studies are required to elucidate the role of WEs in mycolic acid-containing bacteria.

4.2 Overproduction of FcrA provides *de novo* fatty alcohols for WE synthesis

This study established that FcrA is an alcohol-forming fatty acyl-CoA reductase that contributes to the biosynthesis of WEs in RHA1. More specifically, purified FcrA catalyzed the reduction of various fatty acyl-CoAs to the corresponding fatty alcohol in a NADPH dependent manner. Overproduction of FcrA in RHA1 provided an enzymatic route for the production of *de novo* fatty alcohols, which resulted in the bacterium accumulating WEs to greater than 10% of CDW under conditions that promote TAG production. These initial data highlighted the potential of rhodococci for the sustainable production of WEs. More specifically, simply overproducing FcrA from a plasmid in RHA1 yielded a strain able to accumulate ~13% of its CDW in WEs. At the time, this exceeded the levels of any natural or engineered strains, including *A. calcoaceticus* and *M. aquaeolei* VT8, which accumulated *de novo* WEs to ~6% and ~10% CDW, respectively

(174, 259). Similarly, engineered strains of *E. coli* and *Acinetobacter* accumulated WEs to 1% and 3% CDW, respectively (260, 261), or resulted in large reductions to growth yields (262).

Interestingly, the WEs accumulated during the overproduction of FcrA are remarkably similar to spermaceti WEs, which were historically valued as lubricants and cosmetics due to their excellent physicochemical properties (185). The rhodococcal and spermaceti WEs are remarkably similar with respect to several characteristics, including range of chain lengths, with C34 WEs being the majority species, lengths of acyl- and alcohol-components, and degree of unsaturation (172). The similarity of rhodococcal and spermaceti WEs enhances the former's industrial relevance and justifies further research into the production of rhodococcal WEs.

4.3 Synthetic biology tools for rhodococcal biocatalysts

This study created and characterized genetic tool required to develop rhodococci as industrial biocatalysts. Specifically, I created pSYN, a modular integrative-vector for *Rhodococcus*, and used it to characterize a series of strong constitutive rhodococcal promoters. The constitutive promoters identified in this study were used to balance a biosynthetic pathway for WE production. Recently, DeLorenzo *et al* created a library of constitutive rhodococcal promoters (263) using saturation mutagenesis of a constitutive *Streptomyces* promoter (264). While this approach was successful in creating a promoter library with a transcriptional range of ~45-fold, the promoters were not compared to previously characterized constitutive promoters, such as P_{nit} (157). Therefore, the results of DeLorenzo *et al.* study are hard to compare to the constitutive promoters I derived from P_{10}. Interestingly, the authors note that mutagenesis was unable to create a promoter stronger than the original *Streptomyces* promoter (263). The inability to easily

engineer promoters stronger than naturally occurring ones has been extensively reported (265, 266). Therefore, it would be beneficial to use the strong constitutive promoters I discovered to create libraries of mutagenized promoters covering a greater range of strengths. Indeed, libraries of promoters of a wide range of strengths can benefit biocatalyst development. For example, promoters chosen from a library of synthetic T7 promoters of strengths covering a 1000-fold range were used to precisely balance the violacein biosynthetic pathway in *E. coli*, leading to a 3.2-fold increase in violacein production (103).

The constitutive promoters identified in this study, together with their derivatives, will provide a basis on which other genetic tools can be constructed. For example, the P_{10}-derived promoters could be used to create tetracycline-responsive hybrid promoters for both research into fundamental rhodococcal biology and to construct advanced genetic tools (108, 111, 267). Recently, a tetracycline-responsive hybrid promoters from mycobacteria was modified for use in *Rhodococcus*, resulting in a promoter that could be induced ~67-fold (268). Nevertheless, this is almost three times lower than the 200-fold induction seen in the original mycobacterial promoter (269), and much lower than other engineered tetracycline-responsive promoters, which can be induced up to 5000-fold (108). As discussed in Section 1.1.6, hybrid tetracycline-inducible promoters are created by the addition of *tetO* sequences into strong constitutive promoters. As this promoter modification usually results in a decrease of promoter strength (111, 269), developing a hybrid tetracycline-inducible promoter from constitutive P_{10}-derived promoters may provide a stronger and more robust inducible promoter for use in *Rhodococcus*.

The modular, site-specific integrative vectors developed in this study aided in the rapid creation and characterization of rhodococcal strains, allowing for the efficient screening of both promoters and WSs, and the creation of WE biosynthetic pathways. Site-specific integrases have long been a fundamental tool in the genetic manipulation of actinobacteria (270, 271) and have been adapted to a wide range of hosts and applications (272). Such integrases allow for a "plug and play" approach to genetic manipulation and synthetic biology that has enabled a range of technological achievements, such as the assembly of large polyketide synthase complexes in *Streptomyces* (273), rapid genome engineering and promoter discovery in *Pseudomonas* (61), and multipart DNA assembly, both *in vitro* and *in vivo* (272). Expanding the use of site-specific integrases in *Rhodococcus* beyond the ϕC31 integrase used in this study would greatly increase the ability to rapidly create rhodococcal biocatalysts. However, this will require site-specific integrases such as BxB1, RV, FC1, or FBT1 (274) to be characterized in *Rhodococcus*, and the creation of a rhodococcal strain that carries a "docking-site" consisting of multiple unique integrase attachment sequences (272).

The pSYN integrative vector designed in this study is not without drawbacks. In Section 3.3, due to toxicity resulting from the high-levels of gene expression when the plasmid was propagated at high-copy numbers, I was unable to clone the *fcrA* and *ws2* co-expression cassette into *E. coli*. While this was circumvented by direct transformation into RHA1, it would have been advantageous to propagate DNA in *E. coli*. In aid of this, pSYN could be modified to carry a low-copy *E. coli* origin such as those found in the Standard European Vector Architecture database (275).

4.4 The complexities of lipid biosynthesis in *Rhodococcus*

This study highlights the challenges of studying lipid biosynthesis in *Rhodococcus*. Using gene deletions, I investigated the role of five WS/DGATs in WE accumulation. However, while these genes had been previously implicated in WE or TAG biosynthesis, none appeared to play a significant role in WE accumulation. RHA1 possesses 16 *atf* genes, which likely have overlapping functions. This redundancy makes rhodococcal lipid biosynthesis genes challenging to study and further explains why we still lack a clear global understanding of lipid biosynthesis pathways in *Rhodococcus*.

The study of lipid biosynthetic enzymes is further complicated by the limited solubility of these enzymes and their substrates. Many of these enzymes have been shown to be associated with LDs (165, 195) and, like many membrane-bound or associated proteins, are challenging to characterize biochemically. For example, Atf3 from RHA1 was expressed and partially purified as a soluble maltose-binding protein (MBP)-fusion protein, but became unstable when the MBP was removed proteolytically. Furthermore, Atf3 was unable to be solubilized using a series of ionic and non-ionic detergents (Round & Eltis, unpublished). Indeed, although several FARs and WS/DGATs have been purified fused to solubility tags (180, 181, 184, 276), these fusion proteins are relatively poorly characterized. The low solubility of lipid substrates prevents saturation of the enzymes, and thereby the determination of true steady-state kinetic parameters (184, 276). Even when obtained, *in vitro* biochemical data does not always translate to *in vivo* behaviour, as was observed for $Atf1_{PD630}$ (255). These challenges long stymied efforts to obtain structural data for bacteria WS/DGATs (277), and only recently has the first crystal structure

been published (276). Even then, the authors noted that a number of disordered regions with low electron density complicated structural analyses (276). However, this structure may serve as a basis for structural comparisons that could shed light on the substrate specificity of WS/DGATs.

Effectively harnessing the biosynthetic potential of rhodococci for the production of oleochemicals will required further research into the complexities of rhodococcal lipid synthesis. Due to the complex nature of this process, its elucidation will require a multi-layer approach combining transcriptomics, proteomics, and metabolomics data, collected under meticulously controlled growth conditions, into a systems-level understanding of the lipid biosynthesis phenotype. Furthermore, the network regulating this phenotype must be determined. Finally, due to the redundancy of lipid biosynthesis genes, high-throughput genome engineering techniques are needed to efficiently validate this understanding.

4.5 The potential of rhodococci for the sustainable production of WEs

In this study, I created a rhodococcal biocatalyst that accumulated WEs to greater than 15% of CDW, at yields of 0.05 g per g glucose, while maintaining 80% of the specific growth rate of the WT strain. This result exceeds the ~12% WEs (CDW; yield of 0.04 g per g glucose) recently achieved in *A. baylyi* ADP1, a natural WE-producing strain, by overproducing Arc1, an aldehyde-forming fatty acyl-CoA reductase (278). Furthermore, during exponential growth, the rhodococcal biocatalyst designed in this study had a dry biomass yield of 0.64 g per g glucose, higher than both *E. coli* and the oleaginous yeast *Y. lipolytica*, which yielded 0.5 and 0.325 g per g glucose, respectively (169). As biomass yields are directly related to overall process yields (169), the high dry biomass yield of our biocatalyst will help maximize WE yields in a future

bioprocess. The high biomass yield suggests that RHA1 is highly efficient at using glucose as a carbon source. Indeed, in PD630, another oleaginous *Rhodococcus*, ~93% of glucose is utilized through the Entner–Doudoroff (ED) pathway (279). Despite producing less ATP, the ED pathway is more efficient then the classical Embden–Meyerhof–Parnas pathway due to its 3.5-fold lower protein requirement (121).

The ED pathway also provides NADPH required for the synthesis of storage compounds such as neutral lipids. As most glucose is utilized via the ED pathway by PD630 (279), and this pathway is highly upregulated in RHA1 during growth on glucose under lipid accumulating conditions (189), the production of a 32-carbon WE can be defined by the following stoichiometric reaction:

$$8\ \text{Glucose} + 6\ \text{ATP} + 8\ \text{NADPH} \rightarrow \text{C32 WE} + 10\ \text{NADH} \quad (1)$$

Assuming that the remaining ATP requirements are fulfilled by oxidative phosphorylation and NADPH is generated through the pentose phosphate pathway (~5% of glucose flux in PD630 (279)):

$$1\ NADH \rightarrow \sim 2.5\ ATP \quad (2)$$

$$1\ \text{Glucose} + 1\ \text{ATP} \rightarrow 12\ \text{NADPH} + 6CO_2 \quad (3)$$

WE production in *Rhodococcus* can be simplified to:

$$8.66\ \text{Glucose} \rightarrow \text{C32 WE} + 7.6\ \text{NADH} \quad (4)$$

Based on these considerations, the theoretical yield of C32 WEs is ~0.32 g per g glucose.

As theoretical WE yields are much higher than that of our biocatalyst, 0.05 g per g glucose, metabolic engineering has the potential to significantly increase WE yields. One obvious inefficiency in our strain is that WE represented only 40% of the accumulated neutral lipids. As TAG and WE biosynthesis directly compete for acyl-CoA substrates, reducing carbon flow into TAGs has the potential to greatly increase WE yields. This could be accomplished through the deletion of *atf* genes involved in TAG biosynthesis (131) or PAPs involved in the production of TAG intermediates (280). However, as discussed above, the redundancy of rhodococcal lipid biosynthetic enzymes complicates implementation of this approach. Further engineering strategies involve increasing carbon flow into lipid biosynthesis by increasing the expression of ACC, the first committed step in lipid biosynthesis. This strategy has greatly increased lipid synthesis in *E. coli* and *Y. lipolytica* (241, 281). Finally, as lipid and WE biosynthesis requires large amounts of redox co-factors, in particular NADPH, modulating redox co-factors, analogously to what has been done in *Y. lipolytica* (169) has the potential to further increase yields toward the theoretical maximum.

Neutral lipid synthesis in our biocatalyst was lower than expected. Specifically, under lipid-accumulating conditions, our biocatalyst reached a neutral lipid content of ~35% of CDW. This is significantly lower than the >50% of CDW normally reported for rhodococci (129, 131, 282). Unexpectedly, the neutral lipid yields in our strain were similar in both exponential growth and lipid-accumulating conditions, ~0.12 g per g glucose. This yield is lower than the 0.18 g per g glucose that has previously been reported in *Rhodococcus* (283). This suggests that our culture conditions were not ideal for our biocatalyst, and that addressing this through advanced bioprocess design could increase both WE content and yield.

4.6 Remaining questions

There are fundamental questions to be answered about how WEs affect rhodococcal physiology. During the course of this study, the subcellular location of WE was assumed to be within LD. However, WEs are known to be stored in bodies with a range of different morphologies (137). Indeed, at least three different WEs storage bodies have been reported: circular phospholipid-covered lipid bodies, similar to those normally found in rhodococci; small, rectangular inclusions with a phospholipid layer; and large, sheet-like disk structures that do not appear to have a phospholipid layer. In the biocatalyst constructed in this study, it is unclear how the WEs are sequestered. Thus, they may be located in the cytoplasmic membrane, in LDs together with the TAGs, or as separate storage bodies. Answering these questions will require the fractionation and analysis of cellular components (165, 195) using biochemical and electron microscopy techniques.

Similarly, the subcellular localization of FcrA and WS2 need to be determined. Specifically, it is of interest to determine whether these enzymes interact with LDs, WE storage bodies, or the membrane. Interestingly, three of the four characterized WSs that I expressed in RHA1 were active during exponential growth, resulting in large increases in WEs. However, only WS2 resulted in an increase in WE accumulation under lipid-accumulating conditions (Figure 3.17). It is unclear whether this is due to the substrate specificity of the enzymes (e.g., the relative levels of WS and DGAT activities in the enzymes) or some other factor such as their subcellular localization. Overall, these results illustrate the importance of screening approaches in creating

biosynthetic pathways, and highlight our lack of understanding of neutral lipid accumulation in rhodococci.

4.7 Concluding remarks

The work presented in this thesis advances our knowledge of lipid biosynthesis in *Rhodococcus* and describes the potential of an engineered rhodococci for the production of oleochemicals, specifically high-value WEs. In identifying key enzymes involved in WE accumulation, I determined that rhodococci could be harnessed as biocatalysts for the production of WEs. By expanding the genetic tools available in these bacteria, I created a basis on which biocatalysts and future genetic tools can be built. Applying these tools to assembly a rhodococcal biocatalyst, I built a microbial platform for the production of high-value WEs. Finally, I identified future directions to continue the development of these tools and biocatalyst, as well as highlight fundamental research questions that still exist around lipid biosynthesis in *Rhodococcus*. In conclusion, this work contributes to the development of novel bioprocesses for an important class of oleochemicals that may ultimately allow us to phase out their unsustainable production from sources such as petroleum and palm oil.

References

1. **Caplice E, Fitzgerald GF.** 1999. Food fermentations: role of microorganisms in food production and preservation. Int J Food Microbiol **50:**131-149.
2. **Kriwaczek P.** 2012. Babylon: Mesopotamia and the birth of civilization. St. Martin's Press, New York.
3. **Campbell-Platt G.** 2014. Fermented foods. *In* Batt CA (ed), Encyclopedia of food microbiology. Academic Press, New York.
4. **McGovern PE, Zhang J, Tang J, Zhang Z, Hall GR, Moreau RA, Nuñez A, Butrym ED, Richards MP, Wang C-s, Cheng G, Zhao Z, Wang C.** 2004. Fermented beverages of pre- and proto-historic China. Proc Natl Acad Sci USA **101:**17593-17598.
5. **McGovern PE, Fleming SJ, Katz SH.** 2004. The origins and ancient history of wine. Routledge, London.
6. **Leeuwenhoek. Av.** Letter to Thomas Gale of June 14th 1680, pp. 6-10 in the second printing carried out by Hendrik van Croonevelt at Delft in 1694.
7. **Alba-Lois L, Segal-Kischinevzky C.** 2010. Beer & wine makers. Nat Ed **3:**17.
8. **Barnett James A.** 1998. A history of research on yeasts 1: Work by chemists and biologists 1789–1850. Yeast **14:**1439-1451.
9. **Barnett James A.** 2000. A history of research on yeasts 2: Louis Pasteur and his contemporaries, 1850–1880. Yeast **16:**755-771.
10. **Pasteur L.** 1876. Studies on fermentation. Macmillan, London.
11. **Demain AL, Vandamme EJ, Collins J, Buchholz K.** 2016. History of industrial biotechnology. *In* Wittmann C, Liao JC (ed), Industrial biotechnology.
12. **Adams MR.** 2017. The birth of modern industrial microbiology: The acetone–butanol fermentation. Int J Hist Eng Technol **87:**81-95.
13. **Weizmann C.** 1919. Production of acetone and alcohol by bacteriological processes. patent US1315585A.
14. **Nanda S, Dalai AK, Kozinski JA.** 2017. Butanol from renewable biomass: Highlights of downstream processing and recovery techniques. *In* Mondal P, Dalai AK (ed), Sustainable utilization of natural resources. CRC Press, Boca Raton.
15. **Domagk G.** 1935. Chemotherapie der bakteriellen Infektionen. Angew Chem **48:**657-667.
16. **Fleming A.** 1929. On antibacterial action of culture of *Penicillium*, with special reference to their use in isolation of *B. influenzae*. Br J Exp Pathol **10:**226–236.
17. **Davies J, Davies D.** 2010. Origins and evolution of antibiotic resistance. Microbiol Mol Biol Rev **74:**417-433.
18. **Lynn JM.** 1949. Medical progress: Sulfonamide toxicity. Calif Med **70:**58-56.
19. **Neushul P.** 1993. Science, government, and the mass production of penicillin. J Hist Med Allied Sci **48:**371-395.
20. **Daemmrich A.** 2009. Synthesis by microbes or chemists? Pharmaceutical research and manufacturing in the antibiotic era. Hist Technol **25:**237-256.

21. **Raper Kenneth B.** 1946. The development of improved penicillin-producing molds. Ann N Y Acad Sci **48:**41-56.
22. **Demain AL.** 2010. History of industrial biotechnology. *In* Soetaert W, Vandamme EJ (ed), In industrial biotechnology: Sustainable growth and economic success.
23. **Burkovski A, Kramer R.** 2002. Bacterial amino acid transport proteins: occurrence, functions, and significance for biotechnological applications. Appl Microbiol Biotechnol **58:**265-74.
24. **Becker J, Wittmann C.** 2016. Industrial microorganisms: *Corynebacterium glutamicum*. *In* Wittmann C, Liao J (ed), Industrial biotechnology: Microorganisms.
25. **Martens J-H, Barg H, Warren M, Jahn D.** 2002. Microbial production of vitamin B12. Appl Microbiol Biotechnol **58:**275-285.
26. **Cohen SN, Chang ACY.** 1973. Recircularization and autonomous replication of a sheared r-factor DNA segment in *Escherichia coli* transformants. Proc Natl Acad Sci USA **70:**1293-1297.
27. **Cohen SN, Chang ACY, Boyer HW, Helling RB.** 1973. Construction of biologically functional bacterial plasmids *in vitro*. Proc Natl Acad Sci USA **70:**3240-3244.
28. **Efstratiadis A, Kafatos FC, Maxam AM, Maniatis T.** 1976. Enzymatic *in vitro* synthesis of globin genes. Cell **7:**279-288.
29. **Maxam AM, Gilbert W.** 1977. A new method for sequencing DNA. Proc Natl Acad Sci USA **74:**560-564.
30. **Sanger F, Nicklen S, Coulson AR.** 1977. DNA sequencing with chain-terminating inhibitors. Proc Natl Acad Sci USA **74:**5463-5467.
31. **Itakura K, Hirose T, Crea R, Riggs A, Heyneker H, Bolivar F, Boyer H.** 1977. Expression in *Escherichia coli* of a chemically synthesized gene for the hormone somatostatin. Science **198:**1056-1063.
32. **Goeddel DV, Kleid DG, Bolivar F, Heyneker HL, Yansura DG, Crea R, Hirose T, Kraszewski A, Itakura K, Riggs AD.** 1979. Expression in *Escherichia coli* of chemically synthesized genes for human insulin. Proc Natl Acad Sci U S A **76:**106-10.
33. **T. BU, K. B.** 2005. Highlights in biocatalysis – Historical landmarks and current trends. Engineering in Life Sciences **5:**309-323.
34. **Misset O.** 1997. Development of new lipases. *In* Ee JHv, Misset O, Baas EJ (ed), Enzymes in detergency. Marcel Dekker, New York.
35. **Haugen SP, Ross W, Gourse RL.** 2008. Advances in bacterial promoter recognition and its control by factors that do not bind DNA. Nat Rev Microbiol **6:**507.
36. **Pribnow D.** 1975. Bacteriophage T7 early promoters: Nucleotide sequences of two RNA polymerase binding sites. J Mol Biol **99:**419-443.
37. **Schaller H, Gray C, Herrmann K.** 1975. Nucleotide sequence of an RNA polymerase binding site from the DNA of bacteriophage fd. Proc Natl Acad Sci USA **72:**737-741.
38. **Kapanidis AN, Margeat E, Laurence TA, Doose S, Ho SO, Mukhopadhyay J, Kortkhonjia E, Mekler V, Ebright RH, Weiss S.** 2005. Retention of Transcription Initiation Factor σ^{70} in Transcription Elongation: Single-Molecule Analysis. Mol Cell **20:**347-356.

39. **Li J, Zhang Y.** 2014. Relationship between promoter sequence and its strength in gene expression. Eur Phys J E **37:**86.
40. **Salis HM, Mirsky EA, Voigt CA.** 2009. Automated design of synthetic ribosome binding sites to precisely control protein expression. Nat Biotech **27:**946-950.
41. **Bailey J.** 1991. Toward a science of metabolic engineering. Science **252:**1668-1675.
42. **Woolston BM, Edgar S, Stephanopoulos G.** 2013. Metabolic engineering: Past and future. Annu Rev Chem Biomol Eng **4:**259-288.
43. **Stephanopoulos G, Vallino JJ.** 1991. Network rigidity and metabolic engineering in metabolite overproduction. Science **252:**1675-81.
44. **Vallino J, Stephanopoulos G.** 1993. Metabolic flux distributions in *Corynebacterium glutamicum* during growth and lysine overproduction. Biotechnol Bioeng **41:**633-646.
45. **Anderson S, Marks CB, Lazarus R, Miller J, Stafford K, Seymour J, Light D, Rastetter W, Estell D.** 1985. Production of 2-keto-L-gulonate, an intermediate in L-ascorbate synthesis, by a genetically modified *Erwinia herbicola*. Science **230:**144-149.
46. **Peoples OP, Sinskey AJ.** 1989. Poly-beta-hydroxybutyrate (PHB) biosynthesis in *Alcaligenes eutrophus* H16. Identification and characterization of the PHB polymerase gene (*phbC*). J Biol Chem **264:**15298-303.
47. **Yim H, Haselbeck R, Niu W, Pujol-Baxley C, Burgard A, Boldt J, Khandurina J, Trawick JD, Osterhout RE, Stephen R, Estadilla J, Teisan S, Schreyer HB, Andrae S, Yang TH, Lee SY, Burk MJ, Van Dien S.** 2011. Metabolic engineering of *Escherichia coli* for direct production of 1,4-butanediol. Nat Chem Biol **7:**445-52.
48. **Paddon CJ, Westfall PJ, Pitera DJ, Benjamin K, Fisher K, McPhee D, Leavell MD, Tai A, Main A, Eng D, Polichuk DR, Teoh KH, Reed DW, Treynor T, Lenihan J, Jiang H, Fleck M, Bajad S, Dang G, Dengrove D, Diola D, Dorin G, Ellens KW, Fickes S, Galazzo J, Gaucher SP, Geistlinger T, Henry R, Hepp M, Horning T, Iqbal T, Kizer L, Lieu B, Melis D, Moss N, Regentin R, Secrest S, Tsuruta H, Vazquez R, Westblade LF, Xu L, Yu M, Zhang Y, Zhao L, Lievense J, Covello PS, Keasling JD, Reiling KK, Renninger NS, Newman JD.** 2013. High-level semi-synthetic production of the potent antimalarial artemisinin. Nature **496:**528-532.
49. **Wang HH, Isaacs FJ, Carr PA, Sun ZZ, Xu G, Forest CR, Church GM.** 2009. Programming cells by multiplex genome engineering and accelerated evolution. Nature **460:**894-898.
50. **DiCarlo JE, Norville JE, Mali P, Rios X, Aach J, Church GM.** 2013. Genome engineering in *Saccharomyces cerevisiae* using CRISPR-Cas systems. Nucleic Acids Res **41:**4336-4343.
51. **Bikard D, Jiang W, Samai P, Hochschild A, Zhang F, Marraffini LA.** 2013. Programmable repression and activation of bacterial gene expression using an engineered CRISPR-Cas system. Nucleic Acids Res **41:**7429-7437.
52. **Jiang W, Bikard D, Cox D, Zhang F, Marraffini LA.** 2013. RNA-guided editing of bacterial genomes using CRISPR-Cas systems. Nat Biotech **31:**233-239.
53. **Monk JM, Lloyd CJ, Brunk E, Mih N, Sastry A, King Z, Takeuchi R, Nomura W, Zhang Z, Mori H, Feist AM, Palsson BO.** 2017. iML1515, a knowledgebase that computes *Escherichia coli* traits. Nat Biotech **35:**904-908.

54. **Nikel PI, Martinez-Garcia E, de Lorenzo V.** 2014. Biotechnological domestication of pseudomonads using synthetic biology. Nat Rev Micro **12:**368-379.
55. **Johnson CW, Salvachúa D, Khanna P, Smith H, Peterson DJ, Beckham GT.** 2016. Enhancing muconic acid production from glucose and lignin-derived aromatic compounds via increased protocatechuate decarboxylase activity. metab Eng commun **3:**111-119.
56. **Yu S, Plan MR, Winter G, Krömer JO.** 2016. Metabolic engineering of *Pseudomonas putida* KT2440 for the production of para-hydroxy benzoic acid. Front Bioeng Biotechnol **4**.
57. **Park SH, Kim HU, Kim TY, Park JS, Kim S-S, Lee SY.** 2014. Metabolic engineering of *Corynebacterium glutamicum* for L-arginine production. Nat Commun **5:**4618.
58. **Rohles CM, Gießelmann G, Kohlstedt M, Wittmann C, Becker J.** 2016. Systems metabolic engineering of *Corynebacterium glutamicum* for the production of the carbon-5 platform chemicals 5-aminovalerate and glutarate. Microb Cell Fact **15:**154.
59. **Witthoff S, Schmitz K, Niedenführ S, Nöh K, Noack S, Bott M, Marienhagen J.** 2015. Metabolic engineering of *Corynebacterium glutamicum* for methanol metabolism. Appl Environ Microbiol **81:**2215-2225.
60. **Becker J, Zelder O, Haefner S, Schröder H, Wittmann C.** 2011. From zero to hero – Design-based systems metabolic engineering of *Corynebacterium glutamicum* for l-lysine production. Metab Eng **13**.
61. **Elmore JR, Furches A, Wolff GN, Gorday K, Guss AM.** 2017. Development of a high efficiency integration system and promoter library for rapid modification of *Pseudomonas putida* KT2440. metab Eng commun **5:**1-8.
62. **Cleto S, Jensen JVK, Wendisch VF, Lu TK.** 2016. *Corynebacterium glutamicum* metabolic engineering with CRISPR interference (CRISPRi). ACS Synth Biol **5:**375-385.
63. **Rytter JV, Helmark S, Chen J, Lezyk MJ, Solem C, Jensen PR.** 2014. Synthetic promoter libraries for *Corynebacterium glutamicum*. Appl Microbiol Biotechnol **98:**2617-2623.
64. **Smanski MJ, Zhou H, Claesen J, Shen B, Fischbach MA, Voigt CA.** 2016. Synthetic biology to access and expand nature's chemical diversity. Nat Rev Micro **14:**135-149.
65. **Adams BL.** 2016. The next generation of synthetic biology chassis: Moving synthetic biology from the laboratory to the field. ACS Synth Biol **5:**1328-1330.
66. **Gustavsson M, Lee SY.** 2016. Prospects of microbial cell factories developed through systems metabolic engineering. Microb Biotechnol **9:**610-617.
67. **Gay P, Le Coq D, Steinmetz M, Berkelman T, Kado CI.** 1985. Positive selection procedure for entrapment of insertion sequence elements in gram-negative bacteria. J Bacteriol **164:**918-21.
68. **Reyrat J-M, Pelicic V, Gicquel B, Rappuoli R.** 1998. Counterselectable markers: Untapped tools for bacterial genetics and pathogenesis. Infect Immun **66:**4011-4017.
69. **Hmelo LR, Borlee BR, Almblad H, Love ME, Randall TE, Tseng BS, Lin C, Irie Y, Storek KM, Yang JJ, Siehnel RJ, Howell PL, Singh PK, Tolker-Nielsen T, Parsek MR, Schweizer HP, Harrison JJ.** 2015. Precision-engineering the *Pseudomonas aeruginosa* genome with two-step allelic exchange. Nat protoc **10:**1820-1841.

70. **Quandt J, Hynes MF.** 1993. Versatile suicide vectors which allow direct selection for gene replacement in Gram-negative bacteria. Gene **127:**15-21.
71. **van der Geize R, Hessels GI, van Gerwen R, van der Meijden P, Dijkhuizen L.** 2001. Unmarked gene deletion mutagenesis of *kstD*, encoding 3-ketosteroid Δ^1-dehydrogenase, in *Rhodococcus erythropolis* SQ1 using *sacB* as counter-selectable marker. FEMS Microbiol Lett **205:**197-202.
72. **Park KT, Dahl JL, Bannantine JP, Barletta RG, Ahn J, Allen AJ, Hamilton MJ, Davis WC.** 2008. Demonstration of allelic exchange in the slow-growing bacterium *Mycobacterium avium* subsp. *paratuberculosis*, and generation of mutants with deletions at the *pknG*, *relA*, and *lsr2* loci. Appl Environ Microbiol **74:**1687-1695.
73. **Nakashima N, Miyazaki K.** 2014. Bacterial cellular engineering by genome editing and gene silencing. Int J Mol Sci **15:**2773-93.
74. **Vervoort Y, Linares AG, Roncoroni M, Liu C, Steensels J, Verstrepen KJ.** 2017. High-throughput system-wide engineering and screening for microbial biotechnology. Curr Opin Biotechnol **46:**120-125.
75. **Pines G, Freed EF, Winkler JD, Gill RT.** 2015. Bacterial recombineering: Genome engineering via phage-based homologous recombination. ACS Synth Biol **4:**1176-85.
76. **Murphy KC.** 1998. Use of bacteriophage lambda recombination functions to promote gene replacement in *Escherichia coli*. J Bacteriol **180:**2063-71.
77. **Zhang Y, Buchholz F, Muyrers JPP, Stewart AF.** 1998. A new logic for DNA engineering using recombination in *Escherichia coli*. Nat Genet **20:**123.
78. **Datsenko KA, Wanner BL.** 2000. One-step inactivation of chromosomal genes in *Escherichia coli* K-12 using PCR products. Proc Natl Acad Sci USA **97:**6640-6645.
79. **Huang Y, Li L, Xie S, Zhao N, Han S, Lin Y, Zheng S.** 2017. Recombineering using RecET in *Corynebacterium glutamicum* ATCC14067 via a self-excisable cassette. Sci Rep **7:**7916.
80. **Watts AG, Damager I, Amaya ML, Buschiazzo A, Alzari P, Frasch AC, Withers SG.** 2003. Trypanosoma cruzi trans-sialidase operates through a covalent sialyl-enzyme intermediate: tyrosine is the catalytic nucleophile. J Am Chem Soc **125:**7532-3.
81. **Wang HH, Isaacs FJ, Carr PA, Sun ZZ, Xu G, Forest CR, Church GM.** 2009. Programming cells by multiplex genome engineering and accelerated evolution. Nature **460:**894.
82. **Isaacs FJ, Carr PA, Wang HH, Lajoie MJ, Sterling B, Kraal L, Tolonen AC, Gianoulis TA, Goodman DB, Reppas NB, Emig CJ, Bang D, Hwang SJ, Jewett MC, Jacobson JM, Church GM.** 2011. Precise manipulation of chromosomes in vivo enables genome-wide codon replacement. Science **333:**348-53.
83. **Wang HH, Kim H, Cong L, Jeong J, Bang D, Church GM.** 2012. Genome-scale promoter engineering by coselection MAGE. Nat Methods **9:**591-3.
84. **Bao Z, Cobb RE, Zhao H.** 2016. Accelerated genome engineering through multiplexing. Wiley Interdiscip Rev Syst Biol Med **8:**5-21.
85. **Yan Q, Fong SS.** 2017. Challenges and advances for genetic engineering of non-model bacteria and uses in consolidated bioprocessing. Front Microbiol **8:**2060.

86. **Jiang W, Bikard D, Cox D, Zhang F, Marraffini LA.** 2013. RNA-guided editing of bacterial genomes using CRISPR-Cas systems. Nat Biotechnol **31:**233-9.
87. **Jinek M, Chylinski K, Fonfara I, Hauer M, Doudna JA, Charpentier E.** 2012. A programmable dual-RNA-guided DNA endonuclease in adaptive bacterial immunity. Science **337:**816-21.
88. **Qi LS, Larson MH, Gilbert LA, Doudna JA, Weissman JS, Arkin AP, Lim WA.** 2013. Repurposing CRISPR as an RNA-guided platform for sequence-specific control of gene expression. Cell **152:**1173-83.
89. **Jiang Y, Chen B, Duan C, Sun B, Yang J, Yang S.** 2015. Multigene editing in the *Escherichia coli* genome via the CRISPR-Cas9 system. Appl Environ Microbiol **81:**2506-2514.
90. **Ronda C, Pedersen LE, Sommer MOA, Nielsen AT.** 2016. CRMAGE: CRISPR optimized MAGE recombineering. Sci Rep **6:**19452.
91. **Endy D.** 2005. Foundations for engineering biology. Nature **438:**449.
92. **Drubin DA, Way JC, Silver PA.** 2007. Designing biological systems. Genes Dev **21:**242-254.
93. **Shimada T, Yamazaki Y, Tanaka K, Ishihama A.** 2014. The whole set of constitutive promoters pecognized by RNA polymerase RpoD holoenzyme of *Escherichia coli*. PLOS ONE **9:**e90447.
94. **Barnard A, Wolfe A, Busby S.** 2004. Regulation at complex bacterial promoters: how bacteria use different promoter organizations to produce different regulatory outcomes. Curr Opin Microbiol **7:**102-108.
95. **López-Maury L, Marguerat S, Bähler J.** 2008. Tuning gene expression to changing environments: from rapid responses to evolutionary adaptation. Nat Rev Genet **9:**583.
96. **Lewis M.** 2011. A tale of two repressors – a historical perspective. J Mol Biol **409:**14-27.
97. **Gilman J, Love J.** 2016. Synthetic promoter design for new microbial chassis. Biochem Soc Trans **44:**731-737.
98. **Heiss S, Hörmann A, Tauer C, Sonnleitner M, Egger E, Grabherr R, Heinl S.** 2016. Evaluation of novel inducible promoter/repressor systems for recombinant protein expression in *Lactobacillus plantarum*. Microb Cell Fact **15:**50.
99. **Binder D, Drepper T, Jaeger K-E, Delvigne F, Wiechert W, Kohlheyer D, Grünberger A.** 2017. Homogenizing bacterial cell factories: Analysis and engineering of phenotypic heterogeneity. Metab Eng **42:**145-156.
100. **Wang B, Barahona M, Buck M.** 2015. Amplification of small molecule-inducible gene expression via tuning of intracellular receptor densities. Nucleic Acids Res **43:**1955-1964.
101. **Alper H, Fischer C, Nevoigt E, Stephanopoulos G.** 2005. Tuning genetic control through promoter engineering. Proc Natl Acad Sci USA **102:**12678-12683.
102. **Ang J, Harris E, Hussey BJ, Kil R, McMillen DR.** 2013. Tuning response curves for synthetic biology. ACS Synth Biol **2:**547-567.
103. **Xu P, Rizzoni EA, Sul S-Y, Stephanopoulos G.** 2017. Improving metabolic pathway efficiency by statistical model-based multivariate regulatory metabolic engineering. ACS Synth Biol **6:**148-158.

104. **Jacob F, Monod J.** 1961. On the regulation of gene activity. Cold Spring Harb Symp Quant Biol **26:**193-211.
105. **Harley CB, Lawrie J, Betlach M, Crea R, Boyer HW, Hedgpeth J.** 1988. Transcription initiation at the *tet* promoter and effect of mutations. Nucleic Acids Res **16:**7269-7285.
106. **Goldstein MA, Doi RH.** 1995. Prokaryotic promoters in biotechnology, p 105-128. *In* El-Gewely MR (ed), Biotechnol Annu Rev, vol 1. Elsevier.
107. **de Boer HA, Comstock LJ, Vasser M.** 1983. The *tac* promoter: a functional hybrid derived from the *trp* and *lac* promoters. Proc Natl Acad Sci USA **80:**21-25.
108. **Bertram R, Hillen W.** 2008. The application of Tet repressor in prokaryotic gene regulation and expression. Microb Biotechnol **1:**2-16.
109. **Schnappinger D, Ehrt S.** 2014. Regulated expression systems for *Mycobacteria* and their applications. Microbiol Spectr **2:**03.
110. **Debowski AW, Verbrugghe P, Sehnal M, Marshall BJ, Benghezal M.** 2013. Development of a tetracycline-inducible gene expression system for the study of *Helicobacter pylori* pathogenesis. Appl Environ Microbiol **79:**7351-7359.
111. **Li H, Liao JC.** 2015. A synthetic anhydrotetracycline-controllable gene expression system in *Ralstonia eutropha* H16. ACS Synth Biol **4:**101-106.
112. **Scholz O, Henßler E-M, Bail J, Schubert P, Bogdanska-Urbaniak J, Sopp S, Reich M, Wisshak S, Köstner M, Bertram R, Hillen W.** 2004. Activity reversal of Tet repressor caused by single amino acid exchanges. Mol Microbiol **53:**777-789.
113. **Strong PJ, Xie S, Clarke WP.** 2015. Methane as a resource: Can the methanotrophs add value? Environ Sci Technol **49:**4001-4018.
114. **Kyung LO, Hoon HD, Ngoc NDT, Yeol LE.** 2016. Metabolic engineering of methanotrophs and its application to production of chemicals and biofuels from methane. Biofuel Bioprod Biorefin **10:**848-863.
115. **Martin G, Yup LS.** 2016. Prospects of microbial cell factories developed through systems metabolic engineering. Microb Biotechnol **9:**610-617.
116. **Linger JG, Vardon DR, Guarnieri MT, Karp EM, Hunsinger GB, Franden MA, Johnson CW, Chupka G, Strathmann TJ, Pienkos PT, Beckham GT.** 2014. Lignin valorization through integrated biological funneling and chemical catalysis. Proceedings of the National Academy of Sciences **111:**12013-12018.
117. **Calero P, Nikel PI.** 2018. Chasing bacterial chassis for metabolic engineering: A perspective review from classical to non-traditional microorganisms. Microb Biotechnol.
118. **Lindblad P, Lindberg P, Oliveira P, Stensjö K, Heidorn T.** 2012. Design, engineering, and construction of photosynthetic microbial cell factories for renewable solar fuel production. Ambio **41:**163-168.
119. **Wu Y, Shen X, Yuan Q, Yan Y.** 2016. Metabolic engineering strategies for co-utilization of carbon sources in microbes. Bioengineering **3:**10.
120. **Fuhrer T, Sauer U.** 2009. Different biochemical mechanisms ensure network-wide balancing of reducing equivalents in microbial metabolism. J Bacteriol **191:**2112-2121.

121. **Flamholz A, Noor E, Bar-Even A, Liebermeister W, Milo R.** 2013. Glycolytic strategy as a tradeoff between energy yield and protein cost. Proc Natl Acad Sci U S A **110:**10039-10044.
122. **Ng CY, Farasat I, Maranas CD, Salis HM.** 2015. Rational design of a synthetic Entner-Doudoroff pathway for improved and controllable NADPH regeneration. Metab Eng **29:**86-96.
123. **Beites T, Mendes MV.** 2015. Chassis optimization as a cornerstone for the application of synthetic biology based strategies in microbial secondary metabolism. Front Microbiol **6:**906.
124. **Marrakchi H, Lanéelle M-A, Daffé M.** 2014. Mycolic Acids: Structures, Biosynthesis, and Beyond. Chemistry & Biology **21:**67-85.
125. **Holder JW, Ulrich JC, DeBono AC, Godfrey PA, Desjardins CA, Zucker J, Zeng Q, Leach AL, Ghiviriga I, Dancel C, Abeel T, Gevers D, Kodira CD, Desany B, Affourtit JP, Birren BW, Sinskey AJ.** 2011. Comparative and functional genomics of *Rhodococcus opacus* PD630 for biofuels development. PLoS Genet **7:**e1002219.
126. **McLeod MP, Warren RL, Hsiao WWL, Araki N, Myhre M, Fernandes C, Miyazawa D, Wong W, Lillquist AL, Wang D, Dosanjh M, Hara H, Petrescu A, Morin RD, Yang G, Stott JM, Schein JE, Shin H, Smailus D, Siddiqui AS, Marra MA, Jones SJM, Holt R, Brinkman FSL, Miyauchi K, Fukuda M, Davies JE, Mohn WW, Eltis LD.** 2006. The complete genome of *Rhodococcus* sp. RHA1 provides insights into a catabolic powerhouse. Proc Natl Acad Sci USA **103:**15582-15587.
127. **Larkin MJ, Kulakov LA, Allen CCR.** 2006. Biodegradation by members of the genus *Rhodococcus*: Biochemistry, physiology, and genetic adaptation, p 1-29, Adv Appl Microbiol, vol 59. Academic Press.
128. **Larkin MJ, Kulakov LA, Allen CCR.** 2005. Biodegradation and *Rhodococcus* – Masters of catabolic versatility. Curr Opin Biotechnol **16:**282-290.
129. **Hernandez MA, Mohn WW, Martinez E, Rost E, Alvarez AF, Alvarez HM.** 2008. Biosynthesis of storage compounds by *Rhodococcus jostii* RHA1 and global identification of genes involved in their metabolism. BMC Genomics **9:**600.
130. **Dávila Costa JS, Herrero OM, Alvarez HM, Leichert L.** 2015. Label-free and redox proteomic analyses of the triacylglycerol-accumulating *Rhodococcus jostii* RHA1. Microbiology **161:**593-610.
131. **Amara S, Seghezzi N, Otani H, Diaz-Salazar C, Liu J, Eltis LD.** 2016. Characterization of key triacylglycerol biosynthesis processes in rhodococci. Sci Rep **6:**24985.
132. **van der Geize R, Dijkhuizen L.** 2004. Harnessing the catabolic diversity of rhodococci for environmental and biotechnological applications. Curr Opin Microbiol **7:**255-261.
133. **Nishiuchi Y, Baba T, Yano I.** 2000. Mycolic acids from *Rhodococcus, Gordonia*, and *Dietzia*. J Microbiol Methods **40:**1-9.
134. **Hsu F-F, Soehl K, Turk J, Haas A.** 2011. Characterization of mycolic acids from the pathogen *Rhodococcus equi* by tandem mass spectrometry with electrospray ionization. Anal Biochem **409:**112-122.

135. **Lambert PA.** 2002. Cellular impermeability and uptake of biocides and antibiotics in Gram-positive bacteria and mycobacteria. J Appl Microbiol **92:**46S-54S.
136. **De Carvalho CCCR, Da Cruz AARL, Pons M-N, Pinheiro HMRV, Cabral JMS, Da Fonseca MMR, Ferreira BS, Fernandes P.** 2004. *Mycobacterium* sp., *Rhodococcus erythropolis*, and *Pseudomonas putida* behavior in the presence of organic solvents. Microsc Res Tech **64:**215-222.
137. **Waltermann M, Steinbuchel A.** 2005. Neutral lipid bodies in prokaryotes: Recent insights into structure, formation, and relationship to eukaryotic lipid depots. J Bacteriol **187:**3607-19.
138. **Liang M-H, Jiang J-G.** 2013. Advancing oleaginous microorganisms to produce lipid via metabolic engineering technology. Prog Lipid Res **52:**395-408.
139. **Alvarez HM.** 2010. Biotechnological production and significance of triacylglycerols and wax esters, p 2995-3002. *In* Timmis KN (ed), Handbook of hydrocarbon and lipid microbiology. Springer Berlin Heidelberg, Berlin, Heidelberg.
140. **Steen EJ, Kang Y, Bokinsky G, Hu Z, Schirmer A, McClure A, Del Cardayre SB, Keasling JD.** 2010. Microbial production of fatty-acid-derived fuels and chemicals from plant biomass. Nature **463:**559-62.
141. **Creason AL, Davis EW, Putnam ML, Vandeputte OM, Chang JH.** 2014. Use of whole genome sequences to develop a molecular phylogenetic framework for *Rhodococcus fascians* and the *Rhodococcus* genus. Front Plant Sci **5:**406.
142. **Sangal V, Goodfellow M, Jones AL, Schwalbe EC, Blom J, Hoskisson PA, Sutcliffe IC.** 2016. Next-generation systematics: An innovative approach to resolve the structure of complex prokaryotic taxa. Sci Rep **6:**38392.
143. **Gürtler V, Mayall BC, Seviour R.** 2004. Can whole genome analysis refine the taxonomy of the genus *Rhodococcus*? FEMS Microbiol Rev **28:**377-403.
144. **Anastasi E, MacArthur I, Scortti M, Alvarez S, Giguère S, Vázquez-Boland JA.** 2016. Pangenome and phylogenomic analysis of the pathogenic actinobacterium *Rhodococcus equi*. Genome Biol Evol **8:**3140-3148.
145. **Ohshiro T, Hirata T, Hashimoto I, Izumi Y.** 1996. Characterization of dibenzothiophene desulfurization reaction by whole cells of *Rhodococcus erythropolis* H-2 in the presence of hydrocarbon. J Ferment Bioeng **82:**610-612.
146. **Nagasawa T, Shimizu H, Yamada H.** 1993. The superiority of the third-generation catalyst, *Rhodococcus rhodochrous* J1 nitrile hydratase, for industrial production of acrylamide. Appl Microbiol Biotechnol **40:**189-195.
147. **Koen Goethals, Danny Vereecke, Jaziri M, Marc Van Montagu a, Holsters M.** 2001. Leafy gall formation by *Rhodococcus fascians*. Annu Rev Phytopathol **39:**27-52.
148. **Hondalus MK, Mosser DM.** 1994. Survival and replication of *Rhodococcus equi* in macrophages. Infect Immun **62:**4167-4175.
149. **Alvarez HM, Mayer F, Fabritius D, Steinbüchel A.** 1996. Formation of intracytoplasmic lipid inclusions by *Rhodococcus opacus* strain PD630. Arch Microbiol **165:**377-386.
150. **R. CCCC.** 2017. Whole cell biocatalysts: Essential workers from nature to the industry. Microb Biotechnol **10:**250-263.

151. **Fernández-Cabezón L, Galán B, García JL.** 2018. New insights on steroid biotechnology. Front Microbiol **9**.
152. **Vlysidis A, Binns M, Webb C, Theodoropoulos C.** 2011. A techno-economic analysis of biodiesel biorefineries: Assessment of integrated designs for the co-production of fuels and chemicals. Energy **36:**4671-4683.
153. **Balan V.** 2014. Current challenges in commercially producing biofuels from lignocellulosic biomass. ISRN Biotechnol **2014:**463074.
154. **Singer ME, Finnerty WR.** 1988. Construction of an *Escherichia coli-Rhodococcus* shuttle vector and plasmid transformation in *Rhodococcus* spp. J Bacteriol **170:**638-645.
155. **Denis-Larose C, Bergeron H, Labbé D, Greer CW, Hawari J, Grossman MJ, Sankey BM, Lau PCK.** 1998. Characterization of the basic replicon of *Rhodococcus* plasmid pSOX and development of a *Rhodococcus-Escherichia coli* shuttle vector. Appl Environ Microbiol **64:**4363-4367.
156. **Hashimoto Y, Nishiyama M, Yu F, Watanabe I, Horinouchi S, Beppu T.** 1992. Development of a host-vector system in a *Rhodococcus* strain and its use for expression of the cloned nitrile hydratase gene cluster. Microbiology **138:**1003-1010.
157. **Nakashima N, Tamura T.** 2004. Isolation and characterization of a rolling-circle-type plasmid from *Rhodococcus erythropolis* and application of the plasmid to multiple-recombinant-protein expression. Appl Environ Microbiol **70:**5557-68.
158. **Bierman M, Logan R, O'Brien K, Seno ET, Nagaraja Rao R, Schoner BE.** 1992. Plasmid cloning vectors for the conjugal transfer of DNA from *Escherichia coli* to *Streptomyces* spp. Gene **116:**43-49.
159. **Hong Y, Hondalus MK.** 2008. Site-specific integration of StreptomycesΦC31 integrase-based vectors in the chromosome of Rhodococcus equi. FEMS Microbiology Letters **287:**63-68.
160. **Lu J, Tappel RC, Nomura CT.** 2009. Mini-review: Biosynthesis of poly(hydroxyalkanoates). Polym Rev **49:**226-248.
161. **Y.-H. Y, C.J. B, E. S, J.-M. J, C.K. R, A.J. S.** 2012. Biosynthesis of poly(3-hydroxybutyrate-co-3-hydroxyvalerate) containing a predominant amount of 3-hydroxyvalerate by engineered *Escherichia coli* expressing propionate-CoA transferase. J Appl Microbiol **113:**815-823.
162. **Pries A, Priefert H, Krüger N, Steinbüchel A.** 1991. Identification and characterization of two *Alcaligenes eutrophus* gene loci relevant to the poly(beta-hydroxybutyric acid)-leaky phenotype which exhibit homology to *ptsH* and *ptsI* of *Escherichia coli*. J Bacteriol **173:**5843-5853.
163. **Griebel R, Smith Z, Merrick JM.** 1968. Metabolism of poly(β-hydroxybutyrate). I. Purification, composition, and properties of native poly(β-hydroxybutyrate) granules from Bacillus megaterium. Biochemistry **7:**3676-3681.
164. **Chen G-Q, Wu Q.** 2005. The application of polyhydroxyalkanoates as tissue engineering materials. Biomaterials **26:**6565-6578.
165. **Chen Y, Ding Y, Yang L, Yu J, Liu G, Wang X, Zhang S, Yu D, Song L, Zhang H, Zhang C, Huo L, Huo C, Wang Y, Du Y, Zhang H, Zhang P, Na H, Xu S, Zhu Y, Xie Z, He T, Zhang Y, Wang G, Fan Z, Yang F, Liu H, Wang X, Zhang X, Zhang**

MQ, Li Y, Steinbüchel A, Fujimoto T, Cichello S, Yu J, Liu P. 2014. Integrated omics study delineates the dynamics of lipid droplets in *Rhodococcus opacus* PD630. Nucleic Acids Res **42:**1052-1064.
166. **Murphy DJ.** 2001. The biogenesis and functions of lipid bodies in animals, plants and microorganisms. Prog Lipid Res **40:**325-438.
167. **Meng X, Yang J, Xu X, Zhang L, Nie Q, Xian M.** 2009. Biodiesel production from oleaginous microorganisms. Renew Energ **34:**1-5.
168. **Liang M-H, Jiang J-G.** 2013. Advancing oleaginous microorganisms to produce lipid via metabolic engineering technology. Progress in Lipid Research **52:**395-408.
169. **Qiao K, Wasylenko TM, Zhou K, Xu P, Stephanopoulos G.** 2017. Lipid production in *Yarrowia lipolytica* is maximized by engineering cytosolic redox metabolism. Nat Biotech **35:**173-177.
170. **Post-Beittenmiller D.** 1996. Biochemistry and molecular biology of wax production in plants. Annu Rev Plant Physiol Plant Mol Biol **47:**405-430.
171. **Jacobsen E, Billings JK, Frantz RA, Kinney CK, Stewart ME, Downing DT.** 1985. Age-related changes in sebaceous wax ester secretion rates in men and women. J Invest Dermatol **85:**483-5.
172. **Nevenzel JC.** 1970. Occurrence, function and biosynthesis of wax esters in marine organisms. Lipids **5:**308-19.
173. **Kaiser J-P, Hanselmann KW.** 1982. Fermentative metabolism of substituted monoaromatic compounds by a bacterial community from anaerobic sediments. Arch Microbiol **133:**185-194.
174. **Lenneman EM, Ohlert JM, Palani NP, Barney BM.** 2013. Fatty alcohols for wax esters in *Marinobacter aquaeolei* VT8: two optional routes in the wax biosynthesis pathway. Appl Environ Microbiol **79:**7055-62.
175. **Ishige T, Tani A, Sakai Y, Kato N.** 2003. Wax ester production by bacteria. Curr Opin Microbiol **6:**244-250.
176. **Kalscheuer R, Steinbuchel A.** 2003. A novel bifunctional wax ester synthase/acyl-CoA:diacylglycerol acyltransferase mediates wax ester and triacylglycerol biosynthesis in *Acinetobacter calcoaceticus* ADP1. J Biol Chem **278:**8075-82.
177. **Stoveken T, Kalscheuer R, Malkus U, Reichelt R, Steinbuchel A.** 2005. The wax ester synthase/acyl coenzyme A:diacylglycerol acyltransferase from *Acinetobacter* sp. strain ADP1: characterization of a novel type of acyltransferase. J Bacteriol **187:**1369-76.
178. **Rontani J-F.** 2010. Production of wax esters by bacteria, p 459-470. *In* Timmis KN (ed), Handbook of hydrocarbon and lipid microbiology. Springer Berlin Heidelberg, Berlin, Heidelberg.
179. **Reiser S, Somerville C.** 1997. Isolation of mutants of *Acinetobacter calcoaceticus* deficient in wax ester synthesis and complementation of one mutation with a gene encoding a fatty acyl coenzyme A reductase. J Bacteriol **179:**2969-75.
180. **Hofvander P, Doan TT, Hamberg M.** 2011. A prokaryotic acyl-CoA reductase performing reduction of fatty acyl-CoA to fatty alcohol. FEBS Lett **585:**3538-43.

181. **Willis RM, Wahlen BD, Seefeldt LC, Barney BM.** 2011. Characterization of a fatty acyl-CoA reductase from *Marinobacter aquaeolei* VT8: a bacterial enzyme catalyzing the reduction of fatty acyl-CoA to fatty alcohol. Biochemistry **50:**10550-8.
182. **Deb C, Lee C-M, Dubey VS, Daniel J, Abomoelak B, Sirakova TD, Pawar S, Rogers L, Kolattukudy PE.** 2009. A novel *in vitro* multiple-stress dormancy model for *Mycobacterium tuberculosis* generates a lipid-loaded, drug-tolerant, dormant pathogen. PLoS ONE **4:**e6077.
183. **Sirakova TD, Deb C, Daniel J, Singh HD, Maamar H, Dubey VS, Kolattukudy PE.** 2012. Wax ester synthesis is required for *Mycobacterium tuberculosis* to enter in vitro dormancy. PLoS One **7:**e51641.
184. **Barney BM, Wahlen BD, Garner E, Wei J, Seefeldt LC.** 2012. Differences in substrate specificities of five bacterial wax ester synthases. Appl Environ Microbiol **78:**5734-45.
185. **Wolfmeier U, Schmidt H, Heinrichs F-L, Michalczyk G, Payer W, Dietsche W, Boehlke K, Hohner G, Wildgruber J.** 2000. Waxes, Ullmann's Encyclopedia of Industrial Chemistry. Wiley-VCH Verlag GmbH & Co. KGaA.
186. **Gago G, Diacovich L, Arabolaza A, Tsai S-C, Gramajo H.** 2011. Fatty acid biosynthesis in actinomycetes. FEMS Microbiol Rev **35:**475-497.
187. **Schweizer E, Hofmann J.** 2004. Microbial type I fatty acid synthases (FAS): Major players in a network of cellular FAS systems. Microbiol Mol Biol Rev **68:**501-517.
188. **White SW, Zheng J, Zhang Y-M, Rock CO.** 2005. The structural biology of type II fatty acid biosynthesis. Annu Rev Biochem **74:**791-831.
189. **Juarez A, Villa JA, Lanza VF, Lázaro B, de la Cruz F, Alvarez HM, Moncalián G.** 2017. Nutrient starvation leading to triglyceride accumulation activates the Entner Doudoroff pathway in *Rhodococcus jostii* RHA1. microb Cell Fact **16:**35.
190. **Hernandez MA, Arabolaza A, Rodriguez E, Gramajo H, Alvarez HM.** 2013. The *atf2* gene is involved in triacylglycerol biosynthesis and accumulation in the oleaginous *Rhodococcus opacus* PD630. Appl Microbiol Biotechnol **97**.
191. **Alvarez AF, Alvarez HM, Kalscheuer R, Waltermann M, Steinbuchel A.** 2008. Cloning and characterization of a gene involved in triacylglycerol biosynthesis and identification of additional homologous genes in the oleaginous bacterium *Rhodococcus opacus* PD630. Microbiology **154:**2327-35.
192. **Diaz Salazar Albelda C.** 2016. Redundancy in the biosynthesis of triacylglycerol by *Rhodococcus*. MSc Thesis. University of British Columbia.
193. **Marc W, Andreas H, Horst R, David T, Rudolf R, Ursula M, Hans-Joachim G, Rainer K, Tim S, Philipp VL, Alexander S.** 2005. Mechanism of lipid-body formation in prokaryotes: how bacteria fatten up. Molecular Microbiology **55:**750-763.
194. **Londos C, Brasaemle DL, Schultz CJ, Segrest JP, Kimmel AR.** 1999. Perilipins, ADRP, and other proteins that associate with intracellular neutral lipid droplets in animal cells. Semin Cell Dev Biol **10:**51-58.
195. **Ding Y, Yang L, Zhang S, Wang Y, Du Y, Pu J, Peng G, Chen Y, Zhang H, Yu J, Hang H, Wu P, Yang F, Yang H, Steinbüchel A, Liu P.** 2012. Identification of the major functional proteins of prokaryotic lipid droplets. J Lipid Res **53:**399-411.

196. **MacEachran DP, Prophete ME, Sinskey AJ.** 2010. The *Rhodococcus opacus* PD630 heparin-binding hemagglutinin homolog TadA mediates lipid body formation. Appl Environ Microbiol **76**.
197. **Low HH, Sachse C, Amos LA, Löwe J.** 2009. Structure of a bacterial dynamin-like protein lipid tube provides a mechanism for assembly and membrane curving. Cell **139:**1342-1352.
198. **Boström P, Andersson L, Rutberg M, Perman J, Lidberg U, Johansson BR, Fernandez-Rodriguez J, Ericson J, Nilsson T, Borén J, Olofsson S-O.** 2007. SNARE proteins mediate fusion between cytosolic lipid droplets and are implicated in insulin sensitivity. Nat Cell Biol **9:**1286.
199. **Zhang C, Yang L, Ding Y, Wang Y, Lan L, Ma Q, Chi X, Wei P, Zhao Y, Steinbüchel A, Zhang H, Liu P.** 2017. Bacterial lipid droplets bind to DNA via an intermediary protein that enhances survival under stress. Nat Commun **8:**15979.
200. **Bauchop T, Elsden SR.** 1960. The growth of micro-organisms in relation to their energy supply. J Gen Microbiol **23:**457-69.
201. **Sambrook J, Russell DW.** 2001. Molecular cloning: A laboratory manual, 3rd ed. Cold Spring Harbor Laboratory Press, Cold Spring Harbor, NY.
202. **Hong Y, Hondalus MK.** 2008. Site-specific integration of *Streptomyces* ΦC31 integrase-based vectors in the chromosome of *Rhodococcus equi*. FEMS microbiology letters **287:**63-68.
203. **Chin JX, Chung BK-S, Lee D-Y.** 2014. Codon Optimization OnLine (COOL): A web-based multi-objective optimization platform for synthetic gene design. Bioinformatics **30:**2210-2212.
204. **Torella JP, Lienert F, Boehm CR, Chen J-H, Way JC, Silver PA.** 2014. Unique nucleotide sequence-guided assembly of repetitive DNA parts for synthetic biology applications. Nat Protoc **9:**2075-2089.
205. **Goodman AL, Wu M, Gordon JI.** 2011. Identifying microbial fitness determinants by insertion sequencing using genome-wide transposon mutant libraries. Nat Protoc **6:**1969.
206. **Bergmeyer HU.** 1975. New values for the molar extinction coefficients of NADH and NADPH for the use in routine laboratories. Z Klin Chem Klin Biochem **13:**507-8.
207. **Eyer P, Worek F, Kiderlen D, Sinko G, Stuglin A, Simeon-Rudolf V, Reiner E.** 2003. Molar absorption coefficients for the reduced Ellman reagent: reassessment. Anal Biochem **312:**224-227.
208. **Bligh EG, Dyer WJ.** 1959. A rapid method of total lipid extraction and purification. Can J Biochem Physiol **37:**911-7.
209. **Matyash V, Liebisch G, Kurzchalia TV, Shevchenko A, Schwudke D.** 2008. Lipid extraction by methyl-tert-butyl ether for high-throughput lipidomics. J Lipid Res **49:**1137-1146.
210. **Pernet F, Pelletier CJ, Milley J.** 2006. Comparison of three solid-phase extraction methods for fatty acid analysis of lipid fractions in tissues of marine bivalves. J Chromatogr A **1137:**127-37.
211. **Wang C, Lee J, Deng Y, Tao F, Zhang L-H.** 2012. ARF-TSS: an alternative method for identification of transcription start site in bacteria. Biotechniques **52**.

212. **Baranyi J, Roberts TA.** 1994. A dynamic approach to predicting bacterial growth in food. Int J Food Microbiol **23:**277-94.
213. **Urbanová K, Vrkoslav V, Valterová I, Háková M, Cvacˇka J.** 2012. Structural characterization of wax esters by electron ionization mass spectrometry. J Lipid Res **53:**204-213.
214. **Youngquist JT, Schumacher MH, Rose JP, Raines TC, Politz MC, Copeland MF, Pfleger BF.** 2013. Production of medium chain length fatty alcohols from glucose in *Escherichia coli*. Metab Eng **20:**177-86.
215. **Aslan S, Sun C, Leonova S, Dutta P, Dörmann P, Domergue F, Stymne S, Hofvander P.** 2014. Wax esters of different compositions produced via engineering of leaf chloroplast metabolism in *Nicotiana benthamiana*. Metab Eng **25:**103-112.
216. **Kroll J, Klinter S, Schneider C, Voß I, Steinbüchel A.** 2010. Plasmid addiction systems: Perspectives and applications in biotechnology. Microb Biotechnol **3:**634-657.
217. **Silva F, Queiroz JA, Domingues FC.** 2012. Evaluating metabolic stress and plasmid stability in plasmid DNA production by *Escherichia coli*. Biotechnol Adv **30:**691-708.
218. **Barroca M, Rodrigues P, Sobral R, Costa MMR, Chaves SR, Machado R, Casal M, Collins T.** 2016. Antibiotic free selection for the high level biosynthesis of a silk-elastin-like protein. Sci Rep **6:**39329.
219. **Wu G, Yan Q, Jones JA, Tang YJ, Fong SS, Koffas MA.** 2016. Metabolic burden: Cornerstones in synthetic biology and metabolic engineering applications. Trends Biotechnol **34:**652-64.
220. **Round J, Roccor R, Li S-N, Eltis LD.** 2017. A fatty acyl-CoA reductase promotes wax ester accumulation in *Rhodococcus jostii* RHA1. Appl Environ Microbiol **83:**e00902-17.
221. **Linger JG, Vardon DR, Guarnieri MT, Karp EM, Hunsinger GB, Franden MA, Johnson CW, Chupka G, Strathmann TJ, Pienkos PT, Beckham GT.** 2014. Lignin valorization through integrated biological funneling and chemical catalysis. Proc Natl Acad Sci U S A **111:**12013-12018.
222. **Newton-Foot M, Gey van Pittius NC.** 2013. The complex architecture of mycobacterial promoters. Tuberculosis **93:**60-74.
223. **Zhu Y, Mao C, Ge X, Wang Z, Lu P, Zhang Y, Chen S, Hu Y.** 2017. Characterization of a minimal type of promoter containing the −10 element and a guanine at the −14 or −13 position in *Mycobacteria*. J Bacteriol **199**.
224. **Seghezzi N, Amar P, Koebmann B, Jensen PR, Virolle M-J.** 2011. The construction of a library of synthetic promoters revealed some specific features of strong *Streptomyces* promoters. Appl Microbiol Biotechnol **90:**615-623.
225. **Weickert MJ, Adhya S.** 1993. The galactose regulon of *Escherichia coli*. Mol Microbiol **10:**245-251.
226. **Liu X, Matsumura P.** 1996. Differential regulation of multiple overlapping promoters in flagellar class II operons in *Escherichia coli*. mol Microbiol **21:**613-620.
227. **Stewart V, Bledsoe PJ, Williams SB.** 2003. Dual overlapping promoters control *napF* (periplasmic nitrate reductase) operon expression in *Escherichia coli* K-12. J Bacteriol **185:**5862-5870.

228. **Kaiser M, Sawers G.** 1997. Overlapping promoters modulate Fnr- and ArcA-dependent anaerobic transcriptional activation of the *focApfl* operon in *Escherichia coli*. Microbiology **143:**775-783.
229. **Cortes T, Schubert Olga T, Rose G, Arnvig Kristine B, Comas I, Aebersold R, Young Douglas B.** 2013. Genome-wide mapping of transcriptional start sites defines an extensive leaderless transcriptome in *Mycobacterium tuberculosis*. Cell Rep **5:**1121-1131.
230. **Albersmeier A, Pfeifer-Sancar K, Rückert C, Kalinowski J.** 2017. Genome-wide determination of transcription start sites reveals new insights into promoter structures in the actinomycete *Corynebacterium glutamicum*. J Biotechnol **257:**99-109.
231. **Gopaul KK, Brooks PC, Prost J-F, Davis EO.** 2003. Characterization of the two *Mycobacterium tuberculosis recA* promoters. J Bacteriol **185:**6005-6015.
232. **Bibb MJ, Janssen GR, Ward JM.** 1985. Cloning and analysis of the promoter region of the erythromycin resistance gene (*ermE*) of *Streptomyces erythraeus*. Gene **38:**215-226.
233. **Labes G, Bibb M, Wohlleben W.** 1997. Isolation and characterization of a strong promoter element from the *Streptomyces ghanaensis* phage 119 using the gentamicin resistance gene (*aacC1*) of Tn1696 as reporter. Microbiology **143:**1503-1512.
234. **Hook-Barnard IG, Hinton DM.** 2007. Transcription initiation by mix and match elements: Flexibility for polymerase binding to bacterial promoters. Gene Regul Syst Bio **1:**275-293.
235. **Brown NL, Stoyanov JV, Kidd SP, Hobman JL.** 2003. The MerR family of transcriptional regulators. FEMS Microbiol Rev **27:**145-163.
236. **Holmes DJ, Caso JL, Thompson CJ.** 1993. Autogenous transcriptional activation of a thiostrepton-induced gene in *Streptomyces lividans*. EMBO J **12:**3183-3191.
237. **Lund PA, Brown NL.** 1989. Regulation of transcription in *Escherichia coli* from the *mer* and *merR* promoters in the transposon Tn501. J Mol Biol **205:**343-353.
238. **Chan CL, Gross CA.** 2001. The Anti-initial Transcribed Sequence, a Portable Sequence That Impedes Promoter Escape, Requires ς^{70} for Function. J Biol Chem **276:**38201-38209.
239. **Xu P, Gu Q, Wang W, Wong L, Bower AGW, Collins CH, Koffas MAG.** 2013. Modular optimization of multi-gene pathways for fatty acids production in *E. coli*. Nat Commun **4:**1409.
240. **Jones JA, Vernacchio VR, Lachance DM, Lebovich M, Fu L, Shirke AN, Schultz VL, Cress B, Linhardt RJ, Koffas MAG.** 2015. ePathOptimize: A Combinatorial Approach for Transcriptional Balancing of Metabolic Pathways. Sci Rep **5:**11301.
241. **Tai M, Stephanopoulos G.** 2013. Engineering the push and pull of lipid biosynthesis in oleaginous yeast *Yarrowia lipolytica* for biofuel production. Metab Eng **15:**1-9.
242. **Holtzapple E, Schmidt-Dannert C.** 2007. Biosynthesis of isoprenoid wax ester in *Marinobacter hydrocarbonoclasticus* DSM 8798: Identification and characterization of isoprenoid coenzyme a synthetase and wax ester synthases. J Bacteriol **189:**3804-3812.
243. **Kalscheuer R, Stöveken T, Malkus U, Reichelt R, Golyshin PN, Sabirova JS, Ferrer M, Timmis KN, Steinbüchel A.** 2007. Analysis of storage lipid accumulation in

Alcanivorax borkumensis: Evidence for alternative triacylglycerol biosynthesis routes in bacteria. J Bacteriol **189:**918-928.

244. **Villa JA, Cabezas M, de la Cruz F, Moncalian G.** 2014. Use of limited proteolysis and mutagenesis to identify folding domains and sequence motifs critical for wax ester synthase/acyl coenzyme A:diacylglycerol acyltransferase activity. Appl Environ Microbiol **80:**1132-1141, 11 pp.
245. **Kalscheuer R, Uthoff S, Luftmann H, Steinbüchel A.** 2003. *In vitro* and *in vivo* biosynthesis of wax diesters by an unspecific bifunctional wax ester synthase/acyl-CoA:diacylglycerol acyltransferase from *Acinetobacter calcoaceticus* ADP1. Eur J Lipid Sci Technol **105:**578-584.
246. **Uthoff S, Stöveken T, Weber N, Vosmann K, Klein E, Kalscheuer R, Steinbüchel A.** 2005. Thio wax ester biosynthesis utilizing the unspecific bifunctional wax ester synthase/acyl coenzyme A:diacylglycerol acyltransferase of *Acinetobacter* sp. strain ADP1. Appl Environ Microbiol **71:**790-796.
247. **Lin F, Chen Y, Levine R, Lee K, Yuan Y, Lin XN.** 2013. Improving Fatty Acid Availability for Bio-Hydrocarbon Production in *Escherichia coli* by Metabolic Engineering. PLOS ONE **8:**e78595.
248. **Teo WS, Ling H, Yu A-Q, Chang MW.** 2015. Metabolic engineering of *Saccharomyces cerevisiae* for production of fatty acid short- and branched-chain alkyl esters biodiesel. Biotechnol Biofuels **8:**177.
249. **Shi S, Valle-Rodriguez JO, Khoomrung S, Siewers V, Nielsen J.** 2012. Functional expression and characterization of five wax ester synthases in Saccharomyces cerevisiae and their utility for biodiesel production. Biotechnol Biofuels **5:**7.
250. **Ruiz-Lopez N, Broughton R, Usher S, Salas JJ, Haslam RP, Napier JA, Beaudoin F.** 2017. Tailoring the composition of novel wax esters in the seeds of transgenic *Camelina sativa* through systematic metabolic engineering. Plant Biotechnol J **15:**837-849.
251. **Torella JP, Boehm CR, Lienert F, Chen J-H, Way JC, Silver PA.** 2014. Rapid construction of insulated genetic circuits via synthetic sequence-guided isothermal assembly. Nucleic Acids Res **42:**681-689.
252. **Forns X, Bukh J, Purcell RH, Emerson SU.** 1997. How *Escherichia coli* can bias the results of molecular cloning: Preferential selection of defective genomes of hepatitis C virus during the cloning procedure. Proc Natl Acad Sci U S A **94:**13909-13914.
253. **Godiska R, Mead D, Dhodda V, Wu C, Hochstein R, Karsi A, Usdin K, Entezam A, Ravin N.** 2010. Linear plasmid vector for cloning of repetitive or unstable sequences in *Escherichia coli*. Nucleic Acids Res **38:**e88-e88.
254. **Nyström A, Papachristodoulou A, Angel A.** 2018. A dynamic model of resource allocation in response to the presence of a synthetic construct. ACS Synth Biol **7:**1201-1210.
255. **Lanfranconi MP, Alvarez HM.** 2017. Rewiring neutral lipids production for the *de novo* synthesis of wax esters in *Rhodococcus opacus* PD630. J Biotechnol **260:**67-73.
256. **Marrakchi H, Lanéelle M-A, Daffé M.** 2014. Mycolic acids: Structures, biosynthesis, and beyond. Chem Biol **21:**67-85.

257. **Toriyama S, Imaizumi S, Tomiyasu I, Masui M, Yano I.** 1982. Incorporation of ^{18}O into long-chain, secondary alcohols derived from ester mycolic acids in *Mycobacterium phlei*. BBA-Lipid Lipid Met **712:**427-429.
258. **Lacave C, Laneelle M-A, Daffe M, Montrozier H, Laneelle G.** 1989. Mycolic acid metabolic filiation and location in *Mycobacterium aurum* and *Mycobacterium phlei*. Eur J Biochem **181:**459-466.
259. **Fixter LM, Nagi MN, Mccormack JG, Fewson CA.** 1986. Structure, distribution and function of wax esters in *Acinetobacter Calcoaceticus*. J Gen Microbiol **132:**3147-3157.
260. **Kalscheuer R, Stoveken T, Luftmann H, Malkus U, Reichelt R, Steinbuchel A.** 2006. Neutral lipid biosynthesis in engineered *Escherichia coli*: Jojoba oil-like wax esters and fatty acid butyl esters. Appl Environ Microbiol **72:**1373-9.
261. **Santala S, Efimova E, Koskinen P, Karp MT, Santala V.** 2014. Rewiring the wax ester production pathway of *Acinetobacter baylyi* ADP1. ACS Synth Biol **3:**145-51.
262. **Kannisto M, Efimova E, Karp M, Santala V.** 2017. Growth and wax ester production of an *Acinetobacter baylyi* ADP1 mutant deficient in exopolysaccharide capsule synthesis. J Ind Microbiol Biotechnol **44:**99-105.
263. **DeLorenzo DM, Rottinghaus AG, Henson WR, Moon TS.** 2018. Molecular toolkit for gene expression control and genome modification in *Rhodococcus opacus* PD630. ACS Synth Biol **7:**727-738.
264. **Siegl T, Tokovenko B, Myronovskyi M, Luzhetskyy A.** 2013. Design, construction and characterisation of a synthetic promoter library for fine-tuned gene expression in actinomycetes. Metab Eng **19:**98-106.
265. **Gilman J, Love J.** 2016. Synthetic promoter design for new microbial chassis. Biochem Soc Trans **44:**731-7.
266. **McWhinnie RL, Nano FE.** 2014. Synthetic promoters functional in *Francisella novicida* and *Escherichia coli*. Appl Environ Microbiol **80:**226-34.
267. **Rodríguez-García A, Combes P, Pérez-Redondo R, Smith MCA, Smith MCM.** 2005. Natural and synthetic tetracycline-inducible promoters for use in the antibiotic-producing bacteria *Streptomyces*. Nucleic Acids Res **33:**e87-e87.
268. **DeLorenzo DM, Henson WR, Moon TS.** 2017. Development of chemical and metabolite sensors for *Rhodococcus opacus* PD630. ACS Synth Biol **6:**1973-1978.
269. **Ehrt S, Guo XV, Hickey CM, Ryou M, Monteleone M, Riley LW, Schnappinger D.** 2005. Controlling gene expression in mycobacteria with anhydrotetracycline and Tet repressor. Nucleic Acids Res **33:**e21-e21.
270. **Kuhstoss S, Richardson MA, Rao RN.** 1991. Plasmid cloning vectors that integrate site-specifically in *Streptomyces spp*. Gene **97:**143-146.
271. **Boccard F, Pernodet J-L, Friedmann A, Guérineau M.** 1988. Site-specific integration of plasmid pSAM2 in Streptomyces lividans and S. ambofaciens. Mol Gen Genet **212:**432-439.
272. **Merrick CA, Zhao J, Rosser SJ.** 2018. Serine Integrases: Advancing Synthetic Biology. ACS Synth Biol **7:**299-310.
273. **Fayed B, Ashford DA, Hashem AM, Amin MA, El Gazayerly ON, Gregory MA, Smith MC.** 2015. Multiplexed integrating plasmids for engineering of the erythromycin

gene cluster for expression in *Streptomyces* spp. and combinatorial biosynthesis. Appl Environ Microbiol **81:**8402-13.
274. **Brown WRA, Lee NCO, Xu Z, Smith MCM.** 2011. Serine recombinases as tools for genome engineering. Methods **53:**372-379.
275. **Silva-Rocha R, Martínez-García E, Calles B, Chavarría M, Arce-Rodríguez A, de las Heras A, Páez-Espino AD, Durante-Rodríguez G, Kim J, Nikel PI, Platero R, de Lorenzo V.** 2013. The Standard European Vector Architecture (SEVA): A coherent platform for the analysis and deployment of complex prokaryotic phenotypes. Nucleic Acids Res **41:**D666-D675.
276. **Petronikolou N, Nair SK.** 2018. Structural and biochemical studies of a biocatalyst for the enzymatic production of wax esters. ACS Catal **8:**6334-6344.
277. **Stöveken T, Kalscheuer R, Steinbüchel A.** 2009. Both histidine residues of the conserved HHXXXDG motif are essential for wax ester synthase/acyl-CoA:diacylglycerol acyltransferase catalysis. Eur J Lipid Sci Technol **111:**112-119.
278. **Lehtinen T, Efimova E, Santala S, Santala V.** 2018. Improved fatty aldehyde and wax ester production by overexpression of fatty acyl-CoA reductases. Microbial Cell Factories **17:**19.
279. **Hollinshead WD, Henson WR, Abernathy M, Moon TS, Tang YJ.** 2016. Rapid metabolic analysis of *Rhodococcus opacus* PD630 via parallel ^{13}C-metabolite fingerprinting. Biotechnol Bioeng **113:**91-100.
280. **Hernández MA, Comba S, Arabolaza A, Gramajo H, Alvarez HM.** 2015. Overexpression of a phosphatidic acid phosphatase type 2 leads to an increase in triacylglycerol production in oleaginous *Rhodococcus* strains. Applied Microbiology and Biotechnology **99:**2191-2207.
281. **Davis MS, Solbiati J, Cronan JE, Jr.** 2000. Overproduction of acetyl-CoA carboxylase activity increases the rate of fatty acid biosynthesis in *Escherichia coli*. J Biol Chem **275:**28593-8.
282. **Waltermann M, Luftmann H, Baumeister D, Kalscheuer R, Steinbuchel A.** 2000. Rhodococcus opacus strain PD630 as a new source of high-value single-cell oil? Isolation and characterization of triacylglycerols and other storage lipids. Microbiology **146**.
283. **Kurosawa K, Boccazzi P, de Almeida NM, Sinskey AJ.** 2010. High-cell-density batch fermentation of Rhodococcus opacus PD630 using a high glucose concentration for triacylglycerol production. J Biotechnol **147:**212-8.

Appendices

Appendix A - Synthesized DNA[a]

Gene / Fragment	Use
ws1	WS for modulating WE accumulation
ATGACCCCGCTCAACCCTACTGATCAATTATTTTTATGGCTGGAGAAGCGCCAGCAGCCCATGCACGTCGGTGGCCTCCAGCTGTT CTCGTTCCCGGAGGGCGCACCCGACGACTACGTCGCGCAGCTCGCCGACCAGCTCCGCCAGAAGACGGAGGTCACCGCGCCGTTC AATCAGCGGCTTTCGTATCGACTAGGCCAGCCGGTGTGGGTCGAGGACGAGCACCTCGACCTCGAGCACCACTTCCGTTTCGAGGC CCTGCCCACCCCCGGACGTATCCGCGAATTGCTGTCGTTCGTCTCTGCTGAACACTCGCACCTCATGGACCGGGAACGCCCGATGT GGGAGGTGCACCTCATCGAGGGACTAAAGGACCGCCAGTTCGCCCTGTACACGAAGGTCCACCATTCGCTCGTCGACGGCGTAAG TGCGATGCGCATGGCGACCCGGATGCTGTCCGAGAACCCCGACGAGCATGGGATGCCGCCGATCTGGGACCTGCCGTGCCTGTCA CGGGACCGAGGAGAGTCAGATGGGCACAGTCTGTGGCGCTCGGTGACGCACCTGCTGGGACTGTCCGACCGTCAGCTCGGCACGA TCCCTACAGTAGCAAAAGAACTCCTGAAGACCATCAACCAGGCCCGCAAGGACCCGGCGTACGACTCCATCTTCCACGCCCCAAG ATGCATGCTCAACCAGAAGATCACCGGCTCCCGCCGCTTCGCGGCCCAGTCGTGGTGCCTGAAGCGCATTCGCGCGGTTTGCGAGG CCTACGGTACGACGGTCAACGACGTGGTGACAGCTATGTGCGCGGCCGCCCTACGCACGTACCTTATGAACCAAGACGCCTTACCG GAAAAGCCCCTGGTCGCATTCGTGCCTGTGTCGTTGCGACGGGACGATAGCTCGGGCGGCAACCAGGTGGGTGTCATATTAGCGTC CTTGCACACCGACGTGCAGGACGCGGGTGAGCGACTGCTCAAGATCCACCACGGGATGGAGGAAGCGAAGCAGCGTTACCGGCA CATGTCGCCCGAGGAGATCGTGAACTACACGGCCCTAACTTTGGCCCCCGCGGCGTTCCACCTGCTCACCGGTCTGGCTCCGAAGT GGCAGACGTTCAACGTCGTCATCTCCAACGTGCCAGGACCATCGCGGCCTCTGTACTGGAACGGTGCCAAGTTAGAAGGCATGTAC CCGGTCTCGATCGACATGGACAGGCTCGCTCTGAACATGACATTAACCAGCTACAACGACCAGGTCGAGTTCGGCCTCATCGGCTG CCGGCGGACGTTGCCGTCCCTGCAACGCATGCTCGACTACCTGGAGCAGGGCCTGGCCGAACTGGAACTGAACGCCGGCTTA	
ws2	WS for modulating WE accumulation
ATGAAACGACTTGGAACACTTGATGCATCTTGGCTGGCTGTCGAGTCCGAGGATACCCCGATGCACGTCGGCACTTTGCAAATCTT CAGCCTTCCTGAAGGCGCGCCCGAAACGTTCCTGCGCGACATGGTCACCCGCATGAAGGAGGCGGGTGACGTGGCGCCCCCCTGG GGCTACAAGCTCGCCTGGTCGGGCTTCCTCGGGCGGGTGATCGCACCTGCGTGGAAGGTCGACAAGGACATCGACCTTGACTACC ACGTGCGGCACAGTGCGCTTCCCCGACCCGGTGGCGAGCGCGAGCTCGGGATCTTAGTATCAAGACTTCACAGCAACCCGCTGGA CTTCTCGAGGCCGTTATGGGAGTGCCACGTCATCGAGGGGCTCGAGAACAACCGCTTCGCCCTGTACACCAAGATGCACCACTCGA TGATCGACGGCATCAGTGGGGTGCGTCTGATGCAGCGCGTCCTCACCACGGACCCCGAGCGTTGCAACATGCCGCCGCCGTGGACT GTTCGTCCGCACCAGCGGCGTGGTGCCAAGACCGATAAAGAGGCCAGCGTCCCGGCCGCCGTGTCGCAGGCCATGGACGCGCTCA AGCTACAGGCTGACATGGCCCCGAGACTGTGGCAGGCCGGGAATCGACTTGTGCACTCCGTCCGTCACCCGGAGGACGGCCTCAC GGCCCCCTTCACGGGGCCGGTGTCAGTCCTCAACCATCGCGTGACAGCCCAGCGTCGGTTCGCGACCCAGCACTACCAGCTCGATA GGCTTAAGAATCTCGCGCACGCCAGCGGCGGGAGTCTCAACGACATCGTCCTGTACCTGTGCGGCACCGCGCTGAGACGGTTCCTA GCCGAGCAGAACAACCTGCCTGACACGCCGTTAACGGCGGGAATCCCCGTCAACATCAGGCCGGCGGACGACGAGGGAACGGGC ACCCAGATCAGCTTCATGATCGCGTCCTTGGCAACAGACGAGGCAGATCCGCTCAACCGGCTCCAGCAGATCAAGACTTCTACGA GACGTGCCAAGGAACACCTGCAGAAGCTTCCGAAGAGCGCTTTGACACAGTACACGATGCTCCTGATGTCCCCGTACATCCTGCAA TTAATGAGCGGACTGGGTGGCCGGATGCGACCAGTGTTCAACGTCACGATCTCGAACGTGCCGGGCCCTGAGGGTACGCTCTACTA CGAGGGAGCACGTCTCGAAGCGATGTACCCGGTCTCGTTGATCGCCCACGGCGGGGCGCTGAACATCACGTGCCTGTCCTACGCA GGATCGTTGAATTTCGGCTTCACAGGTTGCCGGGACACCTTGCCCTCCATGCAGAAGCTGGCGGTCTACACCGGTGAGGCCCTCGA CGAACTGGAGTCGCTTATCTTACCTCCCAAGAAGCGCGCGAGGACACGCAAG	
atfA	WS for modulating WE accumulation
ATGAGACCGCTGCACCCGATCGACTTCATCTTCCTCTCCCTCGAGAAGCGGCAGCAGCCGATGCACGTGGGCGGCCTGTTCCTGTT CCAGATCCCCGACAACGCGCCCGACACGTTCATCCAGGACCTCGTCAACGACATCCGCATCTCCAAGTCCATCCCGGTCCCGCCGT TCAACAACAAGCTGAACGGTCTGTTCTGGGACGAGGACGAGGAGTTCGACCTGGACCATCACTTCCGGCACATCGCGCTGCCGCA CCCCGGCCGGATCCGTGAGCTCCTCATCTACATCTCGCAGGAGCACTCGACGCTGCTCGACCGCGCCAAGCCGCTGTGGACCTGCA ACATCATCGAAGGCATCGAGGGCAACCGGTTCGCCATGTACTTCAAGATCCACCACGCGATGGTCGACGGCGTCGCCGGGATGCG CCTGATCGAGAAGTCGCTGTCGCACGACGTCACCGAGAAGTCGATCGTCCCCCCGTGGTGCGTCGAGGGCAAGCGCGCGAAGCGT CTGCGCGAGCCGAAGACGGGCAAGATCAAGAAGATCATGTCCGGCATCAAGTCCCAGCTGCAGGCGACCCCGACCGTCATCCAGG AGCTGAGCCAGACCGTGTTCAAGGACATCGGCCGCAACCCGGACCACGTCAGCAGCTTCCAGGCCCCGTGCAGCATCCTGAACCA GCGCGTCTCCTCGTCGCGCCGCTTCGCGGCGCAGTCGTTCGACTTGGACCGGTTCCGCAACATCGCCAAGAGCCTCAACGTCACGA TCAACGACGTCGTCCTCGCCGTCTGCTCGGGCGCCCTGCGGGCGTACCTGATGAGCCACAACTCCCTGCCCAGCAAGCCCCTGATC GCGATGGTGCCCGCGTCCATCCGCAACGACGACTCCGACGTGTCGAACCGCATCACGATGATCCTCGCGAACCTGGCCACCCACA AGGACGACCCGCTCCAGCGTCTCGAGATCATCCGGCGGTCGGTGCAGAACTCGAAGCAGCGGTTCAAGCGGATGACCAGCGACCA GATCCTCAACTACTCGGCGGTGGTCTACGGCCCCGCCGGCCTCAACATCATCAGCGGCATGATGCCCAAGCGCCAGGCGTTCAACC TCGTGATCTCCAACGTGCCGGGCCCGCGGGAGCCCCTCTACTGGAACGGCGCGAAGCTCGACGCCCTGTACCCGGCGTCGATCGTG	

CTCGACGGTCAGGCCCTGAACATCACCATGACGTCGTACCTCGACAAGCTGGAGGTCGGCCTGATCGCCTGCCGGAACGCCCTCCC GCGCATGCAGAACCTGCTGACGCACCTCGAAGAGGAGATCCAGCTCTTCGAGGGTGTCATCGCCAAGCAGGAAGACATCAAGACC GCCAAC	
atfA2	WS for modulating WE accumulation
ATGGCAAGGAAATTAAGTATCATGGACTCAGGTTGGCTCATGATGGAGACCCGCGAGACGCCGATGCACGTCGGTGGACTCGCAC TGTTCGCGATCCCGGAGGGTGCCCCCGAGGACTACGTCGAGTCGATCTACCGCTACCTCGTGGACGTGGACTCCATCTGCCGGCCG TTCAACCAGAAGATCCAGAGCCATCTGCCGCTGTACCTGGACGCCACGTGGGTGGAAGACAAGAACTTCGACATCGACTACCACG TTAGGCACTCGGCTTTGCCACGCCCCGGTCGTGTACGGGAGCTGTTAGCGCTTGTAAGCAGGCTGCACGCCCAGCGCCTCGACCCG AGCCGTCCCCTGTGGGAGTCCTACCTGATTGAAGGCCTGGAAGGTAATAGGTTTGCGCTATATACCAAGATGCACCACTCCATGGT GGACGGTGTCGCAGGCATGCACTTGATGCAGTCGCGACTCGCCACATGCGCCGAGGACCGGCTCCCGGCACCGTGGAGCGGGGAG TGGGACGCGGAGAAGAAGCCGCGGAAATCGCGCGGCGCCGCCGCCGCGAACGCGGGCATGAAGGGCACCATGAACAACCTGCGC CGCGGTGGCGGGCAGTTGGTTGACCTGCTAAGGCAGCCGAAGGACGGCAACGTCAAGACCATCTACCGGGCTCCGAAAACCCAGC TCAACCGCAGGGTCACCGGTGCCCGGAGGTTTGCTGCGCAGTCCTGGAGCCTCAGCCGGATCAAGGCGGCGGGTAAGCAGCACGG CGGTACTGTGAACGACATCTTCCTGGCGATGTGCGGAGGCGCATTGCGACGTTATCTACTGAGCCAGGACGCTCTCTCCGACCAGC CATTGGTGGCGCAGGTCCCGGTGGCCCTGCGTTCGGCCGACCAGGCCGGCGAGGGCGGCAACGCCATCACGACAGTTCAAGTCAG CCTAGGCACCCACATCGCCCAGCCTCTCAACCGGCTTGCCGCGATCCAGGACTCGATGAAGGCAGTCAAATCACGGCTGGGCGAC ATGCAGAAGTCGGAGATCGACGTCTACACCGTGCTCACCAACATGCCGCTGTCGCTCGGCCAGGTGACCGGCTTGTCGGGTCGGGT CTCTCCGATGTTCAACCTGGTCATCTCGAACGTGCCCGGCCCGAAGGAGACCCTACACCTAAACGGCGCTGAGATGCTGGCCACCT ACCCGGTCTCCCTGGTCCTGCATGGCTACGCTCTGAACATCACCGTCGTCTCGTACAAGAACTCGTTAGAGTTCGGGGTTATCGGCT GCCGCGACACCTTGCCGCACATCCAGCGTTTCCTTGTGTACCTCGAGGAGTCACTGGTGGAACTCGAGCCC	
pLB	Universal linkers, linearization sites, Gibson overlaps
GGCTGCAGGTCGACTCTAGACATTACTCGCATCCATTCTCAGGCTGTCTCGTCTCGTCTCGGCGCGCCATCGATCATTTTAATTAAC CAGGATACATAGATTACCACAACTCCGAGCCCTTCCACCATTAATGAATCGGCCAACGC	

[a]Genes encoding WSs were codon-optimized for *Rhodococcus*.